UNIVERSITY OF MARYLAND

National Transportation Center

Project ID: NTC2015-MU-R-05

Data Fusion Aided Freeway Analysis for Highway Capacity Manual
(Final Report)

by

Behzad Aghdashi, Ph.D.
Research Associate, ITRE, NC State University
909 Capability Dr, Raleigh, NC
saghdas@ncsu.edu

J. Lake Trask, Ph.D.
Transportation Analyst
Kittelson & Associates, Inc., Wilmington NC
ltrask@kittelson.com

for

National Transportation Center at Maryland (NTC@Maryland)
1124 Glenn Martin Hall
University of Maryland
College Park, MD 20742

March 2018

ACKNOWLEDGEMENTS

This project received funding from the National Transportation Center @ Maryland (NTC@Maryland), one of the five National Centers that were selected in this nationwide competition, by the Office of the Assistant Secretary for Research and Technology (OST-R), U.S. Department of Transportation (US DOT). Many thanks for the support provided by NTC. Our thanks also go to Justin Babich who helped formatting and editing this report.

DISCLAIMER

TABLE OF CONTENTS

LIST OF TABLES

LIST OF FIGURES

EXECUTIVE SUMMARY

The Highay Capacity Manual (HCM) is one of the widely used refercens in the transportation engineerng. The 6th edition of HCM provides a multimodal framework to broaden the scope of HCM applications. This project focused on the freeway facilities analysis which plays the core role in other freeway analysis types in HCM. Other facility-based analysis in HCM is built on freeway facilities methodology such as travel time reliability, Active Traffic and Demand Management (ATDM), or Work Zone analyses.

FREEVAL is the offcial computational engine for HCM, performing freeway analysis. It is freely avaible to download (freeval.org). It replicates the methods in the HCM, and offers the same analysis types as offered by HCM such as travel time reliability analysis or etc. FREEVAL first developed more than a decade ago using Excel/VBA. The 2015 version used Java as the platform and as a result offered a lot of enhancements in terms of computational speed as well as GUI. This project utilized FREEVAL computational engine and built its findings as additional packages for FREEVAL.

This research focused on the use of avaible data sources to streamline the HCM freeway analysis. Examples of availble data sources were investigated are a) online mapping tools and b) sensor data providing speeds. These data sources can be utilized to aid analysts perform freeway segmentation as well as demand estimation and calibration.

The research team investigated different online mapping services and evaluated information that can be gathered through these data sources. Google Maps API selected to be the best data provider for geometric data needs for freeway analysis. Beside this effort, the project team developed a segmentation procedure that can divide a freeway strech into HCM segments. The resulting HCM segments are completely matching with HCM definitions. The project team implemented the developed segmentation procedure in FREEVAL. Google Maps API also emplyed to assist analysts fill requried information (e.g. sections lengths) automatically. As a result, the entire procedure of segmentatin automated in FREEVAL computational engine.

The project also developed methods to estimate demand and calibrate analysis based on availble sensor data. The most uniform sensor database availble across US is probe-based speed data. There are several number of probe-based speed data providers such as INRIX, Here.com, and etc. The developed models to estimate demand and calibrate FREEVAL to target speed profiles/contours tunes speed, capacity and demand adjustment factors. The proposed method implemented in FREEVAL and can be invoked to perform demand estimation and analysis calibration.

1.0 INTRODUCTION AND BACKGROUND

The Highway Capacity Manual (HCM) is a widely utilized reference document for various planning and operational-level transportation analysis methods (Highway Capacity Manual 2016). Among others, it provides a set of methodologies to evaluate freeway facility performance, as well as freeway reliability analyses. Despite the macroscopic nature of the methods in the HCM, and despite the availability of several software packages implementing the method, performing a correct analysis is difficult and time consuming. This is largely due to 1) time-consuming preliminarily data collection and preparation prior to the analysis, 2) difficulty in correct data collection and data entry, and 3) lacking guidance on data needs for calibration and validation. These factors are not comprehensively covered in the HCM, nor do procedures exist for automating these processes. This research tried to address these shortcomings in order to assist HCM users and agencies and ease the methodologies to be performed correctly.

Furthermore, the developed HCM-based calibration methodology can aid dynamic traffic assignment and corridor-level capacity analysis, which is an increasingly useful tool for traffic analysis and evaluation at the network level. How to understand the data needs and further calibrate dynamic demand and supply elements for large-scale traffic regions and corridors is a challenging issue from both theoretical and practical aspects. It is important and necessary to use observed data, such as probe point-to-end travel time from probe-based data sources (e.g. INRIX) or sensor-based flow and speed data, for constructing time-dependent simulation representations consistent with real-world conditions.

The scope of this research effort is concentrated on "significant" non-recurring sources of congestion, which are expected to have a high impact on the traveling public and are oftentimes located on freeway facilities. As such, the FREEVAL tool is ideally suited for analysis, since it is fundamentally based on the freeway facilities methodology in the 6th edition of HCM. The tool has been effectively used in national level research to model the effects of recurring freeway bottlenecks and was found to be significantly more efficient when compared to simulation-based analysis tools. The reliability version of the FREEVAL considers non-recurring congestion sources such as weather and incident's impact which enables a comprehensive assessment of the freeway facilities.

1.1 PROJECT OBJECTIVES:

The objectives of the proposed project were to:

1. Develop a data preparation framework and methodology for an HCM freeway facility analysis, including the use of online mapping tools for facility segmentation;
2. Develop *'demand estimation'* and *'calibration'* methodologies to adjust demand and capacity in conjunction with freeway characteristics such as capacity reduction due to congestion.
3. Identify possible data sources that can be integrated into HCM (FREEVAL) analysis framework for demand estimation, calibration and also validation;

The research approach built on existing HCM methodologies, the FREEVAL tool (the computational engine for the HCM freeway facilities methodology), available online mapping tools (Google map, open street map, etc.), as well as online data sources (e.g. INRIX, RITIS, PEMS, etc). FREEVAL is the official computational engine for HCM freeway analysis. It has been developed and updated at ITRE for more than a decade. The new version of FREEVAL is developed in a Java environment and utilizes all capabilities of a multiplatform-programming environment that assures the feasibility of possible connections to various online or offline data sources, as well as performing more complex mathematical procedures such as optimizations.

However, the existing HCM procedure is limited to the core method and select extensions for reliability analysis and others. It does not provide guidance on input data needs such as demand input, calibration details, and integration with modern data sources. This research filled this gap, and developed the necessary guidance for implementing agencies, assisted by automation of data input and calibration procedures that streamline the application of the method.

1.2 LITERATURE REVIEW

1.2.1 Overview of Dynamic Traffic Assignment and the Cell Transmission Model

An important analysis technique used in planning and evaluating freeway transportation networks is Dynamic Traffic Assignment (DTA). DTA seeks to model “time-varying network and demand interaction using a behaviorally sound approach" (Chiu et al., 2011). This research is primarily interested in a subset of DTA consisting of equilibrium-seeking mesoscopic models, i.e., models whose resolution falls between microscopic and macroscopic models, but make use of properties of both. DTA models are often used to evaluate travel times and costs of network performance by modeling them as optimization problems. In these formulations, travel time and cost become the objectives to be minimized and are subject to flow conservation and traffic assignment constraints. Throughout the literature reviewed, two different traffic assignment conditions were generally used for the DTA formulations. The first and simpler of the two conditions is the System Optimum (SO) condition. Under SO assignment, the goal is to minimize the travel time or cost of the system as a whole (Ziliaskopoulos, 2000). The second condition, User Equilibrium (UE) or User Optimum (UO) assignment, differs from this in that each individual driver seeks to minimize his/her travel time, even if it comes at the cost of total system performance (Ukkusuri & Waller, 2008). This dynamic can be more difficult to capture in mathematical models, but is generally thought of to be a more realistic representation. It should be noted that under free flow conditions with little to no congestion, the two conditions will converge to the same answer, but when congestion is high, the optimal solutions can differ greatly. An in depth survey on DTA is given by Chiu et al. (2011). One of the more widely used DTA models is the Cell Transmission Model (CTM), which was first proposed by Carlos Daganzo (1994). The CTM primarily consists of a set of difference equations that simulate traffic flow on highways and use shockwaves to model the backward (upstream) propagation of traffic congestion. The equations are presented as a discrete approximation of the differential equations proposed by Lighthill, Witham, and Richards (Lighthill & Whitham, 1955a,b; Richards, 1956). These original differential equations (often referred to as the LWR equations) were developed by applying hydrodynamic flow theory to traffic flow and analytically account for important concepts such as the Flow-Density diagram (Figure 1) and the shockwave propagation of congestion. In his initial paper, Daganzo asserts that the CTM

is the discrete equivalent of the underlying hydrodynamic theory. The eq inputs: the free flow speed (FFS) of the highway, the maximum flow in a cell (segment capacity), the jam density, and the wave speed of the propagation shockwaves. Work was later done by Daganzo (1995) to expand the model to represent traffic networks by allowing for basic, merge (on-ramp), and diverge (off-ramp) segments to be represented in the equations. Due to its accuracy (as shown in (Lin & Ahanotu, 1995; Smilowitz & Daganzo, 1999)) and relative computational simplicity, vast amounts of research have been conducted to expand the core methodology of the CTM.

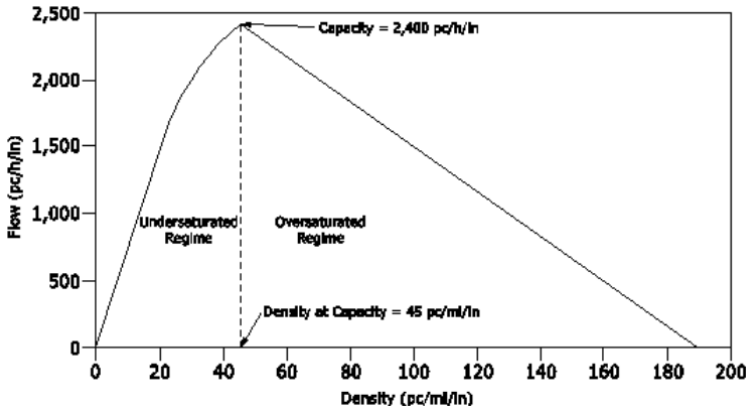

Figure 1: Example fundamental flow-density diagram (Highway Capacity Manual 2016)

1.2.2 Optimization Extensions to the Core CTM Formulation

The first work to utilize the CTM in a pure linear programming framework was presented in the context of the System Optimal Dynamic Traffic Assignment (SO-DTA) problem (Ziliaskopoulos, 2000). Due to the relative computational tractability of linear programming, a large amount of research has since been devoted to building on the work. Waller & Ziliaskopoulos (2001) extended the model into a two stage LP in order to account for stochastic time-dependent demands. Li et al. (2003) developed a Dantzig-Wolfe decomposition scheme for the formulation . Work has also be done to incorporate UE (or UO) route assignment as opposed to the simpler SO assignment. 10 Travis Waller & Ziliaskopoulos (2006) first proposed a combinatorial optimization approach (as opposed to mathematical programming), while later Ukkusuri & Waller (2008) directly extended the CTM linear programming formulation to account for UE conditions. In their work, they also compared the effect of the two route assignment conditions (SO and UE) on solutions for sample TNDP problems. Han et al. (2011) further built on the formulation making use of complementarity theory to improve the calculation of travel time estimates and capture multiple user classes with elastic demands. Active Traffic Management (ATM) techniques such as dynamic congestion pricing for tolls have also been proposed based on sensitivity and dual variable analysis allowed by the linear programming formulations (Lin et al., 2011). In order to model the CTM as a pure linear program, Ziliaskopoulos (2000) used the simplifying assumption that the minimum relationship between flow and capacity could be represented as a set of “less-than" inequality constraints on link flow. However, this assumption does not guarantee that the assigned quantity is truly the minimum of the values, i.e., $x \leq y$, $x \leq z$ does not imply $x = \min\{y , z\}$. This can lead to an issue known as the vehicle-holding or holding-back problem. An overview

of the holding-back problem as well as a survey of the work done to account for it was compiled by Doan & Ukkusuri (2012). Lo (2001) proposed accounting for this nonlinearity by incorporating integer linear constraints that effectively turn sets of constraints on or off, though the work was mostly investigated for its use in signal control applications. In a similar vein, Tampère & Immers (2007) proposed the use of the Heaviside function for the approach. Zheng & Chiu (2011) addressed the issue by proving that the single destination system optimal dynamic traffic assignment (SD SO-DTA) problem is equivalent to the earliest arrival flow (EAF) network problem, and developed a network flow algorithm that eliminated vehicle holding in basic and merge segments (but not necessarily for diverge segments). Doan & Ukkusuri (2012) presented multiple formulations to completely remove vehicle-holding under SO routing for problems with multiple destinations. The removal of vehicle-holding was achieved by using complementarity constraints and converting them to a nonlinear programming model, as well as by incorporating mixed integer programming (MIP) techniques. Next, Ukkusuri et al. (2012) extended the techniques to handle the UE conditions. Unfortunately, each of these formulations requires assumptions that may not accurately reflect realistic conditions, and in addition still contain some nonlinearities or non-convexities (Zhu & Ukkusuri, 2013). Further, in all of the previously mentioned papers the authors acknowledge that the formulations are still impractical for larger and more realistic sizes of networks. Another linear complementarity approach was developed by Zhong et al. (2013) in order to better deal with the nonlinearity of the state jump conditions and hard nonlinear min functions. The proposed formulation readily extends to both DTA and TNDP analysis, and while not as com11 putationally efficient as pure LP formulations, it benefits from the existing work done on linear complementarity problems (LCP) (Hu et al., 2012). More recently, Zhu & Ukkusuri (2013) were able to develop a pure linear programming solution to the vehicle-holding problem for the SD SO-DTA problem by introducing an easily computable penalty function into the formulation. Sun et al. (2014) extended this to incorporate demand uncertainty and developed an adjustable robust optimization (ARO) linear programming formulation.

1.2.3 CTM Formulations and ATM Analysis

The CTM formulation and its extensions have also been used to tune ATM strategies. Gomes & Horowitz (2006) developed the Asymmetric Cell Transmission Model (ACTM) to compute optimal ramp metering rates. While the ACTM formulation remains nonlinear, the authors proved sufficient conditions under which the globally optimal solution could be found through the use of a single linear program. Unfortunately, these sufficiency conditions were rather constrictive, and often highly unrealistic of true freeway conditions. Finding a lack of in-depth theoretical results concerning the CTM/MCTM, Gomes et al. (2008) further investigated the properties of congested and uncongested equilibria for the model and interpreted the findings with respect to the effectiveness of ramp metering strategies. The authors found that optimally computed ramp metering strategies can reduce congestion and travel time on freeways, and that the strategies do more than just move the congestion to on-ramps. A dynamic on-line method to determine Variable Speed Limits (VSL) has been proposed by Li et al. (2014), with benefits stemming from the low computational cost of the CTM vs the more complex existing VSL algorithms.

1.2.4 Overview the Transportation Network Design Problems (TNDP)

Beyond supporting sensitivity analysis, optimization frameworks can also provide a direct path to finding ways of improving existing transportation networks. Most problems of this nature fall

under the umbrella of Transportation Network Design Problems (TNDP). These problems seek to provide an optimization model for the selection of network improvements. For example, if funds for road widening are available, a TNDP formulation could be used to select the optimal portion to be widened. There are a number of appropriate ways to formulate a problem such as this, but often the model would seek to maximize the post-improvement traffic flow, while simultaneously minimizing construction costs, all while satisfying the system's flow conservation and traffic assignment constraints. DTA and TNDP have many important applications beyond just their initial scope. They can be used to improve reliability analysis of transportation networks, especially under abnormal conditions such as evacuations (Lim et al., 2015; Malveo, 2013; Yao et al., 12 2009). Due to the interplay between the equilibrium constraints and the multiple objective functions, single level TNDP formulations are generally nonconvex and nonlinear. These types of problems are known to be at least NP hard (Zeng & Mouskos, 1997). To regain some linearity, TNDP is often formulated as a bilevel program, i.e., one with an upper level and a lower level objective function. Despite the inherent difficulty in finding a solution for formulations such as these, it is still important that at least a near globally optimum solution be found. As such, heuristic algorithms have often been found to be the best choice to efficiently seek an optimal or near-optimal solution. In recent years, much research has been conducted into the use of metaheuristic techniques such as genetic algorithms (GA), simulated annealing (SA), and tabu search for extending and solving TNDP formulations (Delbem et al., 2012; Juan et al., 2012; Karoonsoontawong & Waller, 2006; Luathep et al., 2011; Mudchanatongsuk et al., 2008; Xu et al., 2009; Zeng & Mouskos, 1997).

1.2.5 HCM Calibration and Hourly Demand Profiles

The 6th edition of the Highway Capacity Manual (2016) provides guidance on how to address model calibration in the form of a five-step process as shown in Figure 2. The first step requires the user to 36 gather the required input data for the model including geometric aspects, segment free flow speeds (FFS), and initial demand volume estimates for the mainline and ramps at each analysis period of the study period. No guidance is provided to address the process of initial demand estimation. The manual breaks the calibration adjustment process into three pieces: free flow speed calibration, bottleneck capacity calibration, and demand adjustment. Free flow speeds can be calibrated using observed measures for uncongested or off-peak periods. For bottleneck capacity calibration, the HCM advises a trial and error strategy. In the event the location and or severity of congestion predicted by the model does not match that of an observed set of target performance measures, the manual recommends that an analyst repeatedly adjust the capacity of bottleneck segments by 50 pc/h/ln until an acceptable level of matching is achieved. Identification of bottleneck segments is left up to the analyst's knowledge of the facility. For demand estimation, the manual advises that an analyst manually adjust volumes in increments of 50 pc/h/ln until predicted model travel times and bottleneck queue lengths are within a specified margin of error.

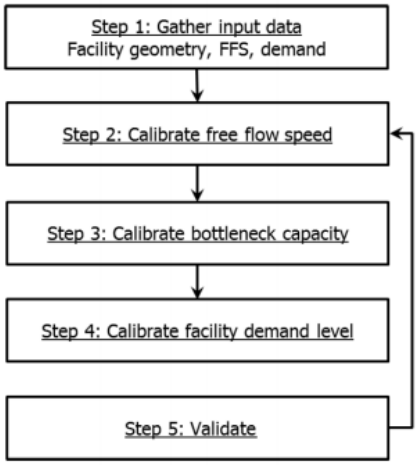

Figure 2: Core freeway analysis calibration framework in the 6th edition of the HCM (Highway Capacity Manual 2016)

In order to estimate the initial set of demand inputs, an analyst generally makes use of an average annual daily traffic (AADT) value projected into individual demand volumes using an hourly demand profile. An hourly demand profile provides a breakdown of the percentage of an AADT value occuring during each hour of the day. Individual profiles are often highly specific to the each 37 location, but general trends are common across most facilities. Demand profiles for weekdays are often bimodal in that they contain two clear peaks. In this case, one peak typically corresponds to travelers on their morning commute, and one corresponds to travelers commuting home from work in the evenings. In contrast, weekend profiles are often unimodal, or have a single peak, that builds more slowly throughout the day. Hallenbeck et al. (1997) developed a set of national default profiles for weekdays and weekends, broken down into both urban and rural categories. Both bimodal and unimodal behavior are reflected in the national default profiles, shown in Figure 3.

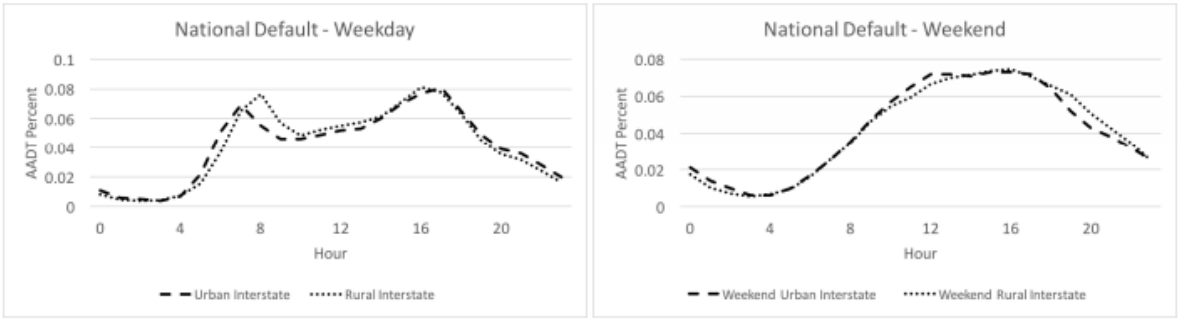

(a) National default weekday profile shape. (b) National default weekend profile shape.

Figure 3: National default hourly demand profiles for weekdays and weekends on urban and rural interstates

Additionally, a study conducted for the state of North Carolina provides a further level of detail and divides the profiles into 3 default categories: unimodal, bimodal with an AM peak, and bimodal with a PM peak (NCDOT, 2016). Figure 2, above, shows examples of each of these three types. The unimodal profiles are very similar to the weekend category of profiles, while the bimodal profiles provide two variations of the weekday profile. Further, six additional profile shapes are provided for each of three main profile types. These represent the minimum, the 25th percentile, the average, the 75th percentile, the maximum, and median of all profiles generated from the collected data.

1.2.6 Calibration of the CTM and Related Models

The cell transmission model is commonly used as a basis for automated density estimation and calibration approaches. Some of the earliest work on this is presented by Munoz et al. (2003) who develop the modified cell transmission model (MCTM) and the switching mode model (SMM). This formulation differs from Daganzo's basic CTM in three key ways. First, cell densities are used as state variables as opposed to cell occupancy, directly leading to the second difference in that the 38 MCTM can handle non-uniform cell lengths. Lastly, the formulation allows congested conditions at the downstream end of a facility. These changes lead to some nonlinearities in the difference equations regarding moving congestion wavefronts, so the authors develop the SMM to return to a piecewise linear formulation. The SMM accounts for five different congestion status modes that allow the model to switch between several sets of linear difference equations. The authors are also able to show that the CTM and the MCTM/SMM can estimate demand within freeway facilities with reasonable accuracy. A fair amount of density estimation research has come out of the development of the MCTM and the SMM. Muñoz et al. (2004) propose a methodological calibration procedure for the CTM/MCTM and further show the methods accurately estimate density on longer stretches of freeway. This procedure is further explored by Zhong et al. (2014), but their proposed nonlinear optimization framework again has the deficiency of an inability to reliably find globally optimal solutions. The MCTM/SMM has been extended to included stochastic variations in traffic, especially with respect to their effects on the fundamental flow-density diagram. The Stochastic Cell Transmission Model (SCTM) directly incorporates stochastic noise into the parameters of the fundamental diagram (Sumalee et al., 2011). Pascale et al. (2013, 2014) develop an alternative approach in which they use a Bayesian framework to account for stochasticity, and propose a particle filtering approach to estimate density. Both methods are shown to be reliably accurate in matching sample detector data. Most recently, a robust switching approach for the SMM is introduced by Morbidi et al. (2014) in situations where the congestion wave speed is unknown. Similar alternatives to the mechanisms of the MCTM/SMM for state detection have also been developed. Stankova & De Schutter (2010) use a jump Markov linear model (JMLM) to account for switching between free-flow and congested states, while Aligawesa and Hwang propose a State Dependent Transition Hybrid Estimation (SDTHE) algorithm motivated by the SMM but with improved state detection. Further research has been conducted into density estimation and state prediction loosely based on the LWR equations and the CTM, though most of the methods developed rely on relaxations and heuristics to even attempt to find solutions (e.g., Lu et al. (2013) and Ma et al. (2015)).

1.2.7 System Identification and Metaheuristics

System identification was initially developed as a technique to construct mathematical models of dynamic systems based on observed data (Ljung, 2010). The approach provides an effective

way of modeling systems where relationships between inputs and outputs are either unknown or poorly understood to the point where an exact model cannot be built. For the approach, systems are 39 generally classified in terms of a "transparency" on the scale between white and black. A “white-box" model of a system is one where all relationships are known and have been defined. For a “black-box" model little to nothing of the true relationships are known or can be defined (De Nicolao, 1997). There also exist a number of variations of “grey-box" models that fall between the two extremes where varying amounts of information are known (Ljung, 2010). In approaching a grey-box model, a basic understanding of the relationships is assumed, but the complexities are not fully or explicitly considered. Metaheuristics are a class of search approaches that “permit an abstract level of description" and are used to “effeciently explore the search space in order to find (near-) optimal solutions" (Blum & Roli, 2003). At their core, metaheuristics are not problem-specific, but implementations can make use of “domain-specific knowledge...controlled by the upper level strategy" (Blum & Roli, 2003). This lack of specificity paired with an abundance of flexibility makes metaheuristic approaches particularly useful for solving grey or even black-box system identification problems. There are a wide variety of types of metaheuristics that have been developed including but not limited to simple local search techniques, evolutionary algorithms, simulated annealing, and artificial neural networks (Gendreau & Potvin, 2005). A genetic algorithm (GA) is an evolutionary search metaheuristic commonly used for complex optimization problems where the underlying mathematics preclude the use of classical approaches. The approach draws from the processes of evolution and natural selection in order to generate an optimal or near-optimal solution by “evolving” a pool of candidate solutions over time (Goldberg, 1989). Each candidate solution is represented as an individual organism, with the decision variables of the problem encoded as the organism’s “genes". An evaluation function is defined in order to calculate the fitness of a candidate solution based on these genes. By choosing an encoding and fitness function such that the problem is framed as a minimization or maximization of fitness, fitnessbased “competition" can be used to make statements on the quality of one candidate solution versus another. In this way, the fitness function is essentially analogous to the objective function of classical optimization techniques like linear programming. The most critical aspect of using a GA is the process of defining the encoding of a candidate solution as the genes of an organism. In fact, the key underlying assumption to the GA approach is that high-quality solutions will contain common “building blocks" in their encoded genetic material (Mitchell, 1998). Maintaining these blocks within a population of organisms, and combining them with other “good" blocks should then theoretically lead to the discovery of better solutions. Blocks can be combined through the use of a crossover operator that represents the “mating" of organisms. While real-valued encodings are occasionally used, most encodings consist of some type of binary representation of the solution. This allows for a straightforward realization of genetic building blocks 40 (e.g., small binary patterns such as “010" or “110"), as well as providing a simple notion of crossover through exchanging binary digits.

2.0 FREEVAL AUTOMATIC SEGMENTATION

This section discusses the research team's efforts to implement automatic segmentation procedure for FREEVAL/HCM. In order to achieve automatic segmentation being useful and applicable for users, first a mapping serice should be added to FREEVAL to assist users to define the spatial scope of the analysis. The first part of this section discusses availble online mapping services that can be incorporated in FREEVAL. The second part introduces a systematic procedure to break freeway strech into HCM segments.

2.1 MAPS INTEGRATION

2.1.1 Google Maps JavaScript API

Google Maps has various free APIs available. The Directions, Distance Matrix, Geocoding, and Roads APIs can use HTTP requests to query the desired data. In FREEVAL A JFX web panel is created in Java Swing so that the Google Maps JavaScript API can be used. The API Reference can be found here: https://developers.google.com/maps/documentation/javascript/3.exp/reference.

The JavaScript API incorporates the other APIs as services. For example, a connection with the Directions API can be made to pass end points and receive a path of points in between. The drawing service can use that path to draw a route. In the case of the JavaScript API, an API key is only required to track access to a project. Without a key, the API limitations are more relaxed since it is counted by session rather than by project. Google Maps has a significant set of features available all in one place and it is highly documented and supported online.

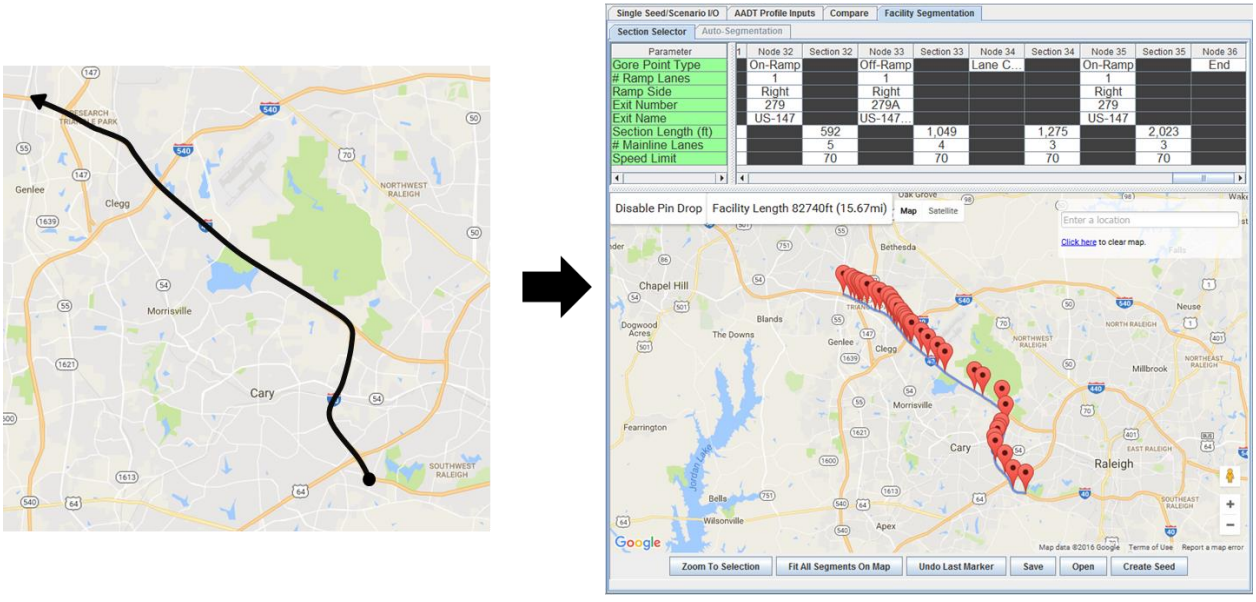

Figure 4: Example of integration of the Google Maps API to improve facility creation

The Google Maps Roads API was initially investigated because of its ability to simply snap points to a road and interpolate a path as the user clicks on the map. However, this came with a severe sever limitation for allowable distance between points. A more elegant solution was found using the Google Maps Directions API. The Directions API allows the user to place multiple points on the map and receive a calculated route between them regardless of the distance.

2.1.2 Open Street Maps

Open Street Maps stores data inside of "Ways" which are segments of "Nodes" which are coordinates. Metadata stored in Ways include things such as the speed limit and number of lanes, however this information is not always present and can be very sparse depending on the area. There is some ambiguity here as well. A segment on a road with two oncoming lanes, a middle lane, and two ongoing lanes will have 5 lanes. A road segment with two lanes on each side of a divider like Western Boulevard will return 2 lanes. A segment that ends at an intersection may have a left turn lane, a right turn lane, and the oncoming traffic lane, so this segment returns 3 lanes. This data is reported by users so they may not follow a standard practice.

The Open Street Maps API is for editing the maps only. Reading Open Street Map data can be done with the Overpass API. The Overpass API is a third party service and has a couple of public instances: http://wiki.openstreetmap.org/wiki/Overpass_API. The Overpass API acts as a database over the web so that data can be queried from Open Street Maps. Overpass API queries can be tested on the web by running them with Overpass Turbo here: http://overpass-turbo.eu. Other third party tools must be used to find routing information using Open Street Map data. These tools usually have limited API requests allowed for free before pricing plans are required.

2.2 FREEVAL AUTOSEGMENTATION PROCEDURE

The first step in creating a model for analysis with the HCM's freeway facilities methodology is to determine the length of freeway being modeled, and divide into "segments" using the manual's specified guidance. The HCM accounts for five separate types of segments: basic, merge, diverge, weaving, and overlap. A merge segment represents an on-ramp and its resulting influence area, while a diverge segment is an analogous representation of an off-ramp. A weave segment represents an on-ramp followed by an off-ramp that includes one or more auxiliary lanes connecting the two ramps. An overlap segment exists when the influence areas of adjacent on and off-ramps overlap and no auxiliary lane exists. Lastly, a basic segment is any other non-ramp stretch of freeway.

While it is straightforward to identify major geometric changes and ramps for a facility, the determination of the corresponding HCM compatible segments can be both challenging and time-consuming. Further, HCM segmentation is highly unlikely to correspond to existing TMC segments over which data is collected by a number of organizations. As such, manual segmentation of a facility represents a major challenge to using the HCM methodology. This work develops a new "autosegmentation" procedure based on the segmentation rules of the HCM in order to reduce the burden placed on an analyst and greatly simplify the facility creation process.

The autosegmentation procedure consists of four main phases, as described in the subsequent sections. Following that, the procedure is further broken down into 12 individual steps, and each

is presented with a detailed description. An example facility is segmented using the 12 steps and presented alongside the description of each step.

2.2.1 Phase 1: Checking for Mainline Geometric and Capacity Changes

The first step identifies all geometric and capacity related changes that occur on the mainline of the facility. These include land drops and lane additions, as well as changes in the speed limit. These represent permanent segment breaks that are not affected by any potential adjustments occurring in subsequent steps.

2.2.2 Phase 2: Identify Ramp Gore Points

In this step, all "gore points" of the facility are identified by the analyst. A gore point is found at each ramp (both on and off-ramps) of the facility. Gore points do not represent segment boundaries, but rather will be used to determine segment type (merge, diverge, weaving) and will adjusted upstream or downstream in the following step to account for influence areas.

Weaving segments are also identified at this step. If the procedure finds that an on-ramp gore point is followed by an off-ramp gore point, and that an auxiliary lane exists between the two points, then the two gore points represent the ends of a weaving segment. However, these gore points do not represent the segment boundary, as they must be adjusted to account for the weave influence areas.

2.2.3 Phase 3: Marking Segment Influence Areas

The HCM segmentation procedure requires that (when possible) both on-ramp and off-ramp segments include 1500ft influence areas. Hence, for each gore point from the previous step denoting an on-ramp, the resulting merge segment's downstream boundary is created 1500ft downstream of the gore point. Analogously, for each gore point denoting an off-ramp, the resulting diverge segment's upstream boundary is created 1500ft upstream of the gore point. For each weaving segment, the gore points marking the on-ramp and off-ramp are shifted upstream and downstream, respectively, by 500ft.

2.2.4 Phase 4: Final Adjustments and Alternatives

In many cases, it is possible that the segment boundaries created in the previous steps will create segmentations that include configurations that are either invalid entirely or conflict with some of the HCM's recommendations (i.e. segments shorter than the minimum length threshold). To account for these occurrences, some of the segment boundaries can be shifted (especially those related to influence areas) in order to eliminate these issues.

Any issues that arise create alternative potential segmentations from which to choose. The analyst will be responsible for deciding which issues to address and how to address them, and should make the decision based on their knowledge of the facility being modeled.

2.3 DETAILED AUTOSEGMENTATION STEPS

Step 1: The start and end points of a facility are permanent segment boundaries

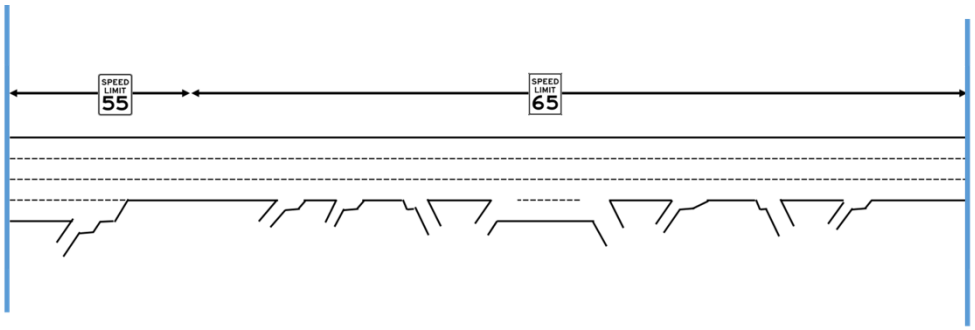

Figure 5: Facility with start and end points marked as segment boundaries

Step 2: All changes in number of lanes and speed limit/free flow speed are permanent segment boundaries. (Note: Accel/deccel lanes do not count as lane changes).

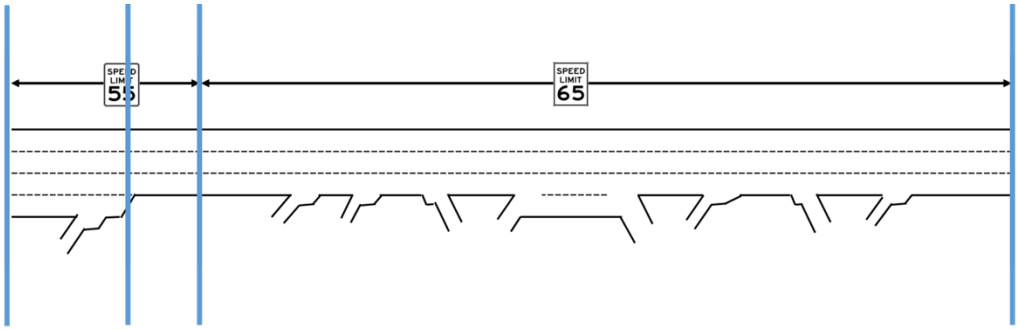

Figure 6: Example facility with geometric and capacity changes marked as segment boundaries

Step 3: Identify all ramp gore points and mark as potential segment boundaries.

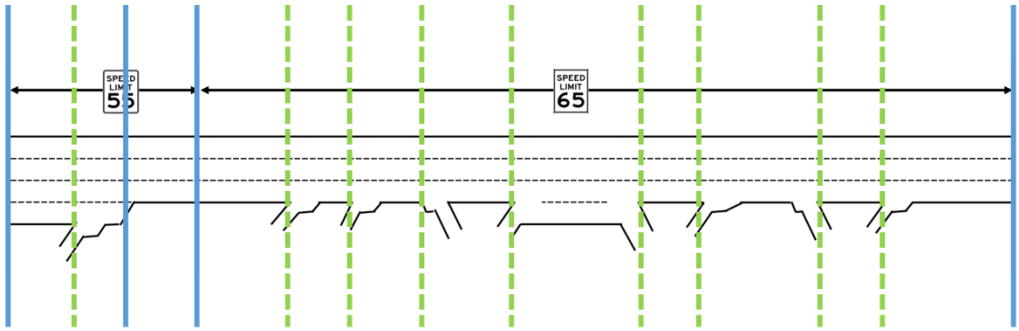

Figure 7: Example facility with each ramp gore point marked as a candidate segment boundary

Step 4: Check to see if an auxiliary lane exists between all sets of adjacent on-ramp and off-ramp gore points. If an auxiliary lane exists, then the two gore points form a weave segment. Next, shift the on-ramp gore point 500ft upstream, and shift the off-ramp gore point 500ft downstream to account for weave influence areas, and mark the shifted gore points as permanent nodes and the result segment as a weave. (Note: if a permanent or candidate segment boundary is within the 500ft influence for the upstream or downstream end, the gore point shift is stopped at the segment boundary.)

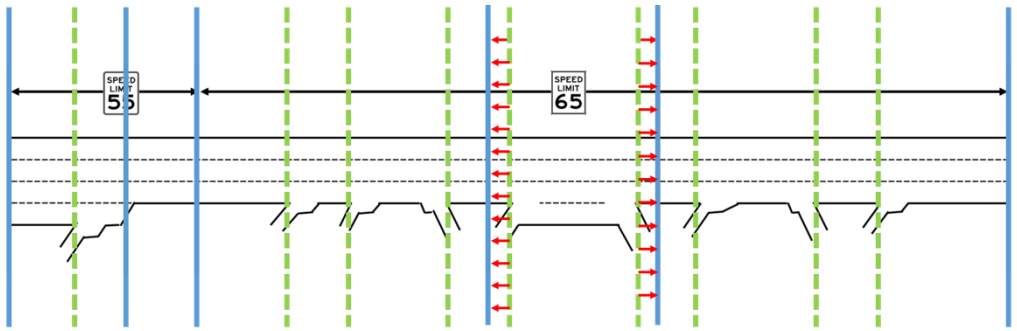

Figure 8: In the case of an on-ramp followed by an off-ramp with an auxiliary lane, the candidate boundaries should be shifted to account for influence areas, and the resulting segment is a weave

Step 5: Mark all remaining gore point candidate boundaries as permanent segment boundaries.

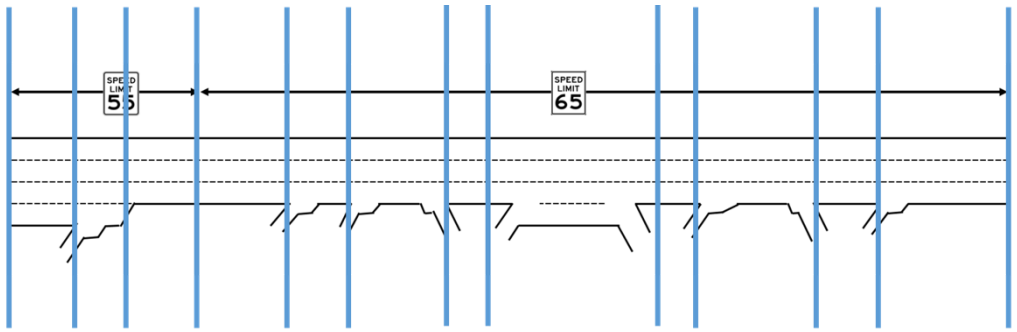

Figure 9: Example facility with the first set of permanent segment boundaries from geometric factors and ramp gore points

Step 6: Determine 1500ft from and to on-ramp and off-ramp gore points, respectively, and mark them as potential segment boundaries.

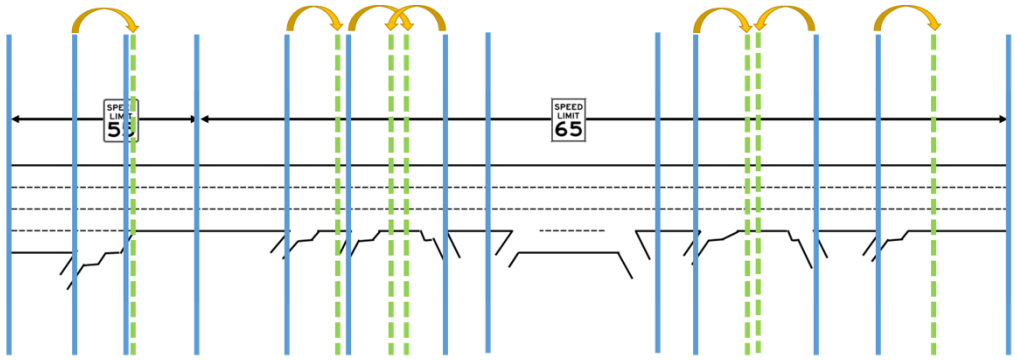

Figure 10: Example facility with candidate segment boundaries created due to ramp influence areas

Step 7: For each new potential boundary, check to see if the 1500ft influence area has passed a segment boundary. If it has, then reduce the 1500ft distance to be aligned with the segment boundary.

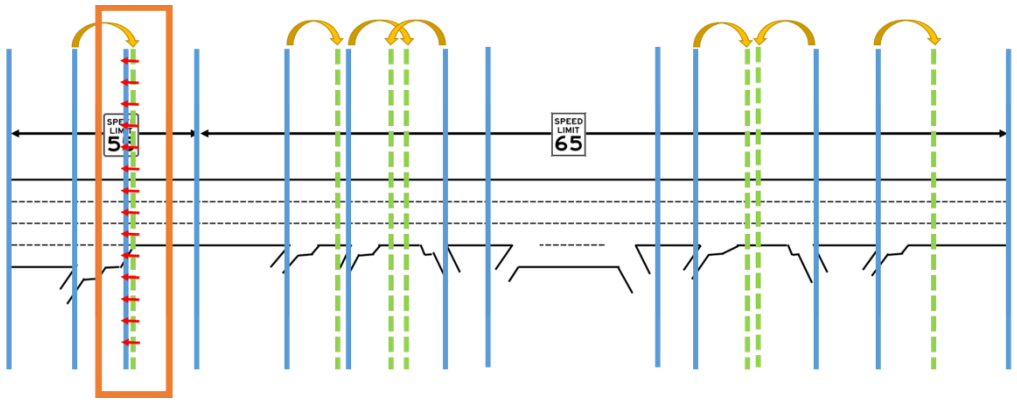

Figure 11: Any influence area that passes a permanent segment boundary should be reduced to match the existing boundary

Step 8: For each new potential boundary, check to see if the 1500ft influence area creates a short (less than the minimum segment length threshold) segment with an adjacent permanent segment boundary. If this occurs, increase the 1500ft threshold to match the adjacent segment boundary.

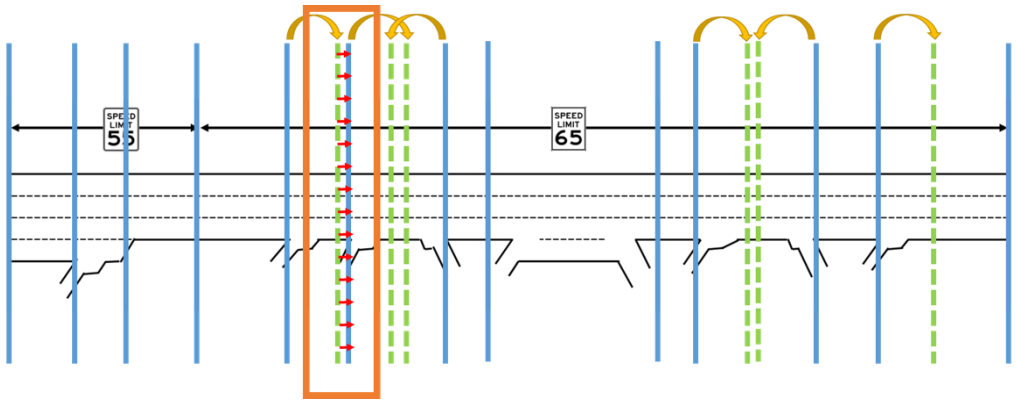

Figure 12: When a small segment will be created between a candidate and permanent segment boundary, the influence area should be increased to match the existing segment boundary

Step 9: For each new potential boundary, check to see if the 1500ft influence areas extending from each pair of adjacent on and off-ramp segment boundaries (with NO auxiliary lane) overlap. If the overlap area is larger than the minimum segment length threshold, mark the candidates as segment boundaries, with the newly created segment being an overlap (R) segment (the resulting layout will be ONR-R-OFR). If the overlap area is smaller than the threshold, select the middle point between the two candidate boundaries as the permanent segment boundary.

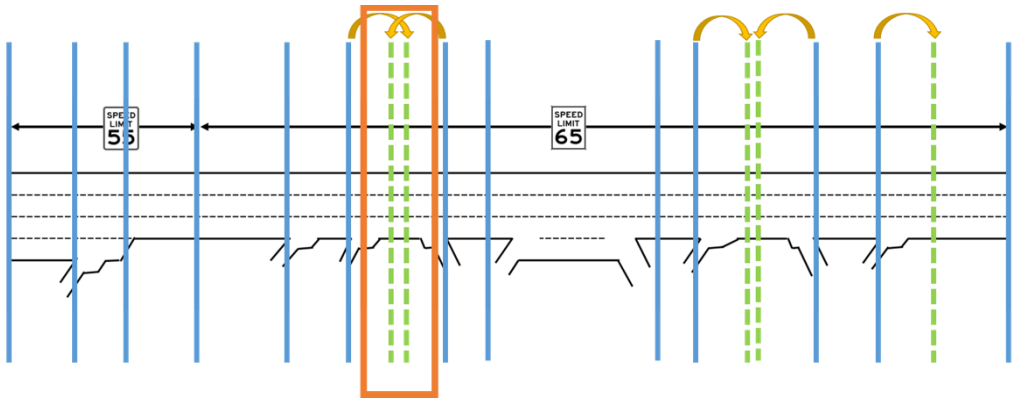

Figure 13: If influence areas between two adjacent ramps overlap, but the segment is not a weave configuration, the candidate boundaries are made permanent, and an overlap (R) segment is created

Step 10: Check to see if any pair of adjacent candidate segment boundaries will create a segment shorter than the minimum length threshold. If an instance is found, merge the two candidates into a single permanent segment boundary placed at the middle point between the two former candidate locations.

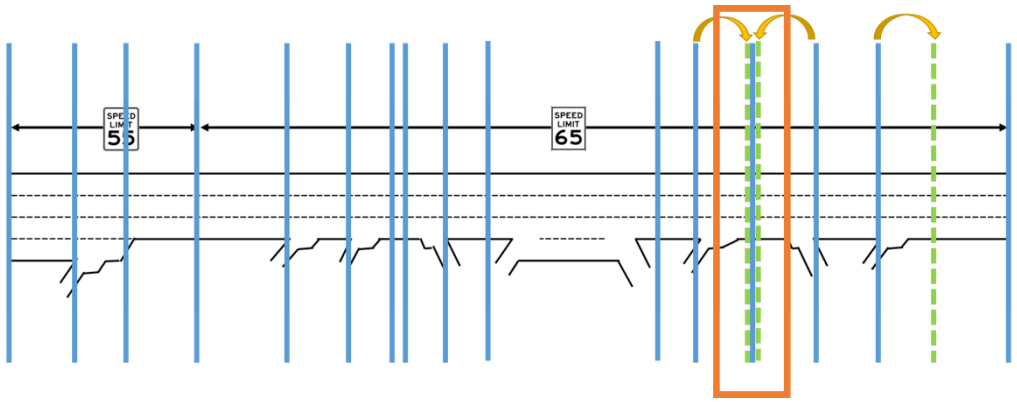

Figure 14: If influence areas of adjacent ramps do not overlap, but the candidate boundaries create a small segment, the middle point between the two becomes a permanent segment boundary

Step 11: Mark any remaining candidate segment boundaries as permanent segment boundaries.

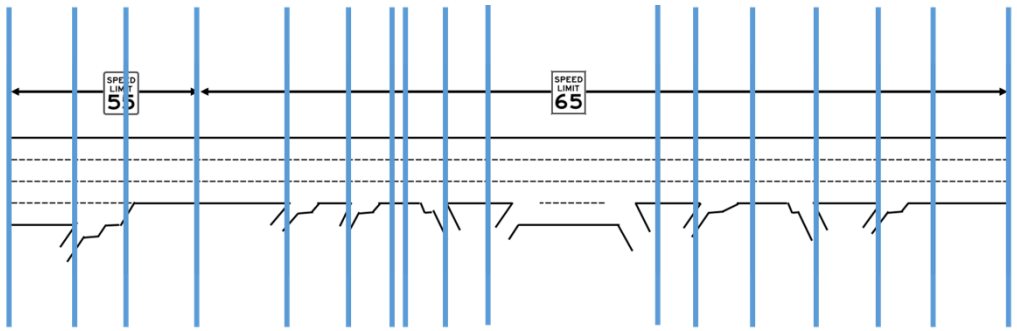

Figure 15: All remaining candidate segments should be valid and can be marked as permanent segment boundaries

Step 12: Mark any segment that has not already been marked as merge, diverge, weave or overlap as a basic segment.

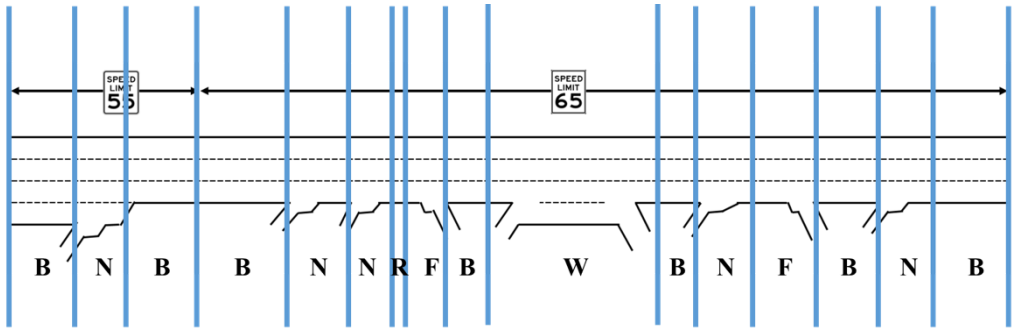

Figure 16: Fully segmented example facility with each segment marked by type (B-Basic, N-On-ramp, F-Off-ramp, W-Weave, R-Overlap)

2.4 IMPLEMENTATION INTO FREEVAL

The autosegmentation procedure as described in the previous sections has been implemented into the FREEVAL computational engine for this project. The procedure is integrated into the program with a new interface utilizing the Google Maps Javascript API. The interface displays a set of Google Maps tiles in order to allow analysts to visually mark gore points for the facility being modeled. This provides a much easier method for creating a facility.

An analyst begins by first placing a marker at the start of the facility. Next, the analyst proceeds to mark all gore points for geometric changes, on-ramps, and off-ramps. Lastly, the analyst places a marker indicating the end of the facility.

As markers are placed on the map, a table is created at the top of the interface. The table includes alternating columns for "nodes" and "sections," which correspond to gore points and the links between them, respectively. The Google Maps API allows for the route along the freeway between each pair of adjacent gore points to be automatically calculated and drawn, and the length of the routed path of each section is given in the table. The interface allows each routed section of the facility to be split into two, creating an additional gore point, or any two adjacent sections can be merged by removing the gore point connecting them. Any gore point placed on the map can be repositioned if necessary by simply dragging and dropping the map marker.

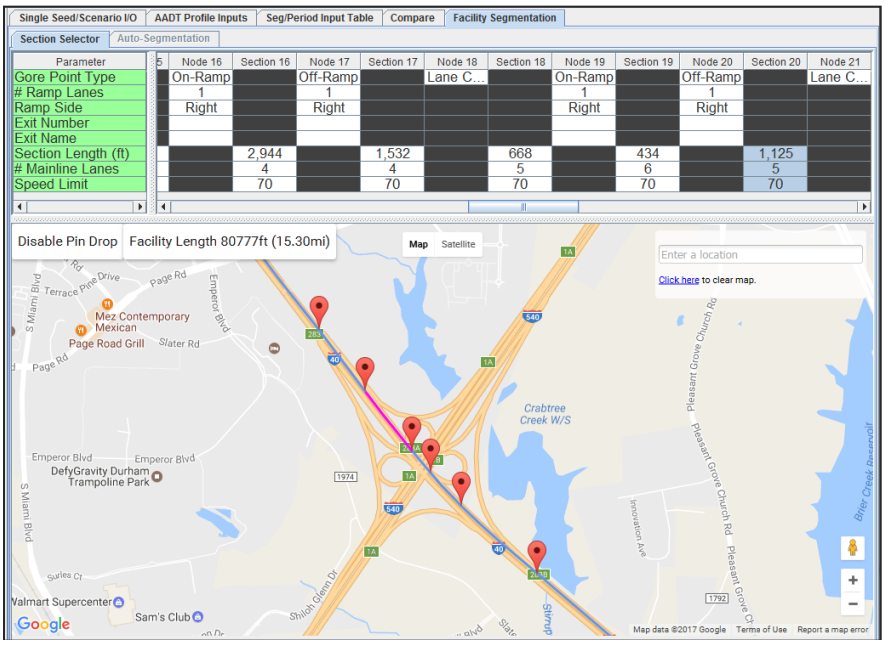

Figure 17: New FREEVAL interface allowing for visual placement of gore points along a facility using Google Maps

The table also allows the analyst to fill in key geometric and capacity parameters required by the segmentation procedure. The principal required value is the number of mainline lanes for each section (from which the procedure identifies auxiliary lanes and weave segments), but an analyst can also enter values for the speed limit, the number of ramp lanes, the exit number, and a name label for each node. These parameters will be carried through the segmentation process and automatically populated into the facility inputs once the segmentation procedure is complete.

Analysts can determine these values in a number different of ways. Previously, the values could only be determined using an analyst's existing knowledge of the facility, or by consulting additional outside maps and data sources. This can still be done, but many of the values can now be determined directly in the interface by way of switching to the satellite view of the facility. For example, by visually inspecting the satellite images, an analyst can determine the number of mainline lanes for each section. The satellite images can also be used to determine the location of certain geometric changes, such as lane drops and lane additions.

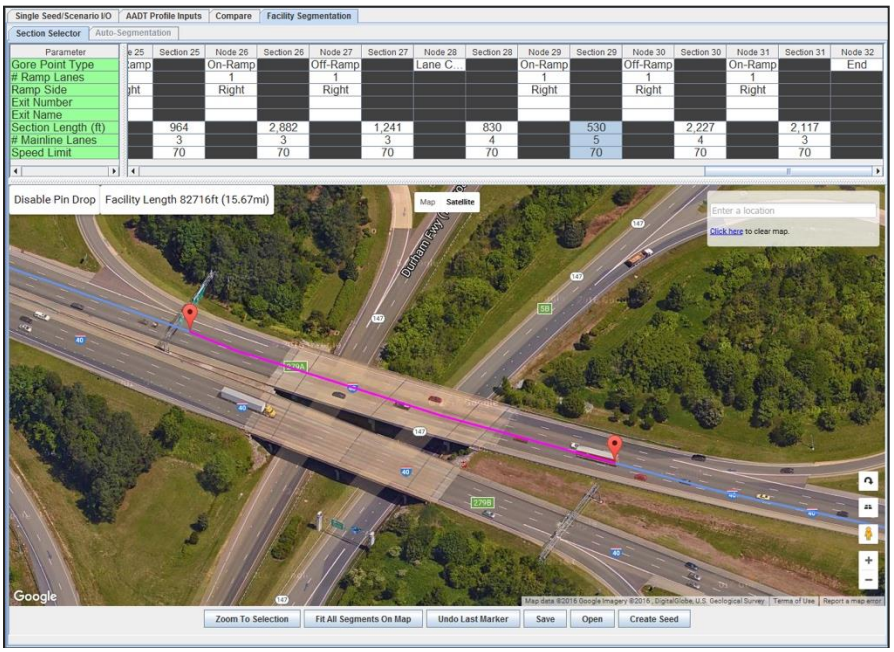

Figure 18: The interface allows an analyst to view satellite images to help determine additional information about the facility

Once all gore points have been marked and the analyst has provided the key input parameters, the autosegmentation described previously is run. At the completion of the procedure, an automated check is run to determine if any issues arose during the segmentation process (e.g. unavoidable short segments). If no issues are found, the analyst is presented with a set of global input parameters that can be adjusted if desired, and the HCM seed file is created.

If the automated check does find one or more segmentation issues, the analyst is presented with a set of options that allow each issue to be addressed individually, or ignored if it is truly unavoidable. It is also possible that issues or improper segmentations can arise due to gore points being placed incorrectly, or incorrect determination of the required inputs (e.g. number of mainline lanes). Consequently, the analyst is also allowed to return to the map and make adjustments as necessary.

3.0 ESTIMATE DEMAND FOR FREEVAL

The freeway facilities methodology of the HCM is tightly built on demand volumes as the main inputs for all freeway segments. These demand volumes are converted into densities and used to estimate flow and congestion. While demand volumes are the critical input for the freeway facilities analysis, they are mostly unknown in real-world situations and hence must be estimated from data provided by a variety of types of sensors (i.e. loop detectors or manual counts). Unfortunately, these sensors can only indicate the actual flow rates, travel times, speeds, observed densities and other measures that are generally considered outputs of the methodology. These types of readings often differ from actual demand volumes, especially at times when a queue is present on the facility, as shown in Figure 19. This puts a challenge on the agencies using the methodology to accurately estimate demand volumes that can produce the desired flow rates in the analysis.

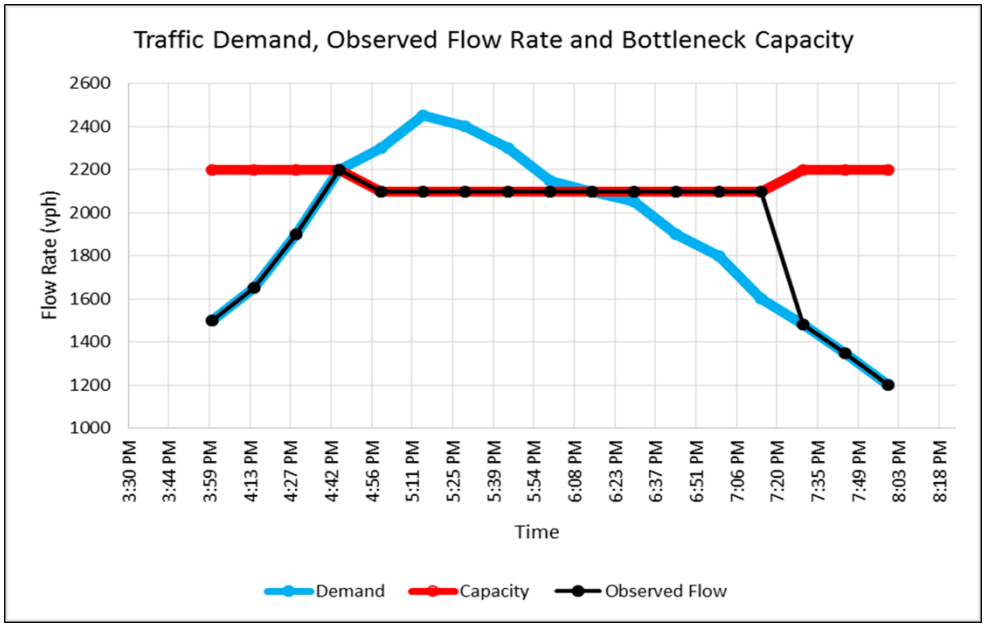

Figure 19: Relationship between demand, observed flow rate, and bottleneck capacity

3.1 PROPOSED FRAMEWORK

A genetic algorithm metaheuristic framework is developed to address the challenges of demand estimation in the context of model calibration. Two encoding approaches for the problem are proposed based on the quality of available data. One approach makes use of existing knowledge of hourly demand profiles, while the second utilizes mixture distributions of random variables in order to allocate demand over the course of a study period when the behavior is unknown. A genetic algorithm is then used to manipulate the individual demand inputs to find a set of overall volumes that minimizes the errors between predicted outputs and a set of target real-world performance measures (e.g., segment speeds).

3.1.1 Profile-Based Encoding

The profile based encoding approach requires that an analyst start with high quality information about both the AADT value for the study period and the shape of the underlying demand profile. This approach is best used when the analyst is confident in his or her projected demand profile, but the performance measures predicted by the methodology do not match observed values. This indicates that the demand volumes are likely close to what they should be, and can be varied within a specified confidence interval to find the optimal distribution of demand. An example of a known demand profile shape with a specified 15% confidence search interval is given in Figure 20.

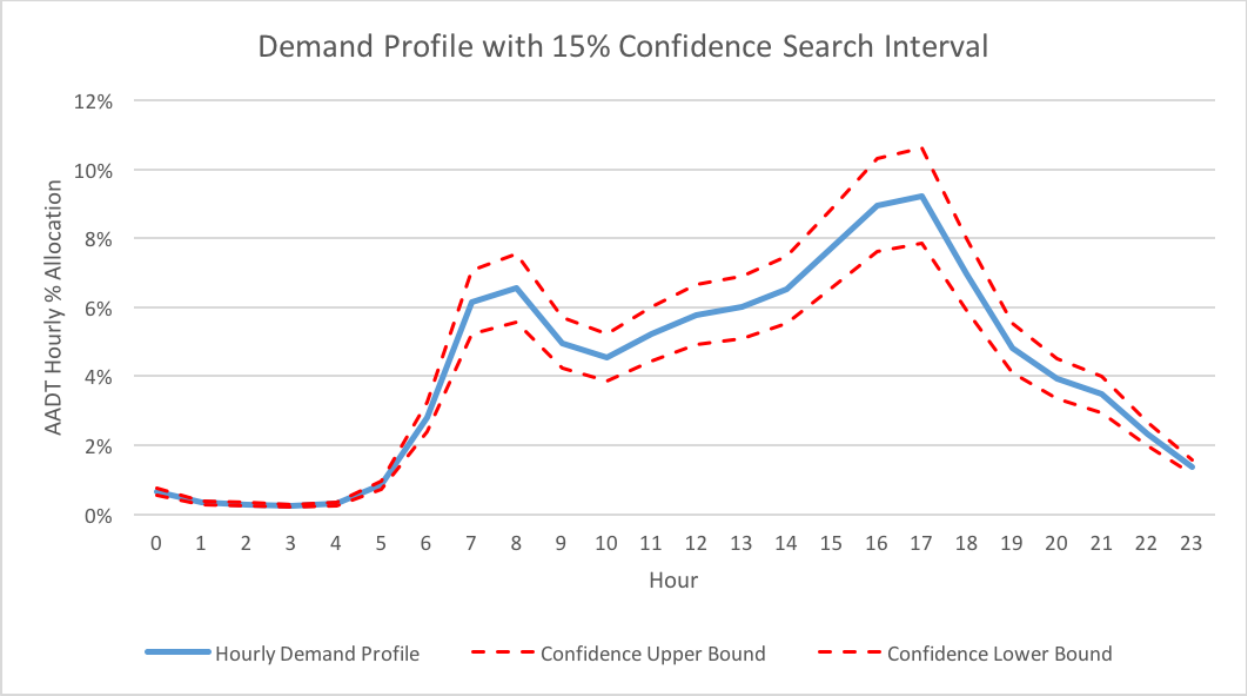

Figure 20: Example of an input demand profile shape with a 15% search interval specified

The HCM freeway facilities methodology includes a set of parameters that can be used to adjust input demand volumes. These values are called Demand Adjustment Factors (DAFs), and exist for every segment where vehicles enter or exit the facility. A DAF for a segment is applied as a multiplier to any existing entering or exiting demand volume input for each analysis period. DAFs provide a straightforward mechanism for this modeling approach as a confidence interval can easily be represented by restricting the value of each DAF to being within a specified range. For example, a confidence interval of 15% would limit the DAF values to the range [0.85,1.15]. In general, a confidence percent of α is represented by a DAF interval of $[1-\alpha, 1+\alpha]$.

For this encoding, each DAF is represented as a binary string of fixed length *n*. By discretizing the given confidence interval with a step size of 1/(2^n), the integer value corresponding to this string can then be projected into the interval to compute the corresponding real-valued DAF. To demonstrate, if the search space is the interval [0.85, 1.15], and an 8-digit binary encoding is used, the discretized step size is 1/(2^8) = 0.00117. If a gene is expressed by the binary string "00001111", it is converted to base 10 as an integer value of 31, and the resulting DAF is 0.85 +

(31*0.00117) = 0.97. Further, the resolution of the search space can easily be adjusted by simply increasing or decreasing the number of binary digits considered.

3.1.2 Mixture Distribution Encoding

While an analyst often has access to reliable information regarding the magnitude and daily behavior of demand for their facility and study period, there are still many cases where such information is unavailable. This renders use of the approach of the previous section largely flawed, as the process is entirely dependent on the initial guess for the shape of the profile. To circumvent this shortcoming, this work developed a demand estimation encoding that can be used to build viable profiles from little or no information. The approach centers on a key assumption: the daily distribution of traffic demand can be represented by the weighted combination of *n* continuous random variable distributions. The density function of the resulting mixture distribution can then be paired with an AADT value to generate a demand profile for the study period. The probability distribution function (PDF) of a mixture distribution is represented by Equation 1.

$$p(x) = \sum_{i=1}^{n} w_i p_i(x), \text{ where } \sum_{i=1}^{n} w_i = 1 \quad (1)$$

In general, a mixture distribution is defined as being the weighted combination of *n* independent probability distributions. Each distribution is assigned a weight w_i, with all weights summing to a value of 1. The probability density function of such a distribution is defined as the weighted sum of the PDFs of each individual distribution, as shown in Equation 1. For the purposes of this work, it is assumed that all random variables making up the mixture distribution have continuous PDFs, which implies that the PDF of Equation 1 is also continuous.

A mixture distribution gives the representation near unlimited flexibility in the shape of the resulting PDF and corresponding demand profile. To reduce the search space to a reasonable size as well as improve convergence, assumptions can be made about the number of distributions *n*, as well as the type of each. In keeping with the intuitive example mentioned above, *n* is always assumed to take on a value of 3 for this research. Further, the type of the individual distributions is limited to either being a skew-normal or a skew-Cauchy distribution. Figures Figure 21 and Figure 22 shows examples of the variety of shapes afforded by these two distributions. However, if for a specific facility these assumptions do not provide acceptable results, both can be altered or relaxed back to their generalized state.

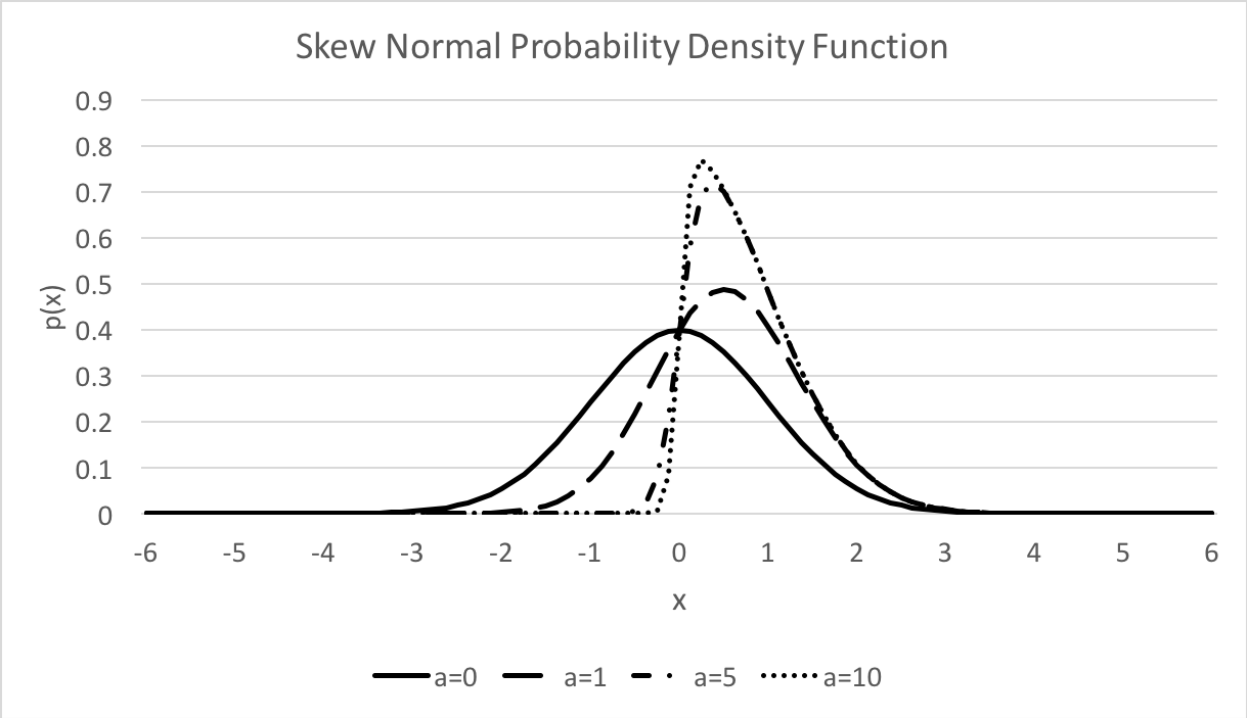

Figure 21: The skew normal distribution with varying values for the skewness parameter

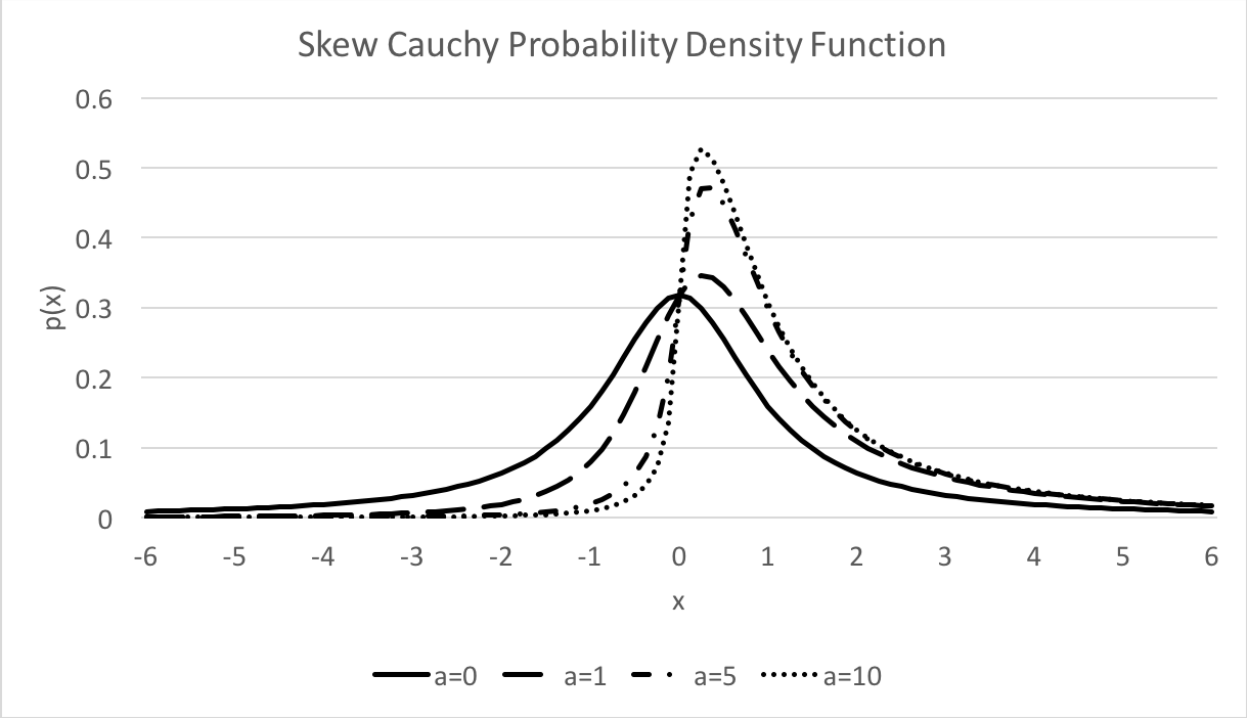

Figure 22: The skew Cauchy distribution with varying values for the skewness parameter

With these assumptions, each of the three distributions has five parameters that become the decision variables in the GA search process. For random variable i of the mixture distribution, these five values are the type Ti, the mixture weight wi, the mean μi, the standard deviation σi, and the skewness ai. The mean μi serves as a location parameter that will anchor distributions around key time intervals such as an AM or PM peak in demand. The shape of each distribution will largely be defined by σi and ai, which will control the steepness of drop-off and amount of probability density located on either side of the mean. The GA can then manipulate these values until they generate demand profile shapes resulting in predicted performance measures matching observed values. Table 1 summarizes these parameters and their functions.

Table 1: Summary of the five parameters of each distribution

Parameter	Description
T_i	Type of the random variable *i.*
w_i	Weight of the random variable *i* in the mixture distribution
μ_i	Mean of the random variable *i.*
σ_i	Standard deviation of the random variable *i.*
a_i	Skewness of the random variable *i.*

If each parameter is represented as a fixed length binary string, then the profile can be represented as one long string formed from a concatenation of the individual values. Since the type T_i of each distribution is limited to being one of two types, it can be represented by a single binary digit. The other four parameters of each distribution can make use of the simple projection method detailed in the previous section. All that is required is that a range of values be specified for each parameter, which can be discretized accordingly with the maximum integer value allowed by the binary encoding.

Reasonable ranges for each of the remaining four parameters can easily be obtained. The weights w_i can be specified to sum to a value of 1, or can be allowed to vary more generally so long as the resulting distribution is normalized before it is used. Each location parameter μ_i must fall somewhere in the 24-hour period, and in many cases, such as for a workday, more specific ranges for AM or PM peak locations can be provided. Using the area covered by normal and Cauchy distributions, a 24-hour study period can be converted to a corresponding range of -6 to 6 for the domain of the mixture distribution PDF. Consequently, a simple linear function $y=0.5x-6$ can be used to project an hour value x into the range as y. For example, if an analyst knows that a morning peak occurs around 8am one of the location parameters μ_i could be limited to a range around a projected value of 0.5*8-6=-2.

Table 2: Distribution parameter ranges

Parameter	Min Value	Max Value	Number Binary Digits	Resulting Step Size
T_i	0	1	1	1
w_i	0	0.5	4	0.3
μ_i	-5	5	4	0.66
σ_i	0.5	5	4	0.3
a_i	-10	10	4	1.33

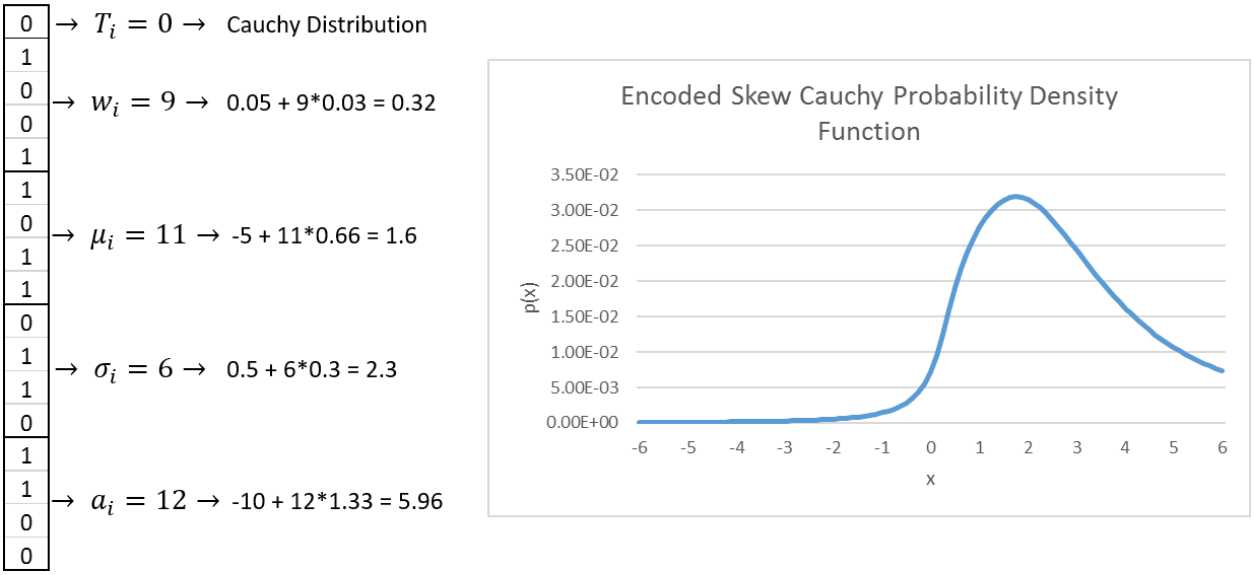

Figure 23: String to random probability density function conversion

Table 2 and Figure 23 demonstrate the process of encoding the five decision parameters for a single random variable into binary string. Table 2 outlines the ranges for the five parameters, and computes the step size based on the number of binary digits of the encoding. Figure 23 explicitly demonstrates the relationship between the binary representation and the values that shape the probability distribution function. Building on this process, Table 3 and Figure 24 show how three random variables are combined to create a mixture distribution representing the demand profile for a study period.

Table 3: Parameters for each of the three random variables of the example mixture distribution

Parameter	Value	Binary
T_1	Normal	1
w_1	0.2	0101
μ_1	-2.33	0100
σ_1	1.7	0100
a_1	-2.02	0110
T_2	Cauchy	0
w_2	0.32	1001
μ_2	-0.33	0111
σ_2	1.0	0111
a_2	1.0	1000
T_3	Cauchy	0
w_3	0.32	1001
μ_3	1.6	1011
σ_3	2.3	0110
a_3	5.96	1100

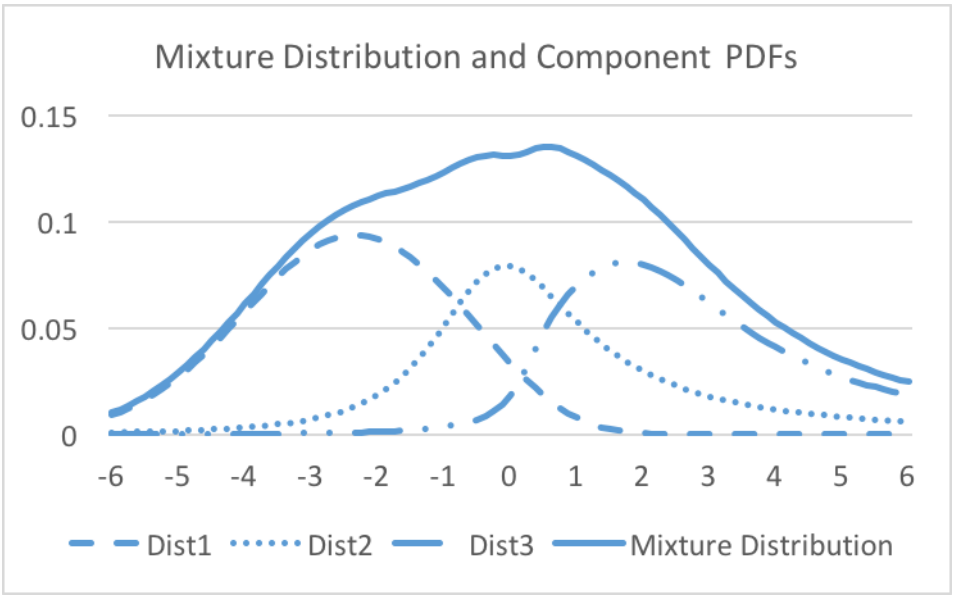

Figure 24: Probability density functions of the full mixture distribution and the component random variables

3.2 COMPUTATIONAL STUDIES AND RESULTS

The encodings of the previous sections were implemented into a genetic algorithm framework built in the Java programming language. The GA framework was built alongside the FREEVAL core computational engine, and integrated into the user interface. The following sections present two computational experiments. The first presents a simple example in which the "ground truth" demand is known. The second presents a case study conducted on a real world stretch of freeway outside of Raleigh, North Carolina in which only limited information is known.

3.2.1 Simple Computational Example

This section tests the ability of the GA to calibrate the methodology for a simple example where the underlying demand is known. This assumption of known ``ground truth" provides an opportunity to analyze how the framework performs in a best case scenario, as opposed to jumping directly to a real-world case study where a lack of ground truth can make it difficult to draw conclusions about its effectiveness. For this example, there is an assumption that the values for free flow speed and capacity are known. Both the profile-based and the n-distribution encodings are tested and compared based on their ability to match predicted facility performance measures to a set of target speeds.

For this case study, a basic facility was designed to be analyzed over a 24-hour study period. The geometry of the test facility is shown in Figure 25. The facility consists of 27 half-mile segments, with a lane-drop in the 26th segment designed to create a flow bottleneck. The facility has a free flow speed of 65 mph, and the HCM default values for capacity are used for each segment. The facility is assigned an unidirectional AADT value of 69,000 at the upstream mainline entrance, which is allocated to the study period according to the 25th percentile bimodal AM peak demand profile shown in Figure 26. The left half of Figure 27 shows the resulting speed contour obtained from the HCM freeway facilities analysis. The contour clearly shows two

congestion areas, with the larger of the two occurring during the morning peak hours. This set of speeds serves as the target data set that the GA framework will be attempt to match.

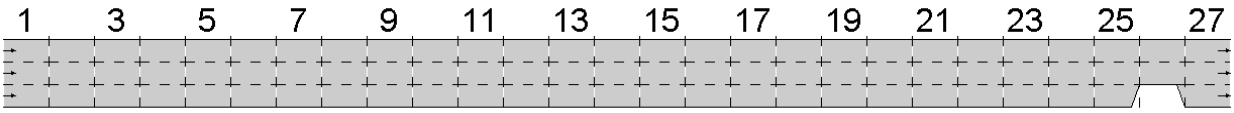

Figure 25: Geometry of the example facility. The bottleneck resulting from the lane drop in segment 26 creates two congestion regimes over the study period.

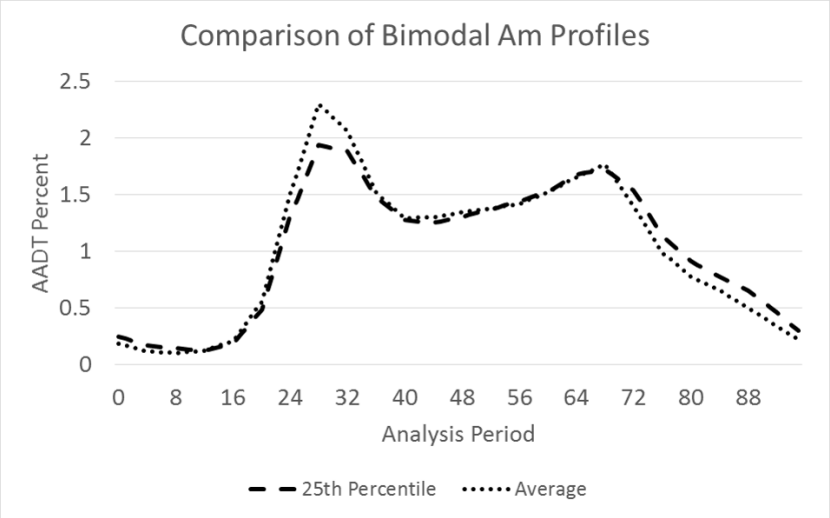

Figure 26: Bimodal-AM Peak 25th Percentile demand profile used to allocate the AADT over the study period

As previously noted, there is an assumption that values for all inputs other than the demand allocation are known a priori to the analyst. For testing the calibration methodology, the GA will be responsible for allocating the demands according to each of the two encoding approaches. Setting the example up in this way allows for analysis to be conducted where the target performance measures are guaranteed to be achievable with the methodology. Additionally, the demand profile estimated by the GA framework can be compared to its underlying ground truth - something that is generally impossible when analyzing real-world facilities.

The following two sections present the results of the using the GA framework to calibrate the facility using both the profile-based and the n-distribution encoding. First, profile-based approach is tested in the context where the analyst has a similar but incorrect demand allocation profile as a starting point. Next, a 3-distribution encoding is used where it is assumed that the analyst only knows the AADT and some basic information about the locations of congestion peaks.

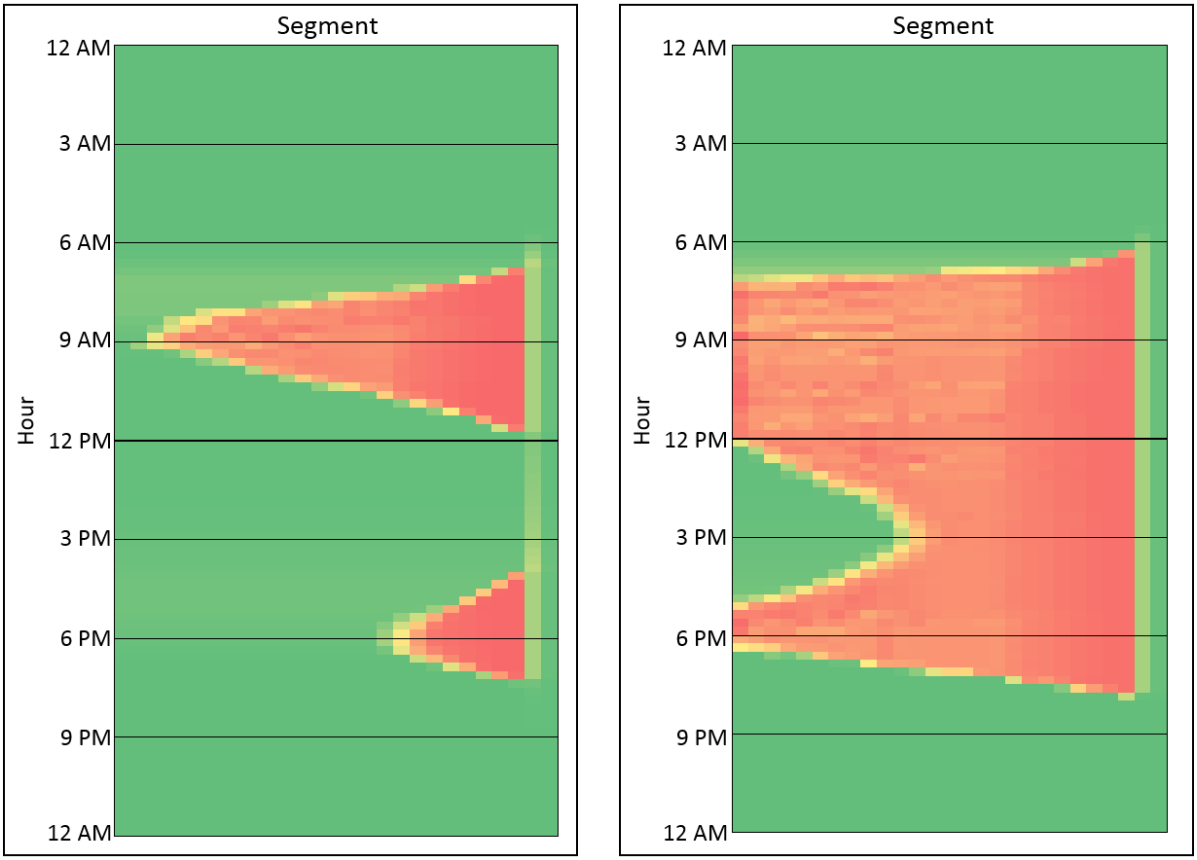

Figure 27: Left: Speed contour obtained after performing the HCM analysis that is used as the target data set for calibration

3.2.1.1 Results Using the Profile-Based Encoding

The first scenario assumes that the analyst starts with the average bimodal AM peak demand profile. A comparison of the 25th percentile and average profile is shown in Figure 26. Additionally, a unidirectional AADT value of 80,000 is initially used to allocate demands volumes to the 15-minute analysis period intervals. The resulting speed contour predicted by the analysis is shown on the right in Figure 27. This contour reveals a much larger congestion regime compared to the target speeds (shown on the left), including problematic spillover beyond the boundary of the analysis. A set of metrics is given in

Table 5 concerning the "fitness" of this initial starting point. These show that on average there is nearly a 15 mph difference between the uncalibrated and target speeds, with some uncalibrated speeds being more than 55 mph off.

The profile-based encoding approach is used to calibrate the demand profile of the facility under this scenario. A confidence interval of 15\% is specified to create the search space for the algorithm. A summary of the additional parameters for the experiment and the GA setup is given in Table 4, and the results of five GA runs are shown in Table 5. These results show that the GA was very successful in calibrating the facility. On average, the overall error in speeds is reduced by 97\%, which translates to an average error of just 0.4 mph per segment per time period. While some large individual errors still exist, an average 90th percentile error of 0.78 mph shows the GA

is able to closely match the speeds for the vast majority of the segments and time periods. Figure 28 shows a contour highlighting the remaining differences in predicted speeds, where red cells indicate larger errors.

Table 4: Summary of the setup parameters for the GA runs

Experiment Parameter	Value
Number of Runs	5
Profile Confidence Interval	15%
Population Size	200
Max Iterations	400
Crossover Mixing %	50%
Mutation Rate (%)	2%

Table 5: Summary of the calibration results for the profile-based encoding runs

Metric	Uncalibrated	GA Average
Total Speed Difference (mph)	38,647.61	1040.41
Average Speed Difference (mph)	14.9	0.4
90th Percentile Speed Difference (mph)	49.96	0.78
Max Speed Difference (mph)	57.04	26.05
GA Run Time (minutes)	-	22

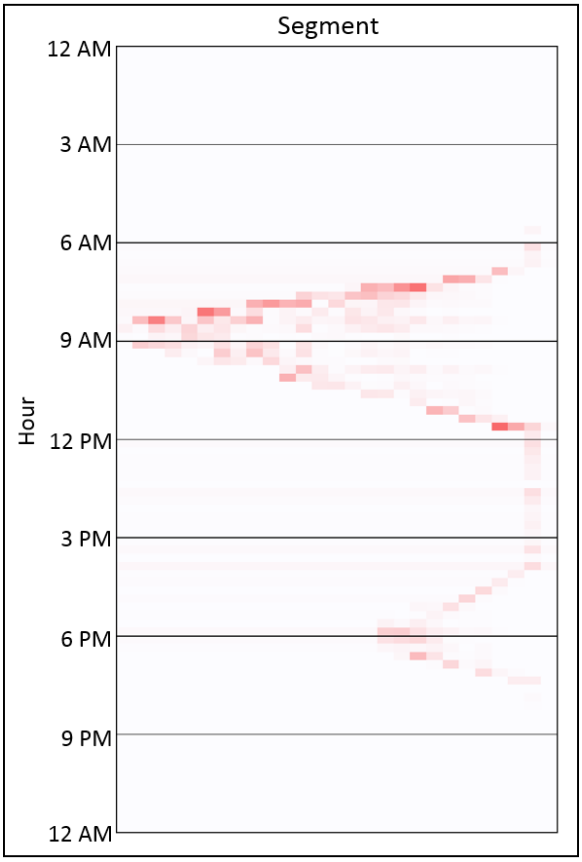

Figure 28: Comparison of the target speeds and the predicted speeds after calibration

Since this example is designed with the explicit goal of being able to compare estimated demands with known ground truth demands, a deeper look can be taken at the underlying profiles generated by the GA framework. However, unlike most other result metrics, multiple demand profiles cannot be averaged into a single profile to gauge the effectiveness. As such, both profiles corresponding to the best and the worst of the GA runs are shown in Figure 29. Each profile plot shows the initial profile guess, the actual underlying profile, and the profile estimated by the GA. While there is some noise within the generated profiles, it is clear that the GA consistently estimated a shape much closer to that of the true profile. The improvement is especially apparent during the AM peak where there is a near perfect reduction from the base profile to the true shape. Much of the error that exists occurs when the methodology is in the undersaturated regime, where speeds do not reflect the underlying demands in a one-to-one way, and additional target data (e.g. observed throughput or volumes) would be required for further accuracy.

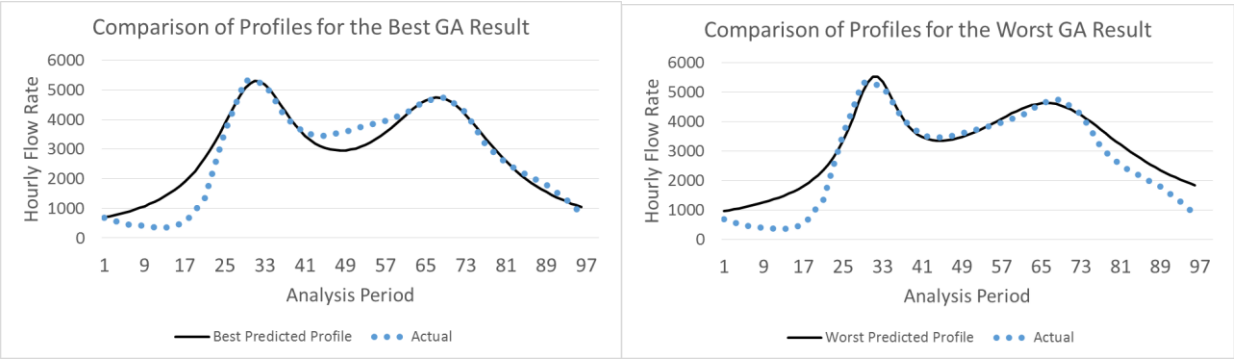

Figure 29: Comparison of profiles generated by the best and the worst of the GA calibration runs, the "ground truth" profile is represented by the dotted line, while the predicted profile is given by the solid line

3.2.2 I-540 Case Study

While the theoretical example of the previous section shows that the GA methodology can accurately calibrate the demands for a facility using a set of target speeds, it is also important to show that the approach is effective for real-world facilities. To accomplish this, a real-world case study was developed based on a stretch of urban freeway on I-540 outside of Raleigh, NC. The 14.5-mile-long facility includes seven on-ramps and eight off-ramps, yielding a total of 16 (including the mainline) demand entry and exit points needing to be estimated or calibrated. The geometry of the case study facility is given in Figure 30. The facility consists largely of three lane segments, and the free flow speed is thought to be 75 mph. The target data speed contour, shown in Figure 31 , was determined for a five-and-a-half-hour study period from 6:00am to 11:30am on Tuesday, August 19th, 2014 (data collected from RITIS.org), and AADT information was gathered from the state department of transportation (NCDOT).

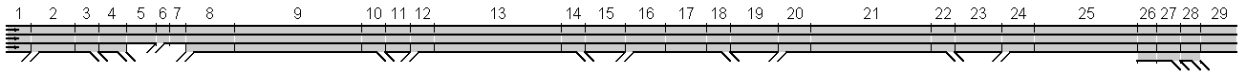

Figure 30: Geometry of the I-540 westbound case study facility

	Segment																												
Analysis Period	1	2	3	4	5	6	7	8	9	10	11	12	13	14	15	16	17	18	19	20	21	22	23	24	25	26	27	28	29
#1 6:00 - 6:15	65.4	72.6	72.6	72.6	73.0	73.0	73.0	73.0	73.0	73.0	73.4	74.1	74.1	74.1	73.6	73.7	73.7	73.7	72.4	70.5	70.5	70.5	71.8	71.1	71.1	71.1	71.1	72.8	72.8
#2 6:15 - 6:30	68.9	70.4	70.4	70.4	72.5	72.5	72.5	72.1	72.1	72.1	73.3	73.9	73.9	73.9	74.0	74.3	74.3	74.3	74.1	73.4	73.4	73.4	74.5	74.5	74.5	74.5	74.5	72.7	72.7
#3 6:30 - 6:45	73.2	70.8	70.8	70.8	71.1	71.1	71.1	71.5	71.5	71.5	73.1	72.5	72.5	72.5	73.5	73.1	73.1	73.1	72.5	72.0	72.0	72.0	71.7	73.7	73.7	73.7	73.7	72.9	72.9
#4 6:45 - 7:00	72.5	72.6	72.6	72.6	71.3	71.3	71.3	71.6	71.6	71.6	70.8	71.0	71.0	71.0	72.4	71.7	71.7	71.7	71.7	70.8	70.8	70.8	72.0	72.9	72.9	72.9	72.9	73.5	73.5
#5 7:00 - 7:15	73.7	70.3	70.3	70.3	70.7	70.7	70.7	71.9	71.9	71.9	73.3	71.9	71.9	71.9	72.5	72.5	72.5	72.5	72.5	70.8	70.8	70.8	71.7	72.1	72.1	72.1	72.1	73.7	73.7
#6 7:15 - 7:30	68.6	67.6	67.6	67.6	68.4	68.4	68.4	68.4	68.4	68.4	67.4	67.3	67.3	67.3	69.4	68.3	68.3	68.3	69.8	69.1	69.1	69.1	71.7	72.1	72.1	72.1	72.1	71.7	71.7
#7 7:30 - 7:45	67.9	64.7	64.7	64.7	68.6	68.6	68.6	60.9	60.9	60.9	46.5	48.8	48.8	48.8	63.9	62.8	62.8	62.8	59.0	59.1	59.1	59.1	66.4	70.1	70.1	70.1	70.1	70.9	70.9
#8 7:45 - 8:00	71.3	68.7	68.7	68.7	67.8	67.8	67.8	53.9	53.9	53.9	31.5	38.7	38.7	38.7	45.3	46.4	46.4	46.4	36.0	53.9	53.9	53.9	64.8	68.5	68.5	68.5	68.5	68.5	68.5
#9 8:00 - 8:15	71.3	68.1	68.1	68.1	67.1	67.1	67.1	56.1	56.1	56.1	36.8	41.0	41.0	41.0	36.9	43.9	43.9	43.9	44.2	55.1	55.1	55.1	62.3	67.6	67.6	67.6	67.6	70.2	70.2
#10 8:15 - 8:30	72.7	68.7	68.7	68.7	67.5	67.5	67.5	67.3	67.3	67.3	55.9	43.0	43.0	43.0	35.8	43.8	43.8	43.8	42.2	56.9	56.9	56.9	64.6	69.1	69.1	69.1	69.1	71.1	71.1
#11 8:30 - 8:45	70.3	70.8	70.8	70.8	73.0	73.0	73.0	70.5	70.5	70.5	64.3	59.0	59.0	59.0	57.7	54.9	54.9	54.9	46.7	57.0	57.0	57.0	63.8	69.5	69.5	69.5	69.5	70.2	70.2
#12 8:45 - 9:00	71.8	70.9	70.9	70.9	71.1	71.1	71.1	70.1	70.1	70.1	70.3	70.0	70.0	70.0	63.4	54.9	54.9	54.9	57.8	62.4	62.4	62.4	65.7	68.1	68.1	68.1	68.1	70.0	70.0
#13 9:00 - 9:15	73.3	70.9	70.9	70.9	69.7	69.7	69.7	70.3	70.3	70.3	72.9	72.9	72.9	72.9	72.6	73.0	73.0	73.0	73.1	71.2	71.2	71.2	72.5	72.2	72.2	72.2	72.2	73.2	73.2
#14 9:15 - 9:30	73.8	69.8	69.8	69.8	71.3	71.3	71.3	73.6	73.6	73.6	73.3	72.6	72.6	72.6	72.5	73.0	73.0	73.0	72.6	72.3	72.3	72.3	74.4	73.3	73.3	73.3	73.3	73.9	73.9
#15 9:30 - 9:45	70.1	68.5	68.5	68.5	68.3	68.3	68.3	69.8	69.8	69.8	71.4	72.7	72.7	72.7	73.1	73.4	73.4	73.4	73.9	71.7	71.7	71.7	72.1	72.2	72.2	72.2	72.2	73.0	73.0
#16 9:45 - 10:00	67.2	68.7	68.7	68.7	68.2	68.2	68.2	68.1	68.1	68.1	68.9	70.1	70.1	70.1	71.0	71.1	71.1	71.1	71.1	70.5	70.5	70.5	71.9	71.3	71.3	71.3	71.3	72.9	72.9
#17 10:00 - 10:15	69.8	69.1	69.1	69.1	67.4	67.4	67.4	67.7	67.7	67.7	68.1	69.7	69.7	69.7	69.0	70.7	70.7	70.7	71.4	70.7	70.7	70.7	72.7	72.3	72.3	72.3	72.3	72.6	72.6
#18 10:15 - 10:30	72.5	66.9	66.9	66.9	69.1	69.1	69.1	72.7	72.7	72.7	74.4	74.0	74.0	74.0	72.9	72.1	72.1	72.1	72.3	71.1	71.1	71.1	73.5	74.2	74.2	74.2	74.2	73.9	73.9
#19 10:30 - 10:45	69.9	69.8	69.8	69.8	70.9	70.9	70.9	70.5	70.5	70.5	70.7	71.4	71.4	71.4	71.1	71.6	71.6	71.6	73.7	73.3	73.3	73.3	73.3	73.6	73.6	73.6	73.6	73.5	73.5
#20 10:45 - 11:00	69.0	67.0	67.0	67.0	68.0	68.0	68.0	68.3	68.3	68.3	69.4	69.7	69.7	69.7	69.6	70.5	70.5	70.5	71.4	70.8	70.8	70.8	71.5	71.8	71.8	71.8	71.8	73.1	73.1
#21 11:00 - 11:15	68.7	70.4	70.4	70.4	67.8	67.8	67.8	68.0	68.0	68.0	69.5	70.3	70.3	70.3	70.5	73.5	73.5	73.5	74.1	72.0	72.0	72.0	71.1	71.5	71.5	71.5	71.5	72.5	72.5
#22 11:15 - 11:30	68.0	70.3	70.3	70.3	67.7	67.7	67.7	70.4	70.4	70.4	68.1	70.2	70.2	70.2	73.2	73.5	73.5	73.5	72.9	72.2	72.2	72.2	71.4	72.4	72.4	72.4	72.4	72.7	72.7

Figure 31: Observed speed contour for the study period used as the target data set for the case study example

The target speed contour shows low speeds indicating congestion around what are considered to be the AM peak travel hours. Based on this observation, an initial population of the demand inputs can be done by allocating the mainline and ramp AADTs using the average Bimodal with AM Peak demand profile. Figure 32 shows the resulting speed contour, which unfortunately differs greatly from the target speeds. In fact, there is a total speed error of 3,901 mph for the study period, which translates to an average error of 6.11 mph per segment and time period.

	Segment																												
Analysis Period	1	2	3	4	5	6	7	8	9	10	11	12	13	14	15	16	17	18	19	20	21	22	23	24	25	26	27	28	29
#1 6:00 - 6:15	75.0	71.0	69.4	74.6	71.9	63.3	70.9	71.0	73.5	68.8	74.3	66.9	72.0	69.4	73.5	69.1	71.6	68.5	73.2	67.7	71.7	68.6	73.1	67.9	71.5	74.7	70.4	74.5	74.4
#2 6:15 - 6:30	74.6	70.4	69.3	73.7	69.1	61.6	67.6	70.2	71.6	68.6	73.1	65.6	69.2	68.9	71.6	67.7	68.5	68.3	71.1	66.6	68.7	68.5	71.0	66.7	68.4	73.8	70.0	74.5	73.3
#3 6:30 - 6:45	73.9	69.8	69.2	72.3	65.4	59.0	63.3	69.0	69.0	68.5	71.3	64.1	65.6	65.6	69.1	64.6	64.6	64.6	68.4	64.8	64.8	64.8	68.2	64.4	64.4	72.4	69.6	74.4	71.6
#4 6:45 - 7:00	72.7	69.0	69.1	70.3	60.8	55.1	57.9	65.7	65.7	65.7	68.9	61.0	61.0	61.0	65.7	59.7	59.7	59.7	64.8	60.0	60.0	60.0	64.5	59.4	59.4	70.5	69.2	73.6	69.3
#5 7:00 - 7:15	71.1	66.4	66.9	29.7	35.9	54.1	56.8	64.3	64.3	64.3	67.8	58.5	58.5	58.5	63.9	56.6	56.6	56.6	62.5	56.7	56.7	56.7	62.0	55.8	55.8	69.0	69.0	72.9	67.5
#6 7:15 - 7:30	71.6	62.5	24.6	18.4	35.1	54.2	56.9	64.6	64.6	64.6	68.0	59.1	59.1	59.1	64.4	57.5	57.5	57.5	63.2	57.6	57.6	57.6	62.7	56.9	56.9	69.4	69.0	73.1	68.1
#7 7:30 - 7:45	66.3	36.3	20.8	18.4	35.3	54.2	56.9	64.9	64.9	64.9	68.2	59.7	59.7	59.7	64.8	58.2	58.2	58.2	63.7	58.4	58.4	58.4	63.3	57.7	57.7	69.8	69.1	73.3	68.5
#8 7:45 - 8:00	61.2	34.4	20.8	18.4	35.5	54.2	56.9	65.1	65.1	65.1	68.4	60.2	60.2	60.2	65.2	58.9	58.9	58.9	64.2	59.2	59.2	59.2	64.0	58.7	58.7	70.2	69.1	73.5	68.9
#9 8:00 - 8:15	67.3	51.7	21.3	18.5	35.6	54.2	56.9	65.3	65.3	65.3	68.6	60.8	60.8	60.8	65.6	59.5	59.5	59.5	64.7	60.0	60.0	60.0	64.5	59.5	59.5	70.5	69.2	73.6	69.3
#10 8:15 - 8:30	73.8	69.3	54.2	26.6	36.4	54.2	56.9	65.9	65.9	65.9	69.0	62.0	62.0	62.0	66.5	61.2	61.2	61.2	65.9	61.8	61.8	61.8	65.9	61.5	61.5	71.3	69.4	74.0	70.3
#11 8:30 - 8:45	74.4	70.2	69.3	73.1	67.3	60.2	65.2	69.6	70.3	68.6	72.2	64.9	67.4	67.4	70.3	66.6	66.6	66.6	69.8	65.8	66.8	66.8	69.6	65.8	66.4	73.1	69.8	74.5	72.5
#12 8:45 - 9:00	74.8	70.6	69.4	74.0	69.8	62.0	68.4	70.4	72.1	68.7	73.4	66.0	69.9	69.1	72.1	68.0	69.3	68.4	71.7	66.9	69.4	68.5	71.6	67.0	69.1	74.0	70.1	74.5	73.6
#13 9:00 - 9:15	75.0	70.9	69.4	74.6	71.7	63.1	70.6	70.9	73.3	68.8	74.2	66.8	71.7	69.4	73.3	68.9	71.3	68.5	73.0	67.6	71.4	68.6	72.9	67.8	71.2	74.6	70.4	74.5	74.3
#14 9:15 - 9:30	75.0	71.1	69.4	74.6	72.4	63.5	71.5	71.1	73.7	68.8	74.5	67.1	72.4	69.5	73.8	69.3	72.0	68.5	73.5	67.9	72.1	68.7	73.4	68.1	71.9	74.8	70.5	74.5	74.6
#15 9:30 - 9:45	75.0	71.2	69.4	74.6	73.0	63.9	72.2	71.3	74.1	68.8	74.5	67.3	73.0	69.6	74.1	69.6	72.7	68.6	73.9	68.2	72.7	68.7	73.8	68.4	72.6	74.9	70.6	74.5	74.7
#16 9:45 - 10:00	75.0	71.3	69.4	74.6	73.5	64.2	72.6	71.5	74.4	68.8	74.5	67.6	73.5	69.8	74.4	69.8	73.2	68.6	74.2	68.4	73.3	68.8	74.2	68.6	73.2	75.0	70.7	74.5	74.9
#17 10:00 - 10:15	75.0	71.5	69.4	74.6	73.9	64.4	72.7	71.6	74.6	68.9	74.5	67.8	74.0	69.9	74.6	70.1	73.7	68.7	74.5	68.6	73.8	68.8	74.5	68.9	73.7	75.0	70.8	74.6	75.0
#18 10:15 - 10:30	75.0	71.5	69.4	74.6	73.9	64.4	72.7	71.6	74.6	68.9	74.5	67.8	73.9	69.9	74.6	70.1	73.7	68.7	74.5	68.6	73.8	68.8	74.5	68.8	73.7	75.0	70.8	74.6	75.0
#19 10:30 - 10:45	75.0	71.5	69.4	74.6	73.9	64.4	72.7	71.6	74.6	68.9	74.5	67.8	73.9	69.9	74.6	70.1	73.7	68.7	74.5	68.6	73.7	68.8	74.5	68.8	73.7	75.0	70.8	74.6	75.0
#20 10:45 - 11:00	75.0	71.5	69.4	74.6	73.9	64.4	72.7	71.6	74.6	68.9	74.5	67.8	73.9	69.9	74.6	70.1	73.7	68.7	74.5	68.6	73.7	68.8	74.5	68.8	73.6	75.0	70.8	74.6	75.0
#21 11:00 - 11:15	75.0	71.4	69.4	74.6	73.8	64.4	72.7	71.6	74.6	68.9	74.5	67.8	73.9	69.9	74.6	70.1	73.7	68.7	74.5	68.6	73.7	68.8	74.5	68.8	73.6	75.0	70.8	74.6	75.0
#22 11:15 - 11:30	75.0	71.4	69.4	74.6	73.8	64.4	72.7	71.6	74.6	68.9	74.5	67.7	73.8	69.8	74.6	70.0	73.6	68.6	74.4	68.6	73.6	68.8	74.4	68.8	73.5	75.0	70.8	74.6	74.9

Figure 32: Uncalibrated speed contour predicted after the initial demand allocation

3.2.2.1 Profile-Based Encoding Results

In order to make use of the profile-based encoding, it is assumed that the AADT values and the average bimodal with AM peak profile are acceptable guesses for the true underlying demands

(which are entirely unknown). Since the speeds of the initial demand allocation differ greatly from the target data, a large confidence bandwidth of 20% is specified to define the search space for the encoding. Five calibrations runs were performed using the GA approach based on the parameters given in Table 6.

Table 6: Summary of the setup parameters for the profile-based GA runs

Experiment Parameter	Value
Number of Runs	5
Profile Confidence Interval	20%
Population Size	200
Max Iterations	400
Crossover Mixing %	50%
Mutation Rate (%)	2%

Table 7 summarizes the results of the five calibration attempts. On average, the GA is able to calibrate the model such that it results in a 48% reduction in total speed error. This corresponds to an average speed difference of around 3 mph for each segment in each time period. Figure 33 shows the speed contour predicted by the best calibration attempt. While there is still a moderate amount of error in the speeds, the contour does show congestion far more consistent with the target data than is seen in the initial guess (see Figure 32).

Table 7: Results summary of the GA Calibration Runs

Metric	Uncalibrated	GA Average
Total Speed Difference (mph)	3901.5	2018.01
Average Speed Difference (mph)	6.12	3.16
90th Percentile Speed Difference (mph)	13.48	6.83
Max Speed Difference (mph)	50.31	32.75
GA Run Time (minutes)	-	4.84

	Segment																												
Analysis Period	1	2	3	4	5	6	7	8	9	10	11	12	13	14	15	16	17	18	19	20	21	22	23	24	25	26	27	28	29
#1 6:00 - 6:15	75.0	71.0	69.4	74.6	71.9	63.2	70.8	70.8	73.2	68.9	74.0	66.8	71.7	69.3	73.3	69.0	71.4	68.7	72.9	67.6	71.3	68.8	72.6	67.8	71.0	74.6	70.7	74.5	74.0
#2 6:15 - 6:30	75.0	71.2	69.3	74.6	73.7	64.2	72.6	71.3	74.1	68.6	74.5	67.3	73.0	69.5	74.3	69.7	72.9	68.1	74.4	68.5	73.5	68.6	74.4	68.7	73.4	75.0	70.6	74.5	75.0
#3 6:30 - 6:45	74.9	70.5	69.2	74.1	71.0	62.7	69.8	70.7	72.9	68.3	74.3	66.7	71.7	69.2	73.5	68.9	71.4	68.4	73.2	67.4	71.0	68.6	72.7	67.4	70.3	74.4	69.8	74.4	74.4
#4 6:45 - 7:00	74.7	70.5	69.3	73.8	71.3	62.7	69.7	70.6	72.6	68.6	73.9	65.6	69.8	68.6	72.8	68.2	70.0	68.2	72.4	67.1	70.1	68.0	72.8	67.5	70.5	74.4	69.8	74.4	74.5
#5 7:00 - 7:15	74.1	69.8	69.1	72.7	68.8	61.1	66.6	69.7	70.6	68.2	72.8	65.2	68.4	68.4	71.8	67.6	68.5	67.5	72.4	66.6	69.4	68.4	71.7	66.6	68.5	73.8	69.5	74.4	73.9
#6 7:15 - 7:30	74.1	69.9	69.1	72.8	68.9	61.3	67.1	69.6	70.5	68.2	72.9	65.2	68.4	68.4	71.9	67.7	68.6	68.1	71.5	66.3	68.4	68.1	71.3	66.5	68.2	73.7	69.0	74.4	74.0
#7 7:30 - 7:45	72.6	68.4	68.4	69.5	60.6	54.4	57.2	64.2	64.2	64.2	68.1	58.0	58.0	58.0	64.2	58.3	58.3	58.3	64.0	59.3	59.3	59.3	64.8	60.5	60.5	70.9	69.6	73.6	69.2
#8 7:45 - 8:00	71.3	67.9	67.9	69.0	58.1	52.5	55.0	62.6	62.6	62.6	66.2	54.8	54.8	54.8	58.3	52.4	46.1	47.7	32.2	56.8	56.8	56.8	62.4	57.5	57.5	69.7	69.4	73.0	67.5
#9 8:00 - 8:15	71.6	68.4	68.4	69.6	59.6	54.5	57.3	63.8	61.8	58.9	32.1	50.5	47.5	43.7	30.1	44.5	44.3	41.7	30.1	56.9	56.9	56.9	62.3	56.8	56.8	69.4	69.0	73.1	68.0
#10 8:15 - 8:30	73.5	69.7	69.3	71.9	64.8	58.5	62.5	67.5	67.5	67.5	58.2	59.2	44.9	65.4	34.4	49.1	43.7	46.2	30.8	56.9	56.9	56.9	62.2	57.8	57.8	69.8	69.3	73.1	67.7
#11 8:30 - 8:45	74.2	70.0	69.3	72.7	66.1	59.6	64.2	68.9	68.9	68.7	70.8	63.6	62.2	59.8	50.4	61.5	57.3	51.9	35.7	56.9	56.9	56.9	62.5	57.6	57.6	69.7	69.6	72.9	67.4
#12 8:45 - 9:00	73.6	69.7	69.3	71.9	64.0	58.4	62.4	69.0	69.0	68.8	70.7	63.7	64.7	64.7	67.3	62.6	62.6	62.6	66.4	62.7	62.7	62.7	66.4	63.3	63.3	72.0	70.0	74.0	70.0
#13 9:00 - 9:15	74.9	70.9	69.5	74.5	71.2	63.0	70.3	70.8	73.1	68.8	74.1	66.3	71.0	69.2	72.8	68.5	70.4	68.5	72.4	67.4	70.7	68.6	72.5	67.6	70.6	74.5	70.5	74.5	74.1
#14 9:15 - 9:30	75.0	71.3	69.4	74.6	73.6	64.2	72.6	71.3	74.2	68.6	74.4	67.4	73.2	69.5	74.4	69.8	73.2	68.6	74.3	68.3	73.2	68.4	74.3	68.5	73.1	75.0	70.9	74.6	74.8
#15 9:30 - 9:45	74.9	70.9	69.4	74.5	71.2	62.9	70.1	70.8	73.1	68.7	74.1	67.1	72.3	69.4	73.8	69.2	71.9	68.4	73.6	67.9	72.1	68.8	73.3	68.1	71.9	74.8	70.9	74.6	74.4
#16 9:45 - 10:00	74.9	70.8	69.5	74.3	69.9	62.2	68.8	70.5	72.4	69.0	73.3	66.2	70.2	69.4	71.7	68.4	69.7	68.7	71.4	67.1	69.9	68.7	71.6	67.4	69.9	74.3	70.7	74.5	73.5
#17 10:00 - 10:15	75.0	71.1	69.4	74.6	71.9	63.4	71.2	71.1	73.8	68.9	74.4	67.0	72.2	69.6	73.5	69.3	72.0	68.9	73.1	67.8	71.8	69.0	72.8	68.1	71.7	74.7	70.6	74.5	74.4
#18 10:15 - 10:30	75.0	71.1	69.5	74.6	71.8	63.2	70.7	70.9	73.4	68.9	74.2	67.2	72.5	69.5	73.8	69.3	72.1	68.8	73.3	68.0	72.1	68.8	73.3	68.2	72.1	74.8	71.3	74.6	74.3
#19 10:30 - 10:45	74.9	70.9	69.4	74.5	70.7	62.8	69.9	71.1	73.7	69.1	74.3	67.2	72.5	69.7	73.5	69.0	71.5	68.6	73.1	67.9	71.9	68.9	73.0	67.9	71.5	74.7	71.3	74.6	73.9
#20 10:45 - 11:00	74.9	70.9	69.4	74.5	70.2	62.5	69.3	70.7	72.9	69.0	73.7	66.7	71.4	69.3	73.0	68.8	70.9	68.8	72.3	67.4	70.7	68.7	72.3	67.6	70.6	74.5	71.3	74.6	73.5
#21 11:00 - 11:15	75.0	71.1	69.5	74.6	71.8	63.3	70.9	71.3	74.1	68.9	74.5	67.3	72.9	69.6	74.0	69.6	72.7	68.7	73.8	68.1	72.6	68.7	73.7	68.4	72.6	74.9	71.2	74.6	74.6
#22 11:15 - 11:30	75.0	71.0	69.4	74.6	71.5	63.0	70.4	70.9	73.3	68.7	74.2	67.0	72.2	69.5	73.5	69.3	72.0	68.7	73.3	67.9	72.0	68.7	73.3	68.0	71.7	74.7	70.9	74.6	74.2

Figure 33: Predicted speed contour resulting from the calibration run with the lowest total speed error

It is important to note that unlike the previous example, this case study is attempting to match target speeds that may not be exactly achievable by the methodology. The reported real-world speeds contain uncertainty in their measurement, and only provide an averaged snapshot of a particular point in time. There is always a guarantee of some degree of error, which holds especially true for segments and time periods where the HCM methodology reports traffic is moving at free flow speed. Free flow speed is an input of the methodology and is assumed to be one constant value for all vehicles. Additionally, one of its primary uses is to serve as an upper bound on predicted speed. However, in real-world conditions, free flow speed will vary from driver to driver independent of the demand volume, even when demands are far below capacity. With this in mind, the calibration shown in Figure 33 can be considered a success as it successfully removes the incorrect congestion regime of the initially estimated contour, and now predicts a speed pattern largely consistent with the target data.

Taking a deeper look at the remaining errors in speed, and breaking them down by speed regime provides additional insight into the calibration process. Table 8 shows a breakdown of the average absolute speed error of the three regimes. The first regime considers any segment and time period combination in which the target speed is greater than 55 mph. The second speed regime considers a target speed less than 55mph, and the final regime considers a target speed of less than 45 mph. It is clear that for the uncalibrated facility, the errors escalate severely as the target speed drops, with mean errors of 17 mph for the second speed regime and 22 mph for the third speed regime. On the other hand, the first attempt at calibration, which uses an unweighted objective function and whose overall results are discussed above, shows a marked improvement. The error breakdown by speed regime is shown in the middle row of Table 8, and the errors for the lower speed regimes drop by 50% and 60%, respectively.

Table 8: Breakdown of the mean absolute speed error of each segment in each time period for three speed regimes using the profile-based encoding

Speed Regime	Overall	>55	<55	<45
Uncalibrated Avg Absolute Speed Error (mph)	6.11	5.31	17.22	21.83
Calibrated (Unweighted) Avg Absolute Speed Error (mph)	3.16	2.81	8.07	8.79
Calibrated (Weighted) Avg Absolute Speed Error (mph)	4.48	4.52	3.95	4.01

In order to improve the calibration accuracy further, the fitness function is altered such that errors occurring when the target speed is lower are weighted more heavily. Any number of weightings can be used, but a simple weighting scheme for the objective is given in Equation 2. This serves to weight errors where the target speed is less than 55 mph twenty times more important than when the target speed is greater than 55 mph. A value of 20 is chosen because the speed regime cutoff of 55 mph is 20 less than the facility free flow speed of 75 mph. Another 5 runs of the calibration GA are made using this new objective function, and the breakdown of the average speed error is given in the final row of Table 8. While the overall average speed error is higher, there is sizable improvement in the predicted speeds for the lower speed regimes, where the average error fell by more than 50% from the unweighted calibration. From this it can be seen that making use of a weighted objective function such as that in Equation 2 can be very helpful to tailor the focus of a calibration. More focused calibration such as this can be particularly useful when the number of periods with low speeds is outnumbered by periods in which speeds are essentially at free flown conditions.

$$\sum_{i=1}^{N}\sum_{p=1}^{P}\lambda_{i,p}\left|v_{i,p}-v'_{i,p}\right|, \text{ where } \lambda_{i,p}=\begin{cases}20 & \text{if } v_{i,p}\geq 55\\ 1 & \text{if } v_{i,p}\geq 55\end{cases} \quad (2)$$

3.2.2.2 3-Distribution Encoding Results

For a second attempt at calibrating the I-540 facility using the GA approach, a 3-distribution encoding approach is utilized and the results are compared to those obtained using the profile-based encoding. Tables Table 9 and

Table 10 provide the parameters used for the GA for a demand estimation approach using a 3-distribution encoding and the unweighted objective function of Equation 2. The ranges specified for the mixture distribution are also mostly the same as with previous examples. However, for this case study, two of the location parameters are left unconstrained (within the 24-hour daily limit), while the target data is used to restrict the location of one of the random variables. Figure 31 shows that the congestion falls entirely between 7:00am and 10:00am, and that range is used to limit the value of μ_1.

Table 9: Summary of the setup parameters for the 3-distribution encoding GA runs

Experiment Parameter	Value
Number of Runs	5
Population Size	400
Max Iterations	200
Crossover Mixing %	50%
Mutation Rate (%)	2%

Table 10: Summary of the distribution parameters for the 3-distribution encoding

Distribution Parameter	Symbol	Range
Weight	w_i	0.05,0.5
Mean 1	μ_1	7:00am, 10:00am
Mean 2	$\mu 2$	12:00am, 11:59pm
Mean 3	μ_3	12:00am, 11:59pm
Standard Deviation	σ_i	0.5,5.0
Skewness	a_i	-10,10

A summary of the results of the experiment is given in Table 11, and the contour predicted by the estimated demands for the best run is shown in

Figure 34. The contour shows a patch of lowered speeds from 7am to 9am, with a shape roughly matching that of the target speed data, indicating a successful calibration. Further, the average error of 3.12 mph is slightly less than that obtained with the profile-based calibration approach. This implies that for a situation with this little of quality input data available, estimating the demand profile using a 3-distribution approach is likely the better alternative.

Table 11: Results summary of the GA Calibration Runs

Metric	Uncalibrated	GA Average
Total Speed Difference (mph)	3901.5	1991.8
Average Speed Difference (mph)	6.12	3.12
90th Percentile Speed Difference (mph)	13.48	6.27
Max Speed Difference (mph)	50.31	28.06
GA Run Time (minutes)	-	8.3

	Segment																												
Analysis Period	1	2	3	4	5	6	7	8	9	10	11	12	13	14	15	16	17	18	19	20	21	22	23	24	25	26	27	28	29
#1 6:00 - 6:15	75.0	71.6	68.6	74.5	74.7	65.1	72.8	71.7	74.8	69.5	74.5	67.9	74.0	70.1	74.6	70.2	73.8	69.5	74.0	68.5	73.4	68.5	74.5	69.3	74.3	75.0	72.4	74.7	74.9
#2 6:15 - 6:30	75.0	71.6	68.8	74.5	74.6	65.0	72.8	71.5	74.6	69.4	74.5	67.9	73.8	70.0	74.4	70.1	73.6	69.5	73.9	68.5	73.3	68.2	74.5	69.4	74.4	75.0	72.5	74.7	74.9
#3 6:30 - 6:45	75.0	71.5	69.0	74.6	74.1	64.7	72.7	70.9	73.7	69.5	74.0	67.4	72.7	69.9	73.5	69.5	72.3	69.5	72.6	67.9	71.8	67.9	73.9	69.0	73.7	75.0	72.5	74.7	74.6
#4 6:45 - 7:00	75.0	71.4	69.2	74.6	73.9	64.6	72.7	70.0	72.5	69.4	72.9	67.0	71.4	69.7	72.4	68.9	70.9	69.4	71.4	67.4	70.3	67.5	73.5	68.8	73.3	75.0	72.4	74.7	74.3
#5 7:00 - 7:15	75.0	71.3	69.3	74.6	73.5	64.4	72.7	68.1	70.1	69.3	70.8	66.0	68.6	68.6	70.0	67.7	67.9	67.9	68.5	66.2	67.1	67.0	72.3	68.4	72.1	74.8	72.1	74.7	73.7
#6 7:15 - 7:30	75.0	71.1	69.3	74.6	73.1	64.2	72.6	64.4	66.7	66.7	67.6	64.9	65.0	65.0	66.8	64.1	64.1	64.1	64.8	63.0	63.0	63.0	70.8	67.9	70.6	74.5	72.1	74.7	72.5
#7 7:30 - 7:45	75.0	71.0	69.4	74.6	72.6	63.9	72.2	58.3	62.6	62.6	63.9	61.4	61.4	61.4	63.7	60.4	60.4	60.4	61.2	59.1	59.1	59.1	69.4	67.4	69.2	74.0	72.0	74.5	71.4
#8 7:45 - 8:00	75.0	70.8	69.4	74.4	71.7	63.5	71.3	49.7	58.4	58.4	59.6	56.4	56.4	56.4	58.8	57.7	48.1	48.2	38.9	56.8	56.8	56.8	68.3	67.0	68.1	73.7	72.0	74.2	70.4
#9 8:00 - 8:15	74.9	70.7	69.5	74.1	71.2	63.2	70.8	49.4	57.9	57.9	59.1	51.3	43.0	61.0	47.6	42.2	40.8	38.9	36.7	56.9	56.9	56.9	68.2	66.9	67.8	73.6	71.9	74.2	70.2
#10 8:15 - 8:30	74.9	70.5	69.5	73.7	70.8	63.0	70.4	56.3	54.8	62.7	50.2	43.6	41.0	59.7	41.4	45.6	46.6	42.7	36.5	56.9	56.9	56.9	67.9	66.8	67.7	73.6	71.8	74.2	70.2
#11 8:30 - 8:45	74.8	70.3	69.5	73.3	70.5	62.9	70.1	62.8	64.2	64.2	64.3	58.5	46.7	60.8	55.8	51.8	42.6	40.6	36.7	56.9	56.9	56.9	67.2	66.6	66.9	73.3	71.7	74.0	69.8
#12 8:45 - 9:00	74.6	70.1	69.5	72.9	70.5	62.9	70.1	66.7	67.4	67.4	68.3	65.5	66.5	66.5	68.1	59.5	60.1	57.3	45.8	59.3	59.3	59.3	67.6	66.8	67.4	73.5	71.8	74.1	70.0
#13 9:00 - 9:15	74.4	70.0	69.5	72.5	70.7	63.0	70.3	68.7	69.8	69.3	70.5	66.3	69.1	69.1	70.5	67.5	67.8	67.8	68.5	66.1	66.8	66.8	71.2	68.0	71.1	74.6	72.1	74.7	72.8
#14 9:15 - 9:30	74.2	69.8	69.5	72.1	70.9	63.0	70.4	69.8	71.3	69.3	71.9	66.9	70.8	69.6	71.9	68.3	69.7	69.3	70.3	66.8	68.8	67.9	72.0	68.3	71.8	74.7	72.3	74.7	73.2
#15 9:30 - 9:45	74.0	69.7	69.5	71.7	71.1	63.2	70.7	70.5	72.5	69.3	73.0	67.3	72.2	69.8	73.1	69.0	71.3	69.4	71.7	67.3	70.3	68.3	72.6	68.5	72.4	74.8	72.3	74.7	73.6
#16 9:45 - 10:00	73.8	69.6	69.5	71.3	71.4	63.3	70.9	70.7	73.1	69.4	73.5	67.5	72.7	69.9	73.5	69.2	71.8	69.4	72.3	67.6	71.0	68.5	72.8	68.5	72.6	74.9	72.2	74.7	73.8
#17 10:00 - 10:15	73.5	69.5	69.5	71.0	71.4	63.3	70.9	70.9	73.4	69.4	73.8	67.7	73.1	69.9	73.9	69.5	72.5	69.4	72.9	67.8	71.7	68.7	73.1	68.7	72.9	74.9	72.3	74.7	74.0
#18 10:15 - 10:30	73.3	69.4	69.5	70.8	71.1	63.1	70.6	71.1	73.6	69.4	74.0	67.8	73.4	70.0	74.1	69.7	72.9	69.4	73.2	68.0	72.2	68.9	73.3	68.8	73.2	75.0	72.4	74.7	74.1
#19 10:30 - 10:45	73.0	69.3	69.5	70.6	70.4	62.8	70.0	71.0	73.6	69.4	73.9	67.8	73.4	69.9	74.1	69.8	73.1	69.4	73.5	68.1	72.5	69.0	73.4	68.8	73.3	75.0	72.5	74.7	74.2
#20 10:45 - 11:00	72.8	69.3	69.5	70.5	69.3	62.2	68.8	70.9	73.3	69.4	73.7	67.7	73.0	69.9	73.8	69.6	72.7	69.4	73.1	67.9	71.9	69.1	72.8	68.5	72.6	74.9	72.3	74.7	73.7
#21 11:00 - 11:15	72.7	69.3	69.5	70.4	67.9	61.4	67.3	70.7	72.9	69.3	73.4	67.6	72.7	69.8	73.6	69.6	72.5	69.4	72.9	67.8	71.6	69.2	72.4	68.4	72.2	74.8	72.3	74.7	73.5
#22 11:15 - 11:30	72.6	69.3	69.5	70.5	66.9	60.8	66.2	70.7	72.7	69.3	73.2	67.5	72.5	69.8	73.5	69.6	72.5	69.4	72.9	67.8	71.7	69.2	72.4	68.4	72.2	74.8	72.4	74.7	73.3

Figure 34: Speed contour of the calibrated facility with the lowest total speed error

Table 12 provides a breakdown of the error for the five calibration runs discussed above with an unweighted objective, as well as for five additional calibration runs made with the same 3-distribution encoding and the regime-weighted objective of Equation 2. The breakdown for the runs with the unweighted objective again shows that the GA was significantly less accurate in matching the lower speed regimes than the higher speed regimes. For the calibration attempts using the weighted objective function, the distribution of error is much more even. There is a large reduction in the average speed error for both of the lower speed regimes, with the lowest regime seeing nearly a 70\% improvement. This strongly reinforces the usefulness of a weighted objective function when the number of periods with high target speeds outnumbers those with lower target speeds.

Table 12: Breakdown of the mean absolute speed error of each segment in each time period for three speed regimes of the 3-distribution encoding calibration

Speed Regime	Overall	>55	<55	<45
Uncalibrated Avg Absolute Speed Error (mph)	6.11	5.31	17.22	21.83
Calibrated (Unweighted) Avg Absolute Speed Error (mph)	3.12	2.71	9.08	10.65
Calibrated (Weighted) Avg Absolute Speed Error (mph)	3.56	3.52	4.48	3.35

4.0 FREEVAL CALIBRATION

4.1 IMPORTANCE OF FREEVAL CALIBRATION

The process of facility calibration is a foundational aspect of using the HCM methodology and a critical step of model creation preceding all analyses. Model calibration is essential because any analysis that uses the HCM methodology hinges on the core model correctly representing daily recurring congestion conditions. In fact, modeling existing real-world conditions for a single representative day is the first step for using the methodology to conduct reliability and active traffic management analyses. This requirement necessitates that every model must be calibrated to match a set of target real-world conditions. The manual's current guidance concerning calibration is very limited, and the process often presents a major barrier to entry for the methodology.

Much of the challenge of the calibration process stems from the fact that each model requires a large number of inputs, with even moderate sized models requiring the input and adjustment of thousands of individual parameters. Further, many of the critical inputs are difficult to measure under real-world conditions. Calibration of both input demand volumes and capacity parameters is vitally important as the driving force of the methodology is the relationship between demand volumes and segment throughput capacities. However, vehicle demand volumes are largely unknown under real world conditions and are essentially impossible to measure when traffic flow is congested. The manual does provide default estimates for the key capacity parameters, but these should ideally be adjusted in conjunction with demand volumes for each specific facility location.

4.2 INTEGER PROGRAMMING APPROACH

While both the freeway facilities method of the HCM and the original CTM can be solved efficiently by iterating through the flow equations, this provides little advantage when attempting to calibrate a facility. Further, this straightforward approach to the analysis is limited in that the unknowns are fixed and the solutions only provide a specific set of performance measures. This yields little real insight into the interplay between variables and sensitivities of each respective model. In order to gain better insight into the workings of the methods, it is thus desirable to formulate them as optimization problems. Much work has already been done to model the CTM using mathematical programming frameworks, but little has been done for the HCM freeways methodology. These approaches have largely used linear programming, integer programming, and nonlinear programming. The CTM was first formulated as linear program (LP) by Ziliaskopoulos (2000) where he defined the System Optimum Dynamic Traffic Assignment (SO DTA) problem. Aghdashi et al. (2013) developed a linear programming model to compute optimal ramp metering strategies based on the undersaturated equations.

This work formulates the oversaturated methodology as a Mixed Integer Linear Program (MILP). The unique ability of the MILP formulation to allow for ``forward", ``backward", or ``inside-out" analysis is explored in an effort to gain better insight into the benefits and limitations of the model.

4.2.1 Formulation of the MILP Model

This work focuses solely on the oversaturated portion of the freeways facility methodology. In part, this is due to the undersaturated algorithm being relatively computationally simple and efficient, and largely because it is of limited usefulness in the context of facility calibration. In cases where the facility is undersaturated, it is known that all demand can and is being met, and thus the demand is simply equivalent to the observed flows. Further, it should be noted that the undersaturated conditions can be analyzed using the oversaturated equations. The methodology as presented in the HCM does not do this in order to eliminate unnecessary computational efforts and costs.

As soon as the demand exceeds capacity on a segment of the facility, the oversaturated procedure is utilized. The oversaturated equations evaluate the facility by computing flows for each node, starting at the first upstream node and moving down the facility. Flows at each node consist of three quantities, mainline flow (MF), on-ramp flow (ONRF), and off-ramp flow (OFRF). Segment flows (SF) are calculated for each intermediate segment, though each can easily be associated with a node to simplify the computations. Figure 35 shows how mainline and segment flows interact at merge and diverge segments.

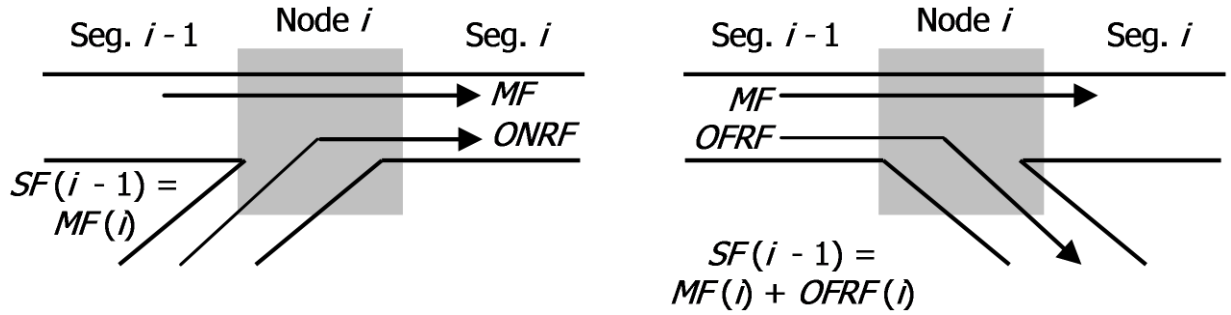

Figure 35: Example of the mainline flow (MF) and the segment flow (SF) calculations with on-ramps and off-ramps

The bulk of the computations of the methodology involve the computation of these flows. Flows for the mainline and ramps are limited both by the input flow desiring to travel through the node, as well as the output flow that can be allowed based on available capacity, adjacent ramp flow, and queue conditions. These computations contain nonlinearities in the form of "min" functions that force the flow to be the minimum of input and output. As an illustration, the following paragraph will briefly discuss the computation of mainline flow at a node, and similar methodology is contained within the oversaturated equations for computing on-ramp and off-ramp flows.

Computing mainline flow at a node consists of computing the mainline input (MI) wishing to travel through the node, as well as computing a number of quantities that can limit the output flow through the node due to the presence of a ramp at the node, or a queue created by a downstream bottleneck. Mainline input at a node is the sum of the mainline flow and on-ramp flow coming from the node immediately upstream, minus any off-ramp flows of the current node. If a queue exists, mainline input also includes any unserved vehicles (UV) stored on the upstream segment. Mainline output is limited by three quantities accounting for turbulence due to merging on-ramp flows, queue accumulation from a downstream bottleneck, and queue dispersion from a

downstream bottleneck, respectively. Mainline output is also limited by the capacity of each of the segments to which it is adjacent. Consequently, the equation to determine mainline flow is presented in the methodology as:

$$MF(i,t,p) = \begin{Bmatrix} MI(i,t,p) \\ MO1(i,t,p) \\ MO2(i,t,p) \\ MO3(i,t,p) \\ SC(i,t,p) \\ SC(i-1,t,p) \end{Bmatrix} \quad (3)$$

While it is sometimes possible to directly linearize an equation such as this with a group of "≤" inequalities, it is unfortunately generally not the case for this model. Depending on the choice of objective functions and the rest of the constraints, simply using inequalities can lead to a phenomenon known as "holding back flows." For example, since this approach is seeking to optimize the system as a whole, flows may be artificially held back from progressing through a node when it benefits this system. This can occur with groups of "≤" inequalities since the flow is only required to be less than both the input and the output, but not exactly the minimum of the two. This type of behavior is highly unrealistic and it is generally accepted that any vehicle traveling through a facility will seek to minimize its own travel time, even at the cost of the performance of the facility as a whole. This type of condition is referred to as the User Optimum (UO) or User Equilibrium (UE) condition. Thus the MILP formulated will make use of binary integer variables in order to model these "min" functions in an exact manner.

The MILP is formulated by using each equation of the oversaturated methodology as a model constraint. The equations are formulated as constraints by using them directly as linear equalities when possible, or by converting them to sets of linear inequalities when necessary. These constraints are then paired with an objective function that minimizes the difference between predicted and target performance measures in order to determine the optimal set of decision variables. In this case, the decision variables are previously determined by the analyst, and are the input parameters (e.g. demand volumes, capacity adjustments) for which the analyst wishes to calibrate the model.

4.2.2 Minimum and Maximum Relationships as Constraints

While linear programming is a very powerful tool, it does have a strict limitation in that it can only model expressions which can be formulated as sets of linear equalities and inequalities. This raised a major issue for this work as many of the most important equations of the HCM methodology require taking the minimum or maximum of a set of values. Consequently, in order to handle min/max constraints, a pure LP model must be expanded to include binary integer decision variables, allowing the min/max relationships to be accurately modeled. The following example shows how a simple "min" relationship can be modeled as a set of linear inequalities through the use of binary variables.

Consider the statement C=min{A,B}. In practice, this statement is essentially an "If-Then" conditional: If A < B, then C=A, and a constraint of C-A=0 must be enforced, and if A>B, then C=B and the constraint C-B=0 must be enforced. By adding a binary decision variable *i*, and a

large positive constant *M*, we can address these two cases with the following set of four inequalities.

$$\begin{aligned} A - B &\le M * i \\ B - A &\le M * (1 - i) \\ -M * i \le C - A &\le M * i \\ -M * (1 - i) \le C - B &\le M * (1 - i) \\ i &\in \{0,1\} \end{aligned} \tag{4}$$

The first pair of inequalities serve to determine the value of the binary variable *i* based on whether or not A>B is a true statement. If A>B, then *i* must equal 0 so that the inequalities read A-B ≤ 0 and B-A ≤ M (A-B ≤ 0 is equivalent to A ≤ B). Alternatively, if A < B, then *i* must equal 1 so that the inequalities read A-B ≤ M and B-A ≤ 0 (B-A ≤ 0 is equivalent to B ≤ A). Next, by looking at the second pair of inequalities, it is easy to see that when *i=0*, we have *C=A*, and when *i=1*, we have *C=B*. Further, since *M* is a sufficiently large constraint, -M ≤ C-A ≤ M and -M ≤ C-B ≤ M are essentially removed from being enforced for the respective value of *i*.

When dealing with equations that set a value to be the minimum of two quantities, this technique can be applied directly. Further, it is easily shown that the minimum of more than two values can be broken down into successive minimums between two values. For example, min{x,y,z} is equivalent to min{x, min{y,z}}.

4.2.3 Issues Due to Computational Complexity

While the MILP formulation provides many new capabilities for analysis using the HCM methodology, it unfortunately comes with an additional major drawback. Since each "min" (and "max") relationship requires a minimum of six constraints (each bounded constraint must be broken into two), the total number of model constraints is large even for small facilities. Each segment is analyzed using 24 equations for each time step of each analysis period of the study period. There are 9 min/max relationships within the 24 equations and 6 If-Then conditionals that must be converted to a set of linear inequalities. In general, for each segment *i*, time step *t*, and analysis period *p*, the added complexity of the model is 140 constraints and 20 binary variables. This poses a major issue as MILP problems are considered to be NP-complete, and therefore unfortunately largely computationally intractable beyond a certain size. As such, even with a commercial solver such as Gurobi or CPLEX, it is only possible to solve small problem instances in a reasonable amount of time.

As an example, consider a facility with 11 total segments, 6 of which are basic, 2 on-ramps, 2 off-ramps, and 1 weaving segment. If the study period is 4 hours (16 analysis periods), and a time step resolution of 15 steps per period (i.e. a one-minute time step), the model would contain approximately 370,000 constraints and 132,000 binary integer variables. Even this relatively small and simple facility almost certainly exceeds the capabilities of most solvers and classical integer programming solution techniques.

4.2.4 Small Computational Example and Results

In order to show the capabilities of the MILP model, a small computational example was developed in which demand volumes for each period are estimated by the model in order to best

match a set of target performance measures. In other words, the mainline demand for each period is the key decision variable of the MILP formulation. The example facility is designed to be simple enough to be solved in a reasonable amount of time by the Guorbi solver. The geometry of the facility is shown in Figure 36. The facility consists of five half-mile length basic segments, with a lane drop from 4 to 3 lanes at the fourth segment to create a bottleneck. A two-hour study period from 5:00pm to 7:00pm was selected for the example. Additionally, the number of time steps per period for the oversaturated methodology was reduced from 60 to 10, with each time step representing 90 seconds as opposed to 15 seconds. Since all segments are a half-mile long, this time step size is valid in accordance with the queue spillback wave speed.

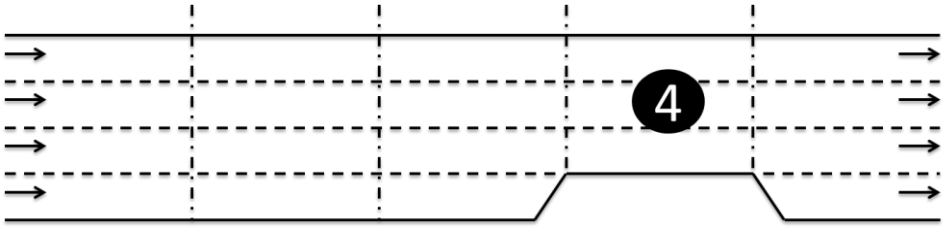

Figure 36: Geometry of the facility for the simple MILP computational example

An initial simulation of the facility was conducted using the FREEVAL computational engine to generate target performance measure outputs. The queuing as predicted by the HCM methodology for the facility can be seen in the contour shown in Figure 37. Observed flows were selected as the target performance measure as they are often available from fixed sensors for many real world facilities. Figure 38 shows the validation process for the example. The MILP model was able to accurately compute the input demands to with ~0.01% of the known underlying value. Additionally, speeds, densities, and queues matched exactly with those computed by FREEVAL.

Analysis Period	Seg. 1	Seg. 2	Seg. 3	Seg. 4	Seg. 5
#1 17:00 - 17:15	0%	0%	0%	0%	0%
#2 17:15 - 17:30	0%	0%	0%	0%	0%
#3 17:30 - 17:45	0%	24%	100%	0%	0%
#4 17:45 - 18:00	49%	100%	100%	0%	0%
#5 18:00 - 18:15	0%	59%	100%	0%	0%
#6 18:15 - 18:30	0%	0%	51%	0%	0%
#7 18:30 - 18:45	0%	0%	0%	0%	0%
#8 18:45 - 19:00	0%	0%	0%	0%	0%

Figure 37: Queue percentage for each segment of the facility for each time period

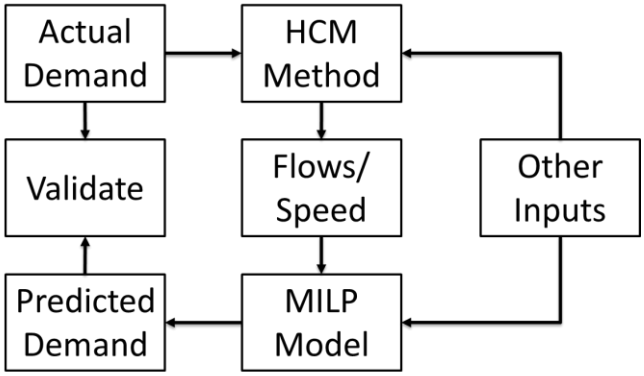

Figure 38: Validation process for the predicted demands computed with the MILP model

While this example demonstrates the power of the approach to accurately estimate inputs based on a set of target performance measures, it also highlights its limitations due to the inherent computational complexity of MILP models. Even for an example this small, there were over 26,000 constraints and over 23,000 variables, 10,000 of which were binary variables. While this problem can be solved quickly in about 10.5 seconds, each additional segment, especially ramp segments, increases the computational burden exponentially, quickly moving the model to the realm of intractability with today's computers.

4.3 A GENETIC ALGORITHM APPROACH

This genetic algorithm framework of this section expands upon the demand estimation approach by adding three key capacity parameters into the existing calibration framework. New genetic encodings for the inputs are developed that allow the metaheuristic to consider pre-breakdown capacity adjustments, the queue discharge flow rate, and the facility-wide jam density alongside demand volumes. These three capacity parameters are important to incorporate as each controls aspects of breakdown occurrence, queue formation and recovery speeds, and overall queue size in a unique way. The resulting framework consists of a two-phase calibration process. During the first phase, the GA adjusts demand volumes and the queue discharge rate, while at the second phase the GA manipulates the jam density and bottleneck segment pre-breakdown capacity adjustments. Further, unlike the initial work, this expanded approach utilizes an updated objective function that considers errors in both facility travel times and individual segment speeds.

4.3.1 Genetic Algorithm Overview

Metaheuristic approaches are often employed for problems in which the underlying mathematical relationships of a system are poorly understood or prohibitively complex. Unlike classical

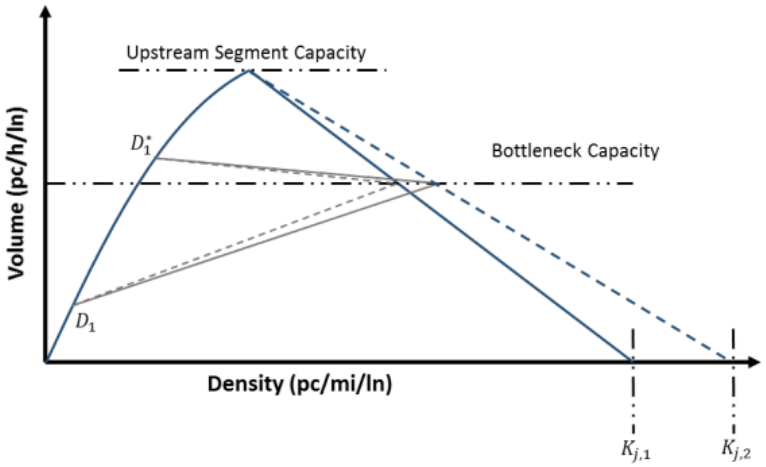

Figure 39: Effects of varying jam density values Kj,1 and Kj,2 on the volume density diagram (Highway Capacity Manual 2016).

approaches that require the use of a gradient or similar quantifiable concept of change, a metaheuristic approach does not need to explicitly consider the underlying mathematics of the system being modeled in order to identify a solution. In particular, evolution based metaheuristics such as genetic algorithms have been widely studied and have been found to be very effective at solving optimization problems related to system identification. A genetic algorithm (GA) seeks to mimic the processes of evolution and natural selection in order to evolve an initial pool of candidate solutions over time until an optimal or near-optimal solution is found. In a GA, each candidate solution is represented as an individual organism, with the decision variables of the problem encoded as the organism's genes or chromosomes. An evaluation function is defined in order to calculate the fitness of a candidate solution based on these "genes". Both the encoding and fitness function are chosen such that the problem is framed as a minimization or maximization of fitness. This allows fitness-based "competition" to be used in order to make determinations on the quality of one candidate solution versus another. In this way, the fitness function is analogous to the objective function of classical optimization techniques such as linear programming. A GA begins with an initial population of randomly generated organisms. The search process operates by "evolving" this population over time, with each new generation of organisms providing an opportunity to identify a better solution. Successive generations are created through competitive 86 selection and crossover of organisms of the previous generation. The evolution process consists of competition-based "mating" of organisms in order to create "offspring" organisms. This is done through the use of a crossover operator, which creates the offspring organisms by "crossing-over" and combining the parents' genetic material into new chromosomes. For example, if one parent's candidate solution was encoded as the binary string "1111," and the other parent's was encoded as "0000," a simple one-point crossover strategy could create two offspring organisms with the chromosomes encoded as "1100" and "0011," respectively. Additional operators such as mutation are utilized to help prevent premature convergence to undesirable local optima. The overall process of a genetic algorithm repeats until either an optimal solution is found or a maximum number of iterations is reached. The most critical aspect of a GA is the encoding of a candidate solution's decision variables as the genes of an organism. The key underlying assumption of the GA approach

is that high-quality solutions contain common “building blocks" found in the encoded genes of the organisms (Mitchell, 1998). Maintaining these blocks within a population of organisms, and combining them with other “good" blocks should then theoretically lead to the discovery of better solutions. Blocks are combined through the use of a crossover operator representing mating and reproduction of organisms. This process produces a number of “offspring" organisms each containing parts of each parent’s genetic material and consequently the encoded decision variable values. While real-valued encodings are occasionally used, most encodings consist of some type of binary representation of the solution. This allows for a straightforward realization of genetic building blocks (e.g. small binary patterns such as “010" or “110"), and provides a simple notion of sharing genetic material through exchanging binary digits. In most cases in which a metaheuristic approach such as a GA is necessary to solve a problem, the solution space is likely to be highly nonlinear, nonconvex, and discontinuous. This makes it extremely difficult for any search process to directly or smoothly move towards a globally optimal solution. Thus, most GA implementations make use of at least one additional operator to guard against premature convergence to locally optimal solutions. The most common of these operators is the mutation operator, which randomly alters an organism’s individual genes or chromosomes in order to introduce additional genetic diversity into the population.

4.3.2 Unifying Demand and Capacity Calibration

Overall, there are three key aspects of capacity that should be considered when calibrating an HCM freeway facilities model, each of which affects the predicted performance measures in a different manner. First, pre-breakdown bottleneck capacity adjustments determine the demand 87 level at which breakdowns occur, and have inverse effects on the shockwave formation and recovery speeds. Second, a reduced queue discharge rate via a capacity drop factor models a known realworld phenomenon and provides an additional control on the breakdown shockwave formation and recovery speeds that only affects conditions post-breakdown. Lastly, the jam density of the facility controls the length of any queues that form, which is reflected in variations in the speeds of individual segments in and around the vehicle queue. As previously mentioned, a genetic algorithm metaheuristic approach was developed to automate the process of demand estimation and adjustment. The approach is able to estimate new or adjust existing demand volume inputs such that the performance predicted by the methodology more accurately matched that of a set of target real-world conditions. While it proved to be an improvement over the current trial and error process, its focus only on demand left it with some inherent limitations. On its own, demand calibration is best suited for matching observed throughput values and travel times. This may be sufficient for some facilities, but in general, and especially when calibrating for individual segment speeds, it is better served when complemented with capacity calibration. By incorporating capacity parameters that control additional relevant aspects of congestion analysis (e.g., breakdown occurrence, formation speed, queue length, and breakdown recovery), the power and flexibility of the system identification framework can be maximized. The proposed framework consists of two-stage approach of successive calibration instances, each of which operates on a different set of variables during the GA search process. The first round of calibration focuses on demand estimation, and incorporates the capacity drop factor alongside the demand volume input variables. The second round utilizes the determined values for these inputs, and operates instead on the pre-breakdown bottleneck adjustments and the jam density. The objective function for both instances

is a weighted combination of error in individual segment speeds and error in the total facility travel times for each analysis period. However, the ratio of the weights will be different for the successive calibration rounds, which will be discussed in more detail in the following sections. Finally, as with the initial demand calibration work, the framework is intended for use with FREEVAL, the HCM freeway facilities computational engine. Figure 40 shows the high-level process flow of the unified two-stage approach.

4.3.3 Fitness Evaluation

The goal of the calibration problem is to ensure that the HCM's methodology predicts performance measures consistent with those observed in the real world. As such, a straightforward choice for quantifying an organism's fitness is to compute the sum of the absolute differences between the predicted and real world values for a given performance measure.

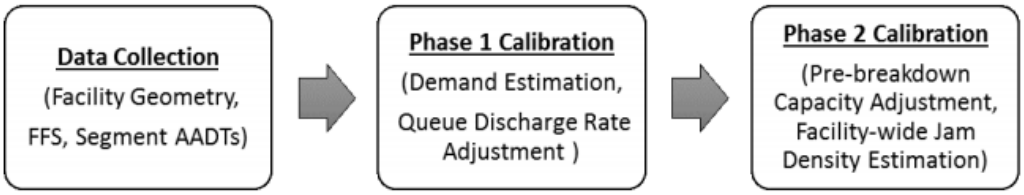

Figure 40: High-level process flow of the unified two-stage calibration process

The overall objective of the GA then be framed as minimizing an organism's fitness, with a fitness value of 0 indicating an optimal solution in which the predicted and real-world performance measures match exactly. Since speeds and travel times are two of the more commonly available types of real world observed data, as well as key quantities for model calibration, it makes sense to center the fitness evaluation around these two performance measures. While a simple objective function could seek to minimize the error around just one of these measures, the dual nature of the calibration approach can benefit from minimizing a linearly weighted combination of the two, simulating a basic multiobjective approach. First let T (p) represent the observed facility travel time of period p, and let $\bar{T}$(p) represent the predicted facility travel time for period p. Similarly, let vi,p represent the observed speed in segment i in analysis period p, and let $\bar{v}$i,p represent the predicted speed for segment i in analysis period p. The overall goal is to minimize the absolute error in between observed and predicted values for each quantity across all segments (1,...,N S) and for all time periods (1,...,P). For two linear weights λ1 and λ2 , the fitness function F (x) for a given organism can be formulated as shown in equation 5.

$$F(x) = \lambda_1 \sum_{p=1}^{P} |T(p) - \bar{T}(p)| + \lambda_2 \sum_{i=1}^{NS} \sum_{p=1}^{P} |v_{i,p} - \bar{v}_{i,p}| \quad (5)$$

While this represents the fitness function in its simplest form, it can be modified in a near endless number of ways and tailored to a specific goal or application. For example, the work developing the demand estimation framework found that it was beneficial to weight errors occurring where targets speed are lower more heavily than those occurring where the target speeds are higher. There are a variety of ways to do this, but a simple linear piecewise weighting scheme was proposed in the demand estimation work that achieved satisfactory results. In this scheme, errors where the target speed is less than 55 mph are weighted as much as twenty times more heavily than where the target speed is greater than 55 mph. This allows the GA to focus on the replicating the congested conditions, as opposed to trying to perfectly match free flow speeds in uncongested periods. While 89 free flow speed is a constant value in the HCM methodology, it can fluctuate widely in the real world depending on the type of driver (e.g. one who speeds versus one who strictly obeys the speed limit) passing through the observation zone in a given time period. Thus the fitness function can be reformulated with this modification as shown in equation set 6.

$$F(x) = \lambda_1 \sum_{p=1}^{P} |T(p) - \bar{T}(p)| + \lambda_2 \sum_{i=1}^{NS} \sum_{p=1}^{P} w_{i,p} |v_{i,p} - \bar{v}_{i,p}|$$

$$\text{where} \quad w_{i,p} = \begin{cases} 20 & \text{if } v_{i,p} < 55 \\ \max\{75 - v_{i,p}, 0\} & \text{if } v_{i,p} \geq 55 \end{cases} \tag{6}$$

In addition to allowing the objective function to consider multiple performance measures, the weights λ1 and λ2 serve an additional purpose for the two-stage calibration process. They allow the focus of the optimization to be shifted between the two quantities based on the phase of the calibration process. The first phase of the calibration process centers on demand estimation, and hence should place a heavier weight on matching the target facility travel times. Alternatively, the second phase of the calibration process centers on pre-breakdown capacity adjustments and jam density, and matching individual segments speeds should be a higher priority and given a heavier weight. The exact ratio of the weights can be adjusted for each particular calibration instance, but a simple two-to-one ratio can serve as a default starting point.

4.3.4 Genetic Encoding of the Capacity Calibration Parameters

The GA framework of the original demand calibration work requires that all decision variables be represented as a string (or strings) of binary digits. As such, a binary encoding process analogous to that of the profile based demand adjustments is used to incorporate capacity calibration parameters into the existing framework. This type of encoding necessitates an assumption of a known range of feasible values for each parameter, which requires that both a minimum and a maximum possible value be specified. The interval created by this range can then be discretized using the maximum integer value allowed by the number of binary digits of the encoding. In this way, the binary value of a gene will represent an integer value, which can then be projected into the discretized search space. To demonstrate, if the search space for a pre-

breakdown CAF is the interval [0.7,1.01], and an 5-digit binary encoding is used, the range is discretized into 31 intervals, which gives a step size of (1.010.70)/(2 5 − 1) = 3.1/31 = 0.01 (projection into the range is inclusive, hence why there are 2 5 − 1 = 31 intervals as opposed to 2 5 = 32). For a gene expressed by the binary string “010100", it 90 is converted to base 10 as an integer value of 20, and the resulting CAF is 0.7 + (20 ∗ 0.01) = 0.90 (a simplified range is used for demonstration purposes). Analogous approaches are used to encode and project both the capacity drop factor and the facility-wide jam density. The specified allowable range for each parameter can vary for each facility and should be chosen using the analyst’s judgment and knowledge of the facility. However, any range should not be too large. For example, pre-breakdown CAFs indicating a drop in capacity of 30% or more are likely to be unrealistic and may indicate that other inputs of the methodology need to be adjusted. Table 13 shows a set of recommended ranges for each of the three parameter types. It should also be noted that the number of binary digits can be varied to increase or decrease the resolution of the CAF search space. For example, a 5-digit binary encoding divides the search interval into 2 5 = 32 values, while a 16-digit binary encoding divides the interval into 65,536 values.

Table 13: Recommended ranges for the capacity calibration parameters

Parameter	Minimum	Maximum
Pre-breakdown CAF	0.80	1.05
Capacity Drop Factor (%)	0	10
Jam Density (veh/mi/ln)	180	220

With a binary representation for each parameter defined, the capacity parameters next need to be incorporated into the GA framework. This requires adding the capacity drop factor to the existing demand calibration process, and creating an additional process for estimating the pre-breakdown capacity adjustments and the facility-wide jam density. Since the demand calibration piece uses uniform crossover and mutation, both of which consider individual binary digits independently, the capacity drop factor can be calibrated in conjunction with demand by simply appending its binary representation to the encoded string of demand values or adjustments. On the other hand, since the framework now functions as a two-stage process, an additional encoding must be utilized for the set of pre-breakdown CAFs and the jam density. In a freeway facilities analysis, each individual segment of a facility has a representative capacity value and a corresponding CAF. This research assumes that capacity of a segment is fixed over time, and thus the number of CAF decision variables considered is equal to the number of segments. The capacity drop factor is considered to be a facility-wide value, and hence constitutes one decision variable. For a facility with NS segments, the set of NS CAF binary encodings are then concatenated into a single binary string. This provides a simpler (albeit analogous) representation as opposed 91 to working with an array of binary strings. Additionally, the binary encoding of the jam density can simply be appended to the end of the single string representation, without altering how GA operators approach it beyond extending its length. Figure 41 demonstrates the process of encoding a set of three pre-breakdown capacity adjustments and the facility-wide jam density into a single binary string.

Table 14: Parameter minimum values and step sizes for the encoding example

Parameter	Minimum Value	Step Size
Pre-breakdown CAF	0.80	0.01
Jam Density (veh/mi/ln)	180	1

	Pre-breakdown Capacity Adjustments			Jam Density
	Seg. 1	Seg. 2	Seg. 3	-
Actual Value	1.0	0.95	1.0	205
# Steps Above Minimum	20	15	20	25
5 Digit Binary Encoding	10100	01111	10100	11001
Final Encoded String	10100011111010011001			

Figure 41: Example of encoding three pre-breakdown CAFs and the facility-wide jam density into binary strings based on the values of Table 14

As a final note on pre-breakdown capacity adjustment factors, this approach initially extends their use to all segments, as opposed to just at bottleneck segments as proposed in the HCM's calibration procedure. The reason for this is two-fold. First, this enables the framework to make small adjustments to segment capacities along the entire facility as the default estimates may be slightly off. However, and more importantly, the second reason is that there is uncertainty in the location of a bottleneck, and its location is likely relatively unknown for an uncalibrated facility. By allowing the GA metaheuristic to adjust the CAFs for every segment, it gives it the freedom to identify bottleneck location(s) while also determining the magnitude of the capacity adjustment(s). Further, while the GA may in some instances adjust capacities when it has no effect on performance measures 92 (e.g., when demand is well below capacity), a simple post-processing check can be employed to replace these adjustments with an unadjusted value of 1.0.

4.3.5 Selection and Crossover

The primary drivers of the evolutionary process of a GA are the selection and crossover operators. The selection operator is used to choose the two organisms (candidate parameter adjustments in our case) that will undergo crossover in order to produce new offspring organisms. There are a number of ways to implement the selection process including random selection, roulette wheel selection, and tournament selection. This research makes use of a simple k-tournament selection strategy in which k solutions are randomly picked from the current generation, and the one with the best (lowest) fitness is selected to be a parent. This process is repeated twice to determine the two parent organisms to undergo crossover. The value of k can be varied to improve the convergence rate of the GA. As with selection, there are a variety of crossover strategies and a vast amount of research conducted in regards to how these strategies impact final solution quality and the speed of convergence. Three commonly used crossover strategies were implemented and tested as part of this research. These included a one and two point

crossovers, as well as uniform crossover. Figure 42 demonstrates each of the three crossover strategies. However, initial testing indicated that the uniform crossover strategy was by far the most effective. Using this strategy, a random number is generated uniformly between 0 and 1 for each binary digit of the encoding. If the generated value is less than a pre-specified mixing percentage (e.g. 0.5 would indicate 50% mixing), the binary digit is swapped between the two strings. As such, for the case study of the subsequent section, a uniform crossover strategy was always used for the Phase 2 capacity calibration process.

4.3.6 Mutation

A uniform mutation strategy was implemented for use in the bottleneck capacity calibration GA framework to help prevent premature convergence to a locally optimal solution. As its name would suggest, a uniform mutation strategy is very similar to the previously described uniform crossover strategy. However, unlike crossover, uniform mutation operates just on a single set of genes in order to randomly introduce changes such that a diverse population of candidate solutions is maintained. Further, instead of a mixing percentage hovering around 50%, mutation of individual genes (e.g., binary digits) is generally specified to occur at a much lower frequency, known as the mutation rate. During the mutation process for a binary string encoding, a random number is again generated 93

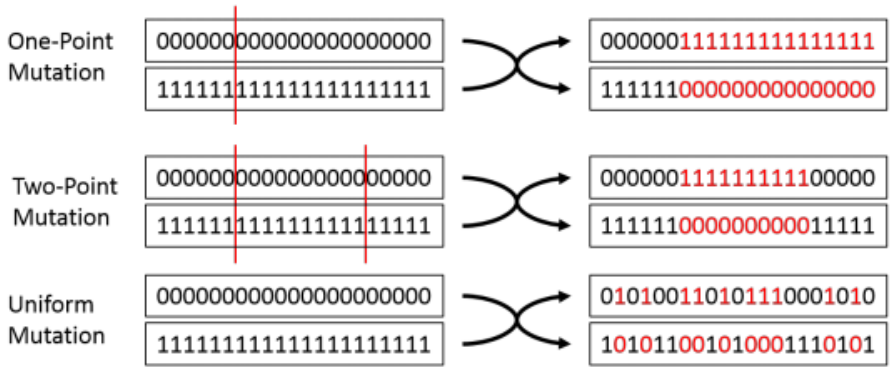

Figure 42: Demonstration of three common crossover operators

uniformly between 0 and 1 for each binary digit. If the number is less than the specified mutation rate, the corresponding binary digit is flipped to its binary alternative. Specifically, a 0 becomes a 1, and a 1 becomes a 0. The optimal mutation rate varies for each specific problem, but research has generally shown that for binary GA encodings, a rate of 0.02 to 0.05 has the most beneficial effect on convergence and final solution quality (Mitchell, 1998).

4.3.7 Computational Experiments and Numerical Results

A case study for testing the approach with real word data was developed for analysis based on a section of I-540 outside of Raleigh, NC. The goal of the case study is to produce a calibrated model by estimating the demand volume inputs and adjusting the core capacity parameters using the genetic algorithm framework. The facility consists of 14.5 miles of largely three-lane urban freeway in the westbound direction, including seven on-ramp segments and eight off-ramp segments. The facility as modeled using the HCM methodology is shown in Figure 43. The facility was then populated with initial demand input values based on AADT estimates available through the North Carolina Department of Transportation and combined with a best estimate of the local hourly demand behavior for the study period (North Carolina Department of Transportation, 2016).

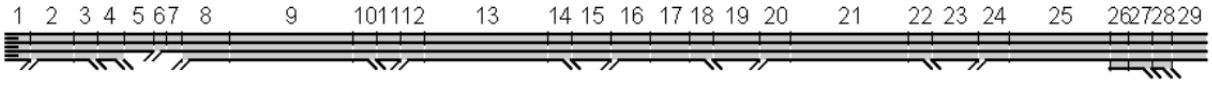

Figure 43: HCM segmentation of 14.5-mile section of I-540 westbound near Raleigh, NC

A set of representative speeds for a five-and-a-half-hour study period between 6:00am and 11:30 am on a Tuesday in August 2014 was collected from RITIS.org and are shown in the top contour of Figure 44 (Maryland CATT Lab, 2008). The bottom contour of Figure 44 shows the speed contours initially predicted by the HCM methodology, which clearly has a very different congestion regime as opposed to the target data. The analysis periods in which the congestion occurs are similar, but the target data shows low speeds in segments 8 to 23, while the uncalibrated facility shows congestion only in segments 2 to 6. A summary of the average speed error for different speed regimes is given in Table 15. A list facility travel times based on the target travel speeds for each analysis period can be found in Table 16. The table also shows the travel times based on the predicted speeds of the uncalibrated facility. It is interesting to note that the travel times are surprisingly similar to the target travel times, though this is unlikely to be the case for most facilities with such clear differences between target and uncalibrated speeds.

Table 15: Summary of the average absolute speed errors for the uncalibrated facility

Error	All Speeds	$v_{i,p} < 65$	$v_{i,p} < 55$	$v_{i,p} < 45$	$v_{i,p} < 35$
Uncalibrated	6.12 mph	12.91 mph	17.21 mph	21.83 mph	36.86 mph

Based on the large differences seen in the speed contours, it is clear that this facility must be calibrated before it can be used for any study or decision-making analysis. Despite having predicted travel times not far off from the target values, it is still desirable to run the model through the demand calibration process (Phase 1) due to the clear misrepresentation of congestion seen in the speeds. The following two sections present the results of applying the two stage calibration process.

Analysis Period	Seg. 1	Seg. 2	Seg. 3	Seg. 4	Seg. 5	Seg. 6	Seg. 7	Seg. 8	Seg. 9	Seg. 10	Seg. 11	Seg. 12	Seg. 13	Seg. 14	Seg. 15	Seg. 16	Seg. 17	Seg. 18	Seg. 19	Seg. 20	Seg. 21	Seg. 22	Seg. 23	Seg. 24	Seg. 25	Seg. 26	Seg. 27	Seg. 28	Seg. 29
#1 6:00 - 6:15	65.4	72.6	72.6	72.6	73.0	73.0	73.0	73.0	73.0	73.0	73.4	74.1	74.1	74.1	73.6	73.7	73.7	73.7	72.4	70.5	70.5	70.5	71.8	71.1	71.1	71.1	71.1	72.8	72.8
#2 6:15 - 6:30	68.9	70.4	70.4	70.4	72.5	72.5	72.5	72.1	72.1	72.1	73.3	73.9	73.9	73.9	74.0	74.3	74.3	74.3	74.1	73.4	73.4	73.4	74.5	74.5	74.5	74.5	74.5	72.7	72.7
#3 6:30 - 6:45	73.2	70.8	70.8	70.8	71.1	71.1	71.1	71.5	71.5	71.5	73.1	72.5	72.5	72.5	73.5	73.1	73.1	73.1	72.5	72.0	72.0	72.0	71.7	73.7	73.7	73.7	73.7	72.9	72.9
#4 6:45 - 7:00	72.5	72.6	72.6	72.6	71.3	71.3	71.3	71.6	71.6	71.6	70.8	71.0	71.0	71.0	72.4	71.7	71.7	71.7	71.7	70.8	70.8	70.8	72.0	72.9	72.9	72.9	72.9	73.5	73.5
#5 7:00 - 7:15	73.7	70.3	70.3	70.3	70.7	70.7	70.7	71.9	71.9	71.9	73.3	71.9	71.9	71.9	72.5	72.5	72.5	72.5	72.5	70.8	70.8	70.8	71.7	72.1	72.1	72.1	72.1	73.7	73.7
#6 7:15 - 7:30	68.6	67.6	67.6	67.6	68.4	68.4	68.4	68.4	68.4	68.4	67.4	67.3	67.3	67.3	69.4	68.3	68.3	68.3	69.8	69.1	69.1	69.1	71.7	72.1	72.1	72.1	72.1	71.7	71.7
#7 7:30 - 7:45	67.9	64.7	64.7	64.7	68.6	68.6	68.6	60.9	60.9	60.9	46.5	48.8	48.8	48.8	63.9	62.8	62.8	62.8	59.0	59.1	59.1	59.1	66.4	70.1	70.1	70.1	70.1	70.9	70.9
#8 7:45 - 8:00	71.3	68.7	68.7	68.7	67.8	67.8	67.8	53.9	53.9	53.9	31.5	38.7	38.7	38.7	45.3	46.4	46.4	46.4	36.0	53.9	53.9	53.9	64.8	68.5	68.5	68.5	68.5	68.5	68.5
#9 8:00 - 8:15	71.3	68.1	68.1	68.1	67.1	67.1	67.1	56.1	56.1	56.1	36.8	41.0	41.0	41.0	36.9	43.9	43.9	43.9	44.2	55.1	55.1	55.1	62.3	67.6	67.6	67.6	67.6	70.2	70.2
#10 8:15 - 8:30	72.7	68.7	68.7	68.7	67.5	67.5	67.5	67.3	67.3	67.3	55.9	43.0	43.0	43.0	35.8	43.8	43.8	43.8	42.2	56.9	56.9	56.9	64.6	69.1	69.1	69.1	69.1	71.1	71.1
#11 8:30 - 8:45	70.3	70.8	70.8	70.8	73.0	73.0	73.0	70.5	70.5	70.5	64.3	59.0	59.0	59.0	57.7	54.9	54.9	54.9	46.7	57.0	57.0	57.0	63.8	69.5	69.5	69.5	69.5	70.2	70.2
#12 8:45 - 9:00	71.8	70.9	70.9	70.9	71.1	71.1	71.1	70.1	70.1	70.1	70.3	70.0	70.0	70.0	63.4	54.9	54.9	54.9	57.8	62.4	62.4	62.4	65.7	68.1	68.1	68.1	68.1	70.0	70.0
#13 9:00 - 9:15	73.3	70.9	70.9	70.9	69.7	69.7	69.7	70.3	70.3	70.3	72.9	72.9	72.9	72.9	72.6	73.0	73.0	73.0	73.1	71.2	71.2	71.2	72.5	72.2	72.2	72.2	72.2	73.2	73.2
#14 9:15 - 9:30	73.8	69.8	69.8	69.8	71.3	71.3	71.3	73.6	73.6	73.6	73.3	72.6	72.6	72.6	72.5	73.0	73.0	73.0	72.6	72.3	72.3	72.3	74.4	73.3	73.3	73.3	73.3	73.9	73.9
#15 9:30 - 9:45	70.1	68.5	68.5	68.5	68.3	68.3	68.3	69.8	69.8	69.8	71.4	72.7	72.7	72.7	73.1	73.4	73.4	73.4	73.9	71.7	71.7	71.7	72.1	72.2	72.2	72.2	72.2	73.0	73.0
#16 9:45 - 10:00	67.2	68.7	68.7	68.7	68.2	68.2	68.2	68.1	68.1	68.1	68.9	70.1	70.1	70.1	71.0	71.1	71.1	71.1	71.1	70.5	70.5	70.5	71.9	71.3	71.3	71.3	71.3	72.9	72.9
#17 10:00 - 10:15	69.8	69.1	69.1	69.1	67.4	67.4	67.4	67.7	67.7	67.7	68.1	69.7	69.7	69.7	69.0	70.7	70.7	70.7	71.4	70.7	70.7	70.7	72.7	72.3	72.3	72.3	72.3	72.6	72.6
#18 10:15 - 10:30	72.5	66.9	66.9	66.9	69.1	69.1	69.1	72.7	72.7	72.7	74.4	74.0	74.0	74.0	72.9	72.1	72.1	72.1	72.3	71.1	71.1	71.1	73.5	74.2	74.2	74.2	74.2	73.9	73.9
#19 10:30 - 10:45	69.9	69.8	69.8	69.8	70.9	70.9	70.9	70.5	70.5	70.5	70.7	71.4	71.4	71.4	71.1	71.6	71.6	71.6	73.7	73.3	73.3	73.3	73.3	73.6	73.6	73.6	73.6	73.5	73.5
#20 10:45 - 11:00	69.0	67.0	67.0	67.0	68.0	68.0	68.0	68.3	68.3	68.3	69.4	69.7	69.7	69.7	69.6	70.5	70.5	70.5	71.4	70.8	70.8	70.8	71.5	71.8	71.8	71.8	71.8	73.1	73.1
#21 11:00 - 11:15	68.7	70.4	70.4	70.4	67.8	67.8	67.8	68.0	68.0	68.0	69.5	70.3	70.3	70.3	70.5	73.5	73.5	73.5	74.1	72.0	72.0	72.0	71.1	71.5	71.5	71.5	71.5	72.5	72.5
#22 11:15 - 11:30	68.0	70.3	70.3	70.3	67.7	67.7	67.7	70.4	70.4	70.4	68.1	70.2	70.2	70.2	73.2	73.5	73.5	73.5	72.9	72.2	72.2	72.2	71.4	72.4	72.4	72.4	72.4	72.7	72.7

Analysis Period	Seg. 1	Seg. 2	Seg. 3	Seg. 4	Seg. 5	Seg. 6	Seg. 7	Seg. 8	Seg. 9	Seg. 10	Seg. 11	Seg. 12	Seg. 13	Seg. 14	Seg. 15	Seg. 16	Seg. 17	Seg. 18	Seg. 19	Seg. 20	Seg. 21	Seg. 22	Seg. 23	Seg. 24	Seg. 25	Seg. 26	Seg. 27	Seg. 28	Seg. 29
#1 6:00 - 6:15	75.0	71.0	69.4	74.6	71.9	63.3	70.9	71.0	73.5	68.8	74.3	66.9	72.0	69.4	73.5	69.1	71.6	68.5	73.2	67.7	71.7	68.6	73.1	67.9	71.5	74.7	70.4	74.5	74.4
#2 6:15 - 6:30	74.6	70.4	69.3	73.7	69.1	61.6	67.6	70.2	71.6	68.6	73.1	65.6	69.2	68.9	71.6	67.7	68.5	68.3	71.1	66.6	68.7	68.5	71.0	66.7	68.4	73.8	70.0	74.5	73.3
#3 6:30 - 6:45	73.9	69.8	69.2	72.3	65.4	59.0	63.3	69.0	69.0	68.5	71.3	64.1	65.6	65.6	69.1	64.6	64.6	64.6	68.4	64.8	64.8	64.8	68.2	64.4	64.4	72.4	69.6	74.4	71.6
#4 6:45 - 7:00	72.7	69.0	69.1	70.3	60.8	55.1	57.9	65.7	65.7	65.7	68.9	61.0	61.0	61.0	65.7	59.7	59.7	59.7	64.8	60.0	60.0	60.0	64.5	59.4	59.4	70.5	69.2	73.6	69.3
#5 7:00 - 7:15	71.1	66.4	66.9	29.7	35.9	54.1	56.8	64.3	64.3	64.3	67.8	58.5	58.5	58.5	63.9	56.6	56.6	56.6	62.5	56.7	56.7	56.7	62.0	55.8	55.8	69.0	69.0	72.9	67.5
#6 7:15 - 7:30	71.6	62.5	24.6	18.4	35.1	54.2	56.9	64.6	64.6	64.6	68.0	59.1	59.1	59.1	64.4	57.5	57.5	57.5	63.2	57.6	57.6	57.6	62.7	56.9	56.9	69.4	69.0	73.1	68.1
#7 7:30 - 7:45	66.3	36.3	20.8	18.4	35.3	54.2	56.9	64.9	64.9	64.9	68.2	59.7	59.7	59.7	64.8	58.2	58.2	58.2	63.7	58.4	58.4	58.4	63.3	57.7	57.7	69.8	69.1	73.3	68.5
#8 7:45 - 8:00	61.2	34.4	20.8	18.4	35.5	54.2	56.9	65.1	65.1	65.1	68.4	60.2	60.2	60.2	65.2	58.9	58.9	58.9	64.2	59.2	59.2	59.2	64.0	58.7	58.7	70.2	69.1	73.5	68.9
#9 8:00 - 8:15	67.3	51.7	21.3	18.5	35.6	54.2	56.9	65.3	65.3	65.3	68.6	60.8	60.8	60.8	65.6	59.5	59.5	59.5	64.7	60.0	60.0	60.0	64.5	59.5	59.5	70.5	69.2	73.6	69.3
#10 8:15 - 8:30	73.8	69.3	54.2	26.6	36.4	54.2	56.9	65.9	65.9	65.9	69.0	62.0	62.0	62.0	66.5	61.2	61.2	61.2	65.9	61.8	61.8	61.8	65.9	61.5	61.5	71.3	69.4	74.0	70.3
#11 8:30 - 8:45	74.4	70.2	69.3	73.1	67.3	60.2	65.2	69.6	70.3	68.6	72.2	64.9	67.4	67.4	70.3	66.6	66.6	66.6	69.8	65.8	66.8	66.8	69.6	65.8	66.4	73.1	69.8	74.5	72.5
#12 8:45 - 9:00	74.8	70.6	69.4	74.0	69.8	62.0	68.4	70.4	72.1	68.7	73.4	66.0	69.9	69.1	72.1	68.0	69.3	68.4	71.7	66.9	69.4	68.5	71.6	67.0	69.1	74.0	70.1	74.5	73.6
#13 9:00 - 9:15	75.0	70.9	69.4	74.6	71.7	63.1	70.6	70.9	73.3	68.8	74.2	66.8	71.7	69.4	73.3	68.9	71.3	68.5	73.0	67.6	71.4	68.6	72.9	67.8	71.2	74.6	70.4	74.5	74.3
#14 9:15 - 9:30	75.0	71.1	69.4	74.6	72.4	63.5	71.5	71.1	73.7	68.8	74.5	67.1	72.4	69.5	73.8	69.3	72.0	68.5	73.5	67.9	72.1	68.7	73.4	68.1	71.9	74.8	70.5	74.5	74.6
#15 9:30 - 9:45	75.0	71.2	69.4	74.6	73.0	63.9	72.2	71.3	74.1	68.8	74.5	67.3	73.0	69.6	74.1	69.6	72.7	68.6	73.9	68.2	72.7	68.7	73.8	68.4	72.6	74.9	70.6	74.5	74.7
#16 9:45 - 10:00	75.0	71.3	69.4	74.6	73.5	64.2	72.6	71.5	74.4	68.8	74.5	67.6	73.5	69.8	74.4	69.8	73.2	68.6	74.2	68.4	73.3	68.8	74.2	68.6	73.2	75.0	70.7	74.5	74.9
#17 10:00 - 10:15	75.0	71.5	69.4	74.6	73.9	64.4	72.7	71.6	74.6	68.9	74.5	67.8	74.0	69.9	74.6	70.1	73.7	68.7	74.5	68.6	73.8	68.8	74.5	68.9	73.7	75.0	70.8	74.6	75.0
#18 10:15 - 10:30	75.0	71.5	69.4	74.6	73.9	64.4	72.7	71.6	74.6	68.9	74.5	67.8	73.9	69.9	74.6	70.1	73.7	68.7	74.5	68.6	73.8	68.8	74.5	68.8	73.7	75.0	70.8	74.6	75.0
#19 10:30 - 10:45	75.0	71.5	69.4	74.6	73.9	64.4	72.7	71.6	74.6	68.9	74.5	67.8	73.9	69.9	74.6	70.1	73.7	68.7	74.5	68.6	73.7	68.8	74.5	68.8	73.7	75.0	70.8	74.6	75.0
#20 10:45 - 11:00	75.0	71.5	69.4	74.6	73.9	64.4	72.7	71.6	74.6	68.9	74.5	67.8	73.9	69.9	74.6	70.1	73.7	68.7	74.5	68.6	73.7	68.8	74.5	68.8	73.6	75.0	70.8	74.6	75.0
#21 11:00 - 11:15	75.0	71.4	69.4	74.6	73.8	64.4	72.7	71.6	74.6	68.9	74.5	67.8	73.9	69.9	74.6	70.1	73.7	68.7	74.5	68.6	73.7	68.8	74.5	68.8	73.6	75.0	70.8	74.6	75.0
#22 11:15 - 11:30	75.0	71.4	69.4	74.6	73.8	64.4	72.7	71.6	74.6	68.9	74.5	67.7	73.8	69.8	74.6	70.0	73.6	68.6	74.4	68.6	73.6	68.8	74.4	68.8	73.5	75.0	70.8	74.6	74.9

Figure 44: Speeds obtained from the real-world sensor data for Tuesday, August 19th, 2014 (top) and those initially predicted by the FREEVAL computational engine for the un-calibrated I-540 case study facility

Table 16: Facility travel times based on the target speeds compared to those from the uncalibrated facility

Analysis Period	Target Facility Travel Time (minutes)	Uncalibrated Travel Time (minutes)	Difference (minutes)	Percent (Difference)
#1 6:00 - 6:15	11.98	12.12	0.14	1.13%
#2 6:15 - 6:30	11.85	12.43	0.59	4.95%
#3 6:30 - 6:45	11.98	12.93	0.95	7.90%
#4 6:45 - 7:00	12.07	13.71	1.64	13.58%
#5 7:00 - 7:15	12.07	14.86	2.80	23.18%
#6 7:15 - 7:30	12.54	15.61	3.07	24.53%
#7 7:30 - 7:45	14.26	16.00	1.74	12.17%
#8 7:45 - 8:00	16.56	15.95	-0.61	-3.68%
#9 8:00 - 8:15	16.27	15.49	-0.77	-4.76%
#10 8:15 - 8:30	15.45	14.25	-1.20	-7.78%
#11 8:30 - 8:45	13.76	12.67	-1.09	-7.94%
#12 8:45 - 9:00	13.08	12.35	-0.73	-5.59%
#13 9:00 - 9:15	12.07	12.15	0.08	0.65%
#14 9:15 - 9:30	11.92	12.07	0.16	1.32%
#15 9:30 - 9:45	12.13	12.01	-0.11	-0.93%
#16 9:45 - 10:00	12.37	11.96	-0.41	-3.30%
#17 10:00 - 10:15	12.37	11.92	-0.45	-3.66%
#18 10:15 - 10:30	12.00	11.92	-0.07	-0.62%
#19 10:30 - 10:45	12.05	11.92	-0.13	-1.08%
#20 10:45 - 11:00	12.39	11.92	-0.47	-3.76%
#21 11:00 - 11:15	12.26	11.93	-0.33	-2.72%
#22 11:15 - 11:30	12.16	11.93	-0.23	-1.90%
Average	12.89	13.10	0.21	1.60%
Avg Absolute Error	-	-	0.81	6.27%

4.3.8 Phase 1 Calibration Results

The phase 1 genetic algorithm approach was applied in order to estimate a set of demand volumes for the first calibration stage. Since the uncalibrated speed contours were significantly different than the target speeds, the n-distribution approach was used in conjunction with the known AADT estimates to determine a new set of demand profiles for the facility entry and exit points. With the new unified approach, the capacity drop factor was considered in conjunction with the demand estimation. 97 Based on the size of the facility and the length of the study period, an initial population size of 200 organisms was specified. Additionally, the recommended 2:1 ratio of weights for $\lambda 1$ and $\lambda 2$ was used, where the facility travel time was given twice as much weight as the individual segment speeds. Table 17 gives a summary of the parameters used to conduct the Phase 1 calibration, including the parameters controlling the estimation of the new demand

profiles. An explanation of these distribution parameters can be found in the previous chapter concerning the demand estimation framework.

Table 17: Summary of the parameters used for the Phase 1 calibration

Phase 1 Calibration and GA Run Parameters	Value
Population Size	200
Max Iterations	400
Binary Encoding Digits	5
Crossover Mixing %	50%
Mutation Rate	5%
Capacity Drop %	0%-10%
Demand Distribution Parameters	**Range**
Random Variable Weight (w_i)	0.05,0.5
Mean 1 (μ_1)	7am - 10am
Mean 1 (μ_1)	Unrestricted
Mean 1 (μ_1)	4pm - 7pm
Std. Deviation (σ_i)	0.5, 5.0
Skewness (α_i)	-10,10

A run of the Phase 1 calibration was successfully able to estimate new demand profiles for the model as well as estimate that the capacity drop factor is 5%. A summary of the average absolute speed errors for different speed regimes can be found in Table 18. Additionally, Figure 45 shows a comparison of the target speed contour and the new partially calibrated speed contour, while Table 19 provides a full breakdown of the remaining error between the target and predicted travel times. It is clear from both the summary table and the speed contours that there was a significant reduction in error for the individual segment speeds. This came despite the error in travel time being weighted significantly more heavily. The overall reduction of error between target and predicted speeds was 98 around 36%, and for the lowest speed regimes, the reduction in error was around 80%! From Table 19 it can be seen that there was an increase in the error in travel time from the uncalibrated model, but this is only due to the uncalibrated model having an unnaturally close travel time estimate, and cannot be viewed as a negative since the uncalibrated travel time was only “good" when considered independently from the clearly incorrect predicted speeds. It is also important to note that the average predicted travel time is only 3.38% off from the average target travel time. This is well within the recommended accuracy of 10% recommended in the HCM’s current calibration procedure (Highway Capacity Manual 2016).

Table 18: Summary results for the Phase 1 calibration run. All errors are the average absolute difference in speed

Error	All Speeds	$v_{i,p} < 65$	$v_{i,p} < 55$	$v_{i,p} < 45$	$v_{i,p} < 35$
Uncalibrated	6.12 mph	12.91 mph	17.21 mph	21.83 mph	36.86 mph
After Phase 1	4.15 mph	7.24 mph	6.55 mph	4.19 mph	7.54 mph
% Improvement	32.09%	43.86%	61.97%	80.78%	79.53%

Analysis Period	Seg. 1	Seg. 2	Seg. 3	Seg. 4	Seg. 5	Seg. 6	Seg. 7	Seg. 8	Seg. 9	Seg. 10	Seg. 11	Seg. 12	Seg. 13	Seg. 14	Seg. 15	Seg. 16	Seg. 17	Seg. 18	Seg. 19	Seg. 20	Seg. 21	Seg. 22	Seg. 23	Seg. 24	Seg. 25	Seg. 26	Seg. 27	Seg. 28	Seg. 29
#1 6:00 - 6:15	65.4	72.6	72.6	72.6	73.0	73.0	73.0	73.0	73.0	73.0	73.4	74.1	74.1	74.1	73.6	73.7	73.7	73.7	72.4	70.5	70.5	70.5	71.8	71.1	71.1	71.1	71.1	72.8	72.8
#2 6:15 - 6:30	68.9	70.4	70.4	70.4	72.5	72.5	72.5	72.1	72.1	72.1	73.3	73.9	73.9	73.9	74.0	74.3	74.3	74.3	74.1	73.4	73.4	73.4	74.5	74.5	74.5	74.5	74.5	72.7	72.7
#3 6:30 - 6:45	73.2	70.8	70.8	70.8	71.1	71.1	71.1	71.5	71.5	71.5	73.1	72.5	72.5	72.5	73.5	73.1	73.1	73.1	72.5	72.0	72.0	72.0	71.7	73.7	73.7	73.7	73.7	72.9	72.9
#4 6:45 - 7:00	72.5	72.6	72.6	72.6	71.3	71.3	71.3	71.6	71.6	71.6	70.8	71.0	71.0	71.0	72.4	71.7	71.7	71.7	71.7	70.8	70.8	70.8	72.0	72.9	72.9	72.9	72.9	73.5	73.5
#5 7:00 - 7:15	73.7	70.3	70.3	70.3	70.7	70.7	70.7	71.9	71.9	71.9	73.3	71.9	71.9	71.9	72.5	72.5	72.5	72.5	72.5	70.8	70.8	70.8	71.7	72.1	72.1	72.1	72.1	73.7	73.7
#6 7:15 - 7:30	68.6	67.6	67.6	67.6	68.4	68.4	68.4	68.4	68.4	68.4	67.4	67.3	67.3	67.3	69.4	68.3	68.3	68.3	69.8	69.1	69.1	69.1	71.7	72.1	72.1	72.1	72.1	71.7	71.7
#7 7:30 - 7:45	67.9	64.7	64.7	64.7	68.6	68.6	68.6	60.9	60.9	60.9	46.5	48.8	48.8	48.8	63.9	62.8	62.8	62.8	59.0	59.1	59.1	59.1	66.4	70.1	70.1	70.1	70.1	70.9	70.9
#8 7:45 - 8:00	71.3	68.7	68.7	68.7	67.8	67.8	67.8	53.9	53.9	53.9	31.5	38.7	38.7	38.7	45.3	46.4	46.4	46.4	36.0	53.9	53.9	53.9	64.8	68.5	68.5	68.5	68.5	68.5	68.5
#9 8:00 - 8:15	71.3	68.1	68.1	68.1	67.1	67.1	67.1	56.1	56.1	56.1	36.8	41.0	41.0	41.0	36.9	43.9	43.9	43.9	44.2	55.1	55.1	55.1	62.3	67.6	67.6	67.6	67.6	70.2	70.2
#10 8:15 - 8:30	72.7	68.7	68.7	68.7	67.5	67.5	67.5	67.3	67.3	67.3	55.9	43.0	43.0	43.0	35.8	43.8	43.8	43.8	42.2	56.9	56.9	56.9	64.6	69.1	69.1	69.1	69.1	71.1	71.1
#11 8:30 - 8:45	70.3	70.8	70.8	70.8	73.0	73.0	73.0	70.5	70.5	70.5	64.3	59.0	59.0	59.0	57.7	54.9	54.9	54.9	46.7	57.0	57.0	57.0	63.8	69.5	69.5	69.5	69.5	70.2	70.2
#12 8:45 - 9:00	71.8	70.9	70.9	70.9	71.1	71.1	71.1	70.1	70.1	70.1	70.3	70.0	70.0	70.0	63.4	54.9	54.9	54.9	57.8	62.4	62.4	62.4	65.7	68.1	68.1	68.1	68.1	70.0	70.0
#13 9:00 - 9:15	73.3	70.9	70.9	70.9	69.7	69.7	69.7	70.3	70.3	70.3	72.9	72.9	72.9	72.9	72.6	73.0	73.0	73.0	73.1	71.2	71.2	71.2	72.5	72.2	72.2	72.2	72.2	73.2	73.2
#14 9:15 - 9:30	73.8	69.8	69.8	69.8	71.3	71.3	71.3	73.6	73.6	73.6	73.3	72.6	72.6	72.6	72.5	73.0	73.0	73.0	72.6	72.3	72.3	72.3	74.4	73.3	73.3	73.3	73.3	73.9	73.9
#15 9:30 - 9:45	70.1	68.5	68.5	68.5	68.3	68.3	68.3	69.8	69.8	69.8	71.4	72.7	72.7	72.7	73.1	73.4	73.4	73.4	73.9	71.7	71.7	71.7	72.1	72.2	72.2	72.2	72.2	73.0	73.0
#16 9:45 - 10:00	67.2	68.7	68.7	68.7	68.2	68.2	68.2	68.1	68.1	68.1	68.9	70.1	70.1	70.1	71.0	71.1	71.1	71.1	71.1	70.5	70.5	70.5	71.9	71.3	71.3	71.3	71.3	72.9	72.9
#17 10:00 - 10:15	69.8	69.1	69.1	69.1	67.4	67.4	67.4	67.7	67.7	67.7	68.1	69.7	69.7	69.7	69.0	70.7	70.7	70.7	71.4	70.7	70.7	70.7	72.7	72.3	72.3	72.3	72.3	72.6	72.6
#18 10:15 - 10:30	72.5	66.9	66.9	66.9	69.1	69.1	69.1	72.7	72.7	72.7	74.4	74.0	74.0	74.0	72.9	72.1	72.1	72.1	72.3	71.1	71.1	71.1	73.5	74.2	74.2	74.2	74.2	73.9	73.9
#19 10:30 - 10:45	69.9	69.8	69.8	69.8	70.9	70.9	70.9	70.5	70.5	70.5	70.7	71.4	71.4	71.4	71.1	71.6	71.6	71.6	73.7	73.3	73.3	73.3	73.3	73.6	73.6	73.6	73.6	73.5	73.5
#20 10:45 - 11:00	69.0	67.0	67.0	67.0	68.0	68.0	68.0	68.3	68.3	68.3	69.4	69.7	69.7	69.7	69.6	70.5	70.5	70.5	71.4	70.8	70.8	70.8	71.5	71.8	71.8	71.8	71.8	73.1	73.1
#21 11:00 - 11:15	68.7	70.4	70.4	70.4	67.8	67.8	67.8	68.0	68.0	68.0	69.5	70.3	70.3	70.3	70.5	73.5	73.5	73.5	74.1	72.0	72.0	72.0	71.1	71.5	71.5	71.5	71.5	72.5	72.5
#22 11:15 - 11:30	68.0	70.3	70.3	70.3	67.7	67.7	67.7	70.4	70.4	70.4	68.1	70.2	70.2	70.2	73.2	73.5	73.5	73.5	72.9	72.2	72.2	72.2	71.4	72.4	72.4	72.4	72.4	72.7	72.7

Analysis Period	Seg. 1	Seg. 2	Seg. 3	Seg. 4	Seg. 5	Seg. 6	Seg. 7	Seg. 8	Seg. 9	Seg. 10	Seg. 11	Seg. 12	Seg. 13	Seg. 14	Seg. 15	Seg. 16	Seg. 17	Seg. 18	Seg. 19	Seg. 20	Seg. 21	Seg. 22	Seg. 23	Seg. 24	Seg. 25	Seg. 26	Seg. 27	Seg. 28	Seg. 29
#1 6:00 - 6:15	75.0	72.1	69.3	74.6	75.0	65.7	73.0	72.2	75.0	68.6	74.4	67.9	74.6	70.5	74.8	70.0	73.7	69.4	74.1	68.4	73.3	68.8	74.1	68.7	73.3	75.0	71.3	74.6	74.7
#2 6:15 - 6:30	75.0	71.8	69.4	74.6	75.0	65.5	72.9	72.0	75.0	68.6	74.5	67.5	74.1	70.3	74.5	69.7	73.1	69.4	73.5	68.2	72.6	68.7	73.8	68.5	72.9	74.9	71.5	74.6	74.4
#3 6:30 - 6:45	75.0	71.5	69.6	74.6	74.7	65.0	72.8	71.7	74.7	68.8	74.5	66.7	72.7	70.0	73.3	68.8	71.1	69.3	71.7	67.3	70.3	68.5	72.2	67.8	70.9	74.5	71.4	74.6	73.3
#4 6:45 - 7:00	75.0	71.0	69.6	74.6	73.1	64.0	72.4	71.1	73.8	68.8	74.5	65.3	70.0	69.7	70.9	67.3	67.7	67.7	68.5	65.9	66.5	66.5	69.6	66.7	67.9	73.6	71.3	74.5	71.1
#5 7:00 - 7:15	74.5	70.4	69.6	73.4	69.6	62.0	68.3	70.3	71.9	68.8	73.1	62.9	65.5	65.5	66.8	62.3	62.3	62.3	63.3	60.7	60.7	60.7	65.4	63.0	63.0	71.9	71.2	73.2	67.2
#6 7:15 - 7:30	73.3	69.7	69.5	71.6	64.6	58.7	62.8	69.5	69.7	68.7	71.4	60.1	61.0	61.0	62.6	57.1	57.1	57.1	58.3	55.0	55.0	55.0	61.4	58.4	58.4	70.1	70.1	71.7	63.4
#7 7:30 - 7:45	72.1	69.2	69.5	70.0	60.2	55.1	58.0	67.6	67.6	67.6	69.5	56.1	49.5	42.5	32.7	56.8	50.5	54.4	38.5	56.8	56.8	56.8	63.0	60.3	60.3	70.8	70.8	72.3	64.7
#8 7:45 - 8:00	71.8	69.0	69.1	69.4	57.9	53.0	55.5	66.1	59.6	37.1	24.0	40.0	40.1	34.9	30.2	49.4	48.0	41.2	35.7	56.9	56.9	56.9	63.3	60.6	60.6	71.0	71.0	72.3	64.7
#9 8:00 - 8:15	72.6	69.3	69.5	70.5	60.3	55.2	58.1	67.3	48.1	31.1	20.4	37.1	40.7	35.8	29.5	48.0	45.8	48.5	36.7	56.9	56.9	56.9	63.7	61.1	61.1	71.1	71.1	72.4	65.1
#10 8:15 - 8:30	73.9	70.0	69.6	72.3	65.0	58.9	63.1	69.4	64.4	44.4	22.2	37.0	42.0	44.0	32.6	47.3	45.4	40.3	35.3	56.9	56.9	56.9	63.9	61.2	61.2	71.2	71.2	72.5	65.3
#11 8:30 - 8:45	74.8	70.6	69.6	73.8	69.3	61.8	67.9	70.2	71.8	68.8	66.1	56.7	47.7	39.7	31.3	49.3	42.1	37.6	35.2	56.9	56.9	56.9	64.1	61.5	61.5	71.3	71.2	72.6	65.7
#12 8:45 - 9:00	75.0	71.2	69.6	74.6	72.5	63.6	71.6	71.0	73.6	68.8	74.4	60.9	61.5	62.9	43.7	48.0	41.0	39.5	35.3	56.9	56.9	56.9	64.2	61.5	61.5	71.3	71.1	72.7	66.0
#13 9:00 - 9:15	75.0	71.6	69.5	74.6	74.3	64.6	72.7	71.5	74.5	68.8	74.5	62.7	68.1	68.1	69.4	68.4	62.7	62.3	48.3	59.8	59.8	59.8	66.1	63.6	63.6	72.1	71.2	73.3	67.6
#14 9:15 - 9:30	75.0	71.8	69.4	74.6	74.9	65.2	72.8	71.8	74.9	68.7	74.5	63.6	69.8	69.5	71.0	67.2	67.6	67.6	68.3	65.7	66.0	66.0	70.1	66.8	68.2	73.7	71.5	74.5	71.1
#15 9:30 - 9:45	75.0	72.0	69.2	74.6	75.0	65.5	72.9	72.1	75.0	68.6	74.4	64.5	71.2	69.7	72.3	68.0	69.4	69.3	70.0	66.4	68.0	68.0	71.3	67.3	69.6	74.2	71.6	74.6	72.2
#16 9:45 - 10:00	75.0	72.2	69.1	74.6	75.0	65.7	73.0	72.2	75.0	68.4	74.4	65.0	72.1	69.7	73.1	68.6	70.6	69.4	71.2	67.0	69.4	68.1	72.1	67.7	70.7	74.5	71.5	74.6	73.0
#17 10:00 - 10:15	75.0	72.3	69.1	74.6	75.0	65.8	73.0	72.4	75.0	68.3	74.4	65.3	72.7	69.8	73.6	69.0	71.5	69.4	72.1	67.3	70.5	68.2	72.7	68.0	71.4	74.7	71.7	74.6	73.4
#18 10:15 - 10:30	75.0	72.3	69.0	74.6	75.0	65.9	73.0	72.4	75.0	68.3	74.4	65.6	73.1	69.8	74.0	69.2	72.0	69.4	72.5	67.5	71.0	68.3	73.1	68.1	71.8	74.7	71.6	74.6	73.7
#19 10:30 - 10:45	75.0	72.4	68.9	74.6	75.0	65.9	73.0	72.5	75.0	68.3	74.4	68.0	74.9	70.5	74.8	70.6	74.6	69.5	74.8	68.8	74.2	68.6	74.8	69.2	74.3	75.0	72.0	74.7	74.9
#20 10:45 - 11:00	75.0	72.4	68.9	74.5	75.0	65.9	73.0	72.5	75.0	68.3	74.4	68.2	75.0	70.5	74.8	70.6	74.7	69.5	74.8	68.9	74.3	68.6	74.8	69.2	74.3	75.0	72.0	74.7	74.9
#21 11:00 - 11:15	75.0	72.4	68.9	74.5	75.0	66.0	73.0	72.6	75.0	68.3	74.4	68.3	75.0	70.6	74.8	70.8	74.9	69.5	74.8	69.0	74.6	68.6	74.8	69.4	74.6	75.0	71.7	74.7	75.0
#22 11:15 - 11:30	75.0	72.3	68.8	74.5	75.0	66.0	73.0	72.6	75.0	68.3	74.4	68.5	75.0	70.6	74.8	71.0	74.9	69.4	74.8	69.2	74.8	68.6	74.8	69.6	74.8	75.0	71.8	74.7	75.0

Figure 45: Comparison of the target speed contour (top) and the speed contour as predicted by the partially calibrated facility after Phase 1

Table 19: Facility travel times based on the target speeds compared to those from the facility after Phase 1 calibration

Analysis Period	Target Facility Travel Time (minutes)	Phase 1 Calibration Travel Time (minutes)	Difference (minutes)	Percent (Difference)
#1 6:00 - 6:15	11.98	11.90	-0.08	-0.67%
#2 6:15 - 6:30	11.85	11.95	0.10	0.87%
#3 6:30 - 6:45	11.98	12.11	0.13	1.05%
#4 6:45 - 7:00	12.07	12.43	0.36	2.95%
#5 7:00 - 7:15	12.07	13.12	1.05	8.72%
#6 7:15 - 7:30	12.54	13.95	1.41	11.27%
#7 7:30 - 7:45	14.26	15.19	0.93	6.51%
#8 7:45 - 8:00	16.56	17.05	0.49	3.01%
#9 8:00 - 8:15	16.27	17.53	1.26	7.78%
#10 8:15 - 8:30	15.45	16.61	1.16	7.51%
#11 8:30 - 8:45	13.76	15.47	1.71	12.43%
#12 8:45 - 9:00	13.08	14.52	1.44	11.04%
#13 9:00 - 9:15	12.07	13.06	0.99	8.23%
#14 9:15 - 9:30	11.92	12.41	0.49	4.13%
#15 9:30 - 9:45	12.13	12.25	0.12	1.00%
#16 9:45 - 10:00	12.37	12.15	-0.22	-1.81%
#17 10:00 - 10:15	12.37	12.08	-0.29	-2.36%
#18 10:15 - 10:30	12.00	12.04	0.04	0.39%
#19 10:30 - 10:45	12.05	11.85	-0.20	-1.72%
#20 10:45 - 11:00	12.39	11.84	-0.55	-4.44%
#21 11:00 - 11:15	12.26	11.83	-0.43	-3.51%
#22 11:15 - 11:30	12.16	11.82	-0.34	-2.85%
Average	12.89	13.32	0.43	3.38%
Avg Absolute Error	-	-	0.62	4.82%

4.3.9 Phase 2 Calibration Results

Overall, the Phase 1 calibration showed a large improvement over the initial uncalibrated model and reduced many of the largest speed errors. Though there was a small increase in the average facility error, the maximum error for an individual study period was reduced, and the speed contour reflects the target behavior much more faithfully. However, this only represents a partial calibration, and two key aspects of capacity calibration have yet to be addressed. This partially calibrated model can now be run through Phase 2 of the calibration to estimate the set of pre-breakdown capacity adjustments, as well as the adjust the facility wide jam density. A range of 0.85 to 1.05 was specified for the set of pre-breakdown CAFs of each HCM segment. A range of 180 to 220 veh/mi/ln was used for the facility-wide jam density. Based on the size of the facility and the length of the study period, an initial population size of 200 organisms was specified. Table 20 summarizes the parameters, and five GA runs were conducted to calibrate the facility.

Table 20: Summary of the parameters used for the Phase 2 calibration runs

Phase 2 Calibration and GA Run Parameters	Value
Population Size	200
Max Iterations	400
Binary Encoding Digits	5
Crossover Mixing %	50%
Mutation Rate	5%
Pre-breakdown CAF Range	0.85 - 1.05
Jam Density Range	180-220 veh/mi/ln

Running Phase 2 calibration successfully estimated a set of pre-breakdown capacity adjustments as well as the facility-wide jam density. The set of pre-breakdown CAFs can be seen in Figure 47, and the capacity drop was estimated to be 5%, while the facility-wide jam density was estimated to be 189 veh/mi/ln. A summary of the average absolute speed errors for different speed regimes can be found in Table 21. Additionally, Figure 46 shows a comparison of the target speed contour and the new partially calibrated speed contour, while Table 22 provides a full breakdown of the remaining error between the target and predicted travel times, as well as improvements over the Phase 1 calibration. The Phase 2 calibration show improvement on both the total speed error, as well as for the individual speed regimes. Perhaps most importantly, a model calibrated through the two stage process showed a reduction in speed error of over 60% for speeds lower than 65mph, and a reduction of 70% for all speeds lower than 55 mph! In terms of travel time, Table 22 shows a further reduction in error for most analysis periods. All but one analysis period falls within 10% of the target travel time, and the average error is just 2.1%.

Table 21: Summary results for the Phase 1 calibration run. All errors are the average absolute difference in speed

Error	All Speeds	$v_{i,p} < 65$	$v_{i,p} < 55$	$v_{i,p} < 45$	$v_{i,p} < 35$
Uncalibrated	6.12 mph	12.91 mph	17.21 mph	21.83 mph	36.86 mph
After Phase 1	4.15 mph	7.24 mph	6.55 mph	4.19 mph	7.54 mph
% Improvement	32.09%	43.86%	61.97%	80.78%	79.53%
After Phase 2	3.73 mph	4.85 mph	4.67 mph	3.32 mph	2.62 mph
% Improvement over Phase 1	10.13%	33.05%	28.55%	20.86%	65.28%
% Improvement over uncalibrated	39.05%	62.43%	72.86%	84.79%	92.89%

These results clearly indicate that the model predicts performance far more consistent with the real world performance measures after the two-stage calibration process. While the predicted speeds do not match the real world data perfectly, they clearly show a congested regime far more consistent with the observed recurring congestion. Further, not only did each phase of the process improve upon the previous “best" calibration, but the process overall resulted in a model in which all key calibration parameters have at least been considered, and likely adjusted when necessary.

Analysis Period	Seg. 1	Seg. 2	Seg. 3	Seg. 4	Seg. 5	Seg. 6	Seg. 7	Seg. 8	Seg. 9	Seg. 10	Seg. 11	Seg. 12	Seg. 13	Seg. 14	Seg. 15	Seg. 16	Seg. 17	Seg. 18	Seg. 19	Seg. 20	Seg. 21	Seg. 22	Seg. 23	Seg. 24	Seg. 25	Seg. 26	Seg. 27	Seg. 28	Seg. 29
#1 6:00 - 6:15	65.4	72.6	72.6	72.6	73.0	73.0	73.0	73.0	73.0	73.0	73.4	74.1	74.1	74.1	73.6	73.7	73.7	73.7	72.4	70.5	70.5	70.5	71.8	71.1	71.1	71.1	71.1	72.8	72.8
#2 6:15 - 6:30	68.9	70.4	70.4	70.4	72.5	72.5	72.5	72.1	72.1	72.1	73.3	73.9	73.9	73.9	74.0	74.3	74.3	74.3	74.1	73.4	73.4	73.4	74.5	74.5	74.5	74.5	74.5	72.7	72.7
#3 6:30 - 6:45	73.2	70.8	70.8	70.8	71.1	71.1	71.1	71.5	71.5	71.5	73.1	72.5	72.5	72.5	73.5	73.1	73.1	73.1	72.5	72.0	72.0	72.0	71.7	73.7	73.7	73.7	73.7	72.9	72.9
#4 6:45 - 7:00	72.5	72.6	72.6	72.6	71.3	71.3	71.3	71.6	71.6	71.6	70.8	71.0	71.0	71.0	72.4	71.7	71.7	71.7	71.7	70.8	70.8	70.8	72.0	72.9	72.9	72.9	72.9	73.5	73.5
#5 7:00 - 7:15	73.7	70.3	70.3	70.3	70.7	70.7	70.7	71.9	71.9	71.9	73.3	71.9	71.9	71.9	72.5	72.5	72.5	72.5	72.5	70.8	70.8	70.8	71.7	72.1	72.1	72.1	72.1	73.7	73.7
#6 7:15 - 7:30	68.6	67.6	67.6	67.6	68.4	68.4	68.4	68.4	68.4	68.4	67.4	67.3	67.3	67.3	69.4	68.3	68.3	68.3	69.8	69.1	69.1	69.1	71.7	72.1	72.1	72.1	72.1	71.7	71.7
#7 7:30 - 7:45	67.9	64.7	64.7	64.7	68.6	68.6	68.6	60.9	60.9	60.9	46.5	48.8	48.8	48.8	63.9	62.8	62.8	62.8	59.0	59.1	59.1	59.1	66.4	70.1	70.1	70.1	70.1	70.9	70.9
#8 7:45 - 8:00	71.3	68.7	68.7	68.7	67.8	67.8	67.8	53.9	53.9	53.9	31.5	38.7	38.7	38.7	45.3	46.4	46.4	46.4	36.0	53.9	53.9	53.9	64.8	68.5	68.5	68.5	68.5	68.5	68.5
#9 8:00 - 8:15	71.3	68.1	68.1	68.1	67.1	67.1	67.1	56.1	56.1	56.1	36.8	41.0	41.0	41.0	36.9	43.9	43.9	43.9	44.2	55.1	55.1	55.1	62.3	67.6	67.6	67.6	67.6	70.2	70.2
#10 8:15 - 8:30	72.7	68.7	68.7	68.7	67.5	67.5	67.5	67.3	67.3	67.3	55.9	43.0	43.0	43.0	35.8	43.8	43.8	43.8	42.2	56.9	56.9	56.9	64.6	69.1	69.1	69.1	69.1	71.1	71.1
#11 8:30 - 8:45	70.3	70.8	70.8	70.8	73.0	73.0	73.0	70.5	70.5	70.5	64.3	59.0	59.0	59.0	57.7	54.9	54.9	54.9	46.7	57.0	57.0	57.0	63.8	69.5	69.5	69.5	69.5	70.2	70.2
#12 8:45 - 9:00	71.8	70.9	70.9	70.9	71.1	71.1	71.1	70.1	70.1	70.1	70.3	70.0	70.0	70.0	63.4	54.9	54.9	54.9	57.8	62.4	62.4	62.4	65.7	68.1	68.1	68.1	68.1	70.0	70.0
#13 9:00 - 9:15	73.3	70.9	70.9	70.9	69.7	69.7	69.7	70.3	70.3	70.3	72.9	72.9	72.9	72.9	72.6	73.0	73.0	73.0	73.1	71.2	71.2	71.2	72.5	72.2	72.2	72.2	72.2	73.2	73.2
#14 9:15 - 9:30	73.8	69.8	69.8	69.8	71.3	71.3	71.3	73.6	73.6	73.6	73.3	72.6	72.6	72.6	72.5	73.0	73.0	73.0	72.6	72.3	72.3	72.3	74.4	73.3	73.3	73.3	73.3	73.9	73.9
#15 9:30 - 9:45	70.1	68.5	68.5	68.5	68.3	68.3	68.3	69.8	69.8	69.8	71.4	72.7	72.7	72.7	73.1	73.4	73.4	73.4	73.9	71.7	71.7	71.7	72.1	72.2	72.2	72.2	72.2	73.0	73.0
#16 9:45 - 10:00	67.2	68.7	68.7	68.7	68.2	68.2	68.2	68.1	68.1	68.1	68.9	70.1	70.1	70.1	71.0	71.1	71.1	71.1	71.1	70.5	70.5	70.5	71.9	71.3	71.3	71.3	71.3	72.9	72.9
#17 10:00 - 10:15	69.8	69.1	69.1	69.1	67.4	67.4	67.4	67.7	67.7	67.7	68.1	69.7	69.7	69.7	69.0	70.7	70.7	70.7	71.4	70.7	70.7	70.7	72.7	72.3	72.3	72.3	72.3	72.6	72.6
#18 10:15 - 10:30	72.5	66.9	66.9	66.9	69.1	69.1	69.1	72.7	72.7	72.7	74.4	74.0	74.0	74.0	72.9	72.1	72.1	72.1	72.3	71.1	71.1	71.1	73.5	74.2	74.2	74.2	74.2	73.9	73.9
#19 10:30 - 10:45	69.9	69.8	69.8	69.8	70.9	70.9	70.9	70.5	70.5	70.5	70.7	71.4	71.4	71.4	71.1	71.6	71.6	71.6	73.7	73.3	73.3	73.3	73.3	73.6	73.6	73.6	73.6	73.5	73.5
#20 10:45 - 11:00	69.0	67.0	67.0	67.0	68.0	68.0	68.0	68.3	68.3	68.3	69.4	69.7	69.7	69.7	69.6	70.5	70.5	70.5	71.4	70.8	70.8	70.8	71.5	71.8	71.8	71.8	71.8	73.1	73.1
#21 11:00 - 11:15	68.7	70.4	70.4	70.4	67.8	67.8	67.8	68.0	68.0	68.0	69.5	70.3	70.3	70.3	70.5	73.5	73.5	73.5	74.1	72.0	72.0	72.0	71.1	71.5	71.5	71.5	71.5	72.5	72.5
#22 11:15 - 11:30	68.0	70.3	70.3	70.3	67.7	67.7	67.7	70.4	70.4	70.4	68.1	70.2	70.2	70.2	73.2	73.5	73.5	73.5	72.9	72.2	72.2	72.2	71.4	72.4	72.4	72.4	72.4	72.7	72.7

Analysis Period	Seg. 1	Seg. 2	Seg. 3	Seg. 4	Seg. 5	Seg. 6	Seg. 7	Seg. 8	Seg. 9	Seg. 10	Seg. 11	Seg. 12	Seg. 13	Seg. 14	Seg. 15	Seg. 16	Seg. 17	Seg. 18	Seg. 19	Seg. 20	Seg. 21	Seg. 22	Seg. 23	Seg. 24	Seg. 25	Seg. 26	Seg. 27	Seg. 28	Seg. 29
#1 6:00 - 6:15	75.0	72.0	69.3	74.6	75.0	65.7	73.0	72.1	74.5	68.6	74.5	67.8	74.6	70.5	74.2	69.9	74.0	69.4	74.0	68.3	73.8	68.8	73.0	68.5	74.0	75.0	71.2	74.6	74.7
#2 6:15 - 6:30	75.0	71.8	69.5	74.6	75.0	65.4	72.9	71.9	74.0	68.6	74.5	67.4	74.2	70.2	73.5	69.5	73.4	69.3	73.4	68.0	73.3	68.6	72.4	68.4	73.6	75.0	71.4	74.6	74.4
#3 6:30 - 6:45	74.9	71.4	69.6	74.6	74.9	64.9	72.8	71.5	72.7	68.7	74.3	66.5	72.8	70.0	71.5	68.5	71.6	69.3	71.5	67.0	71.3	68.4	70.1	67.5	72.1	74.7	71.3	74.6	73.2
#4 6:45 - 7:00	74.2	70.9	69.6	74.6	73.8	63.7	72.5	70.4	70.1	68.8	72.8	64.9	70.1	68.5	67.9	66.8	68.4	69.1	68.2	65.5	68.1	68.1	66.5	66.3	69.6	74.0	71.2	73.8	70.9
#5 7:00 - 7:15	72.5	70.3	69.6	73.4	71.0	61.5	70.0	66.3	65.9	68.8	69.7	62.2	65.6	63.1	62.0	63.4	63.4	64.4	62.8	62.7	63.0	63.0	60.8	64.0	65.5	72.5	68.9	72.0	66.8
#6 7:15 - 7:30	69.9	68.1	67.0	71.6	66.8	57.7	65.3	62.2	61.6	65.7	66.7	57.1	61.0	57.8	56.2	58.5	58.5	59.8	57.6	57.9	57.9	57.9	55.4	61.5	61.6	70.9	66.2	70.0	62.9
#7 7:30 - 7:45	67.6	65.7	64.2	70.0	63.1	53.5	61.2	58.4	57.7	62.6	63.5	52.2	47.5	42.6	37.9	58.3	58.3	58.7	42.4	58.9	58.9	58.9	56.7	62.2	62.6	71.3	67.0	70.4	63.7
#8 7:45 - 8:00	67.0	64.8	63.3	69.4	61.1	50.9	59.1	55.8	54.9	62.8	28.9	47.1	39.5	37.7	37.1	58.3	52.7	41.6	40.3	58.9	58.9	58.9	57.2	62.4	62.9	71.5	67.2	70.5	63.8
#9 8:00 - 8:15	68.5	66.4	65.1	70.5	63.2	53.5	61.3	57.9	56.1	60.4	30.1	46.0	47.8	42.3	37.6	43.7	40.8	38.9	39.7	58.9	58.9	58.9	57.8	62.7	63.4	71.6	67.5	70.7	64.2
#10 8:15 - 8:30	71.1	69.3	68.3	72.3	67.2	57.9	65.6	62.0	61.5	65.4	39.1	42.3	38.6	41.0	38.6	48.4	45.8	40.0	39.6	58.9	58.9	58.9	57.9	62.8	63.4	71.7	67.5	70.8	64.4
#11 8:30 - 8:45	73.3	70.5	69.6	73.9	70.8	61.2	69.6	66.2	65.8	68.8	58.8	49.2	42.5	60.4	52.5	52.9	46.8	41.1	39.6	58.9	58.9	58.9	58.3	62.9	63.7	71.8	67.7	71.0	64.8
#12 8:45 - 9:00	74.6	71.0	69.6	74.6	73.4	63.3	72.4	69.9	69.6	68.8	72.4	60.4	65.8	62.1	61.6	59.1	57.5	50.2	43.0	59.0	59.0	59.0	58.5	63.0	63.8	71.8	67.8	71.1	65.2
#13 9:00 - 9:15	75.0	71.5	69.6	74.6	74.7	64.5	72.7	71.4	72.1	68.8	74.0	62.3	68.5	66.6	66.2	65.7	66.8	67.5	66.2	64.4	66.1	66.1	65.6	65.8	68.8	73.7	71.2	73.3	69.7
#14 9:15 - 9:30	75.0	71.8	69.4	74.6	75.0	65.1	72.8	71.7	73.4	68.7	74.5	63.4	70.2	68.6	68.4	66.9	68.7	69.2	68.3	65.4	68.0	67.8	67.4	66.5	70.1	74.2	71.5	73.9	71.1
#15 9:30 - 9:45	75.0	72.0	69.3	74.6	75.0	65.4	72.9	72.0	74.2	68.6	74.4	64.3	71.5	69.6	70.2	67.8	70.3	69.3	70.0	66.2	69.7	68.0	69.1	67.1	71.2	74.5	71.5	74.4	72.2
#16 9:45 - 10:00	75.0	72.1	69.2	74.6	75.0	65.6	72.9	72.2	74.6	68.4	74.4	64.8	72.4	69.7	71.5	68.4	71.4	69.3	71.2	66.8	70.9	68.1	70.2	67.5	72.1	74.7	71.5	74.6	73.0
#17 10:00 - 10:15	75.0	72.2	69.1	74.6	75.0	65.7	73.0	72.3	74.9	68.4	74.4	65.2	72.9	69.7	72.3	68.8	72.2	69.3	72.1	67.2	71.7	68.2	71.1	67.8	72.6	74.8	71.6	74.6	73.4
#18 10:15 - 10:30	75.0	72.3	69.0	74.6	75.0	65.8	73.0	72.4	75.0	68.4	74.4	65.4	73.3	69.7	72.8	69.1	72.6	69.4	72.5	67.4	72.2	68.3	71.5	68.0	72.9	74.9	71.6	74.6	73.7
#19 10:30 - 10:45	75.0	72.3	68.9	74.6	75.0	65.9	73.0	72.5	75.0	68.3	74.4	67.1	74.6	70.1	74.4	70.0	74.3	69.4	74.2	68.3	73.9	68.5	73.5	68.7	74.2	75.0	71.8	74.7	74.7
#20 10:45 - 11:00	75.0	72.3	68.9	74.6	75.0	65.9	73.0	72.5	75.0	68.3	74.4	68.1	75.0	70.5	74.8	70.5	74.8	69.5	74.8	68.7	74.6	68.6	74.3	69.1	74.7	75.0	71.9	74.7	74.9
#21 11:00 - 11:15	75.0	72.3	68.9	74.5	75.0	65.9	73.0	72.5	75.0	68.3	74.4	68.3	75.0	70.5	74.8	70.7	74.9	69.5	74.8	68.9	74.8	68.6	74.6	69.3	74.9	75.0	71.7	74.7	75.0
#22 11:15 - 11:30	75.0	72.3	68.8	74.5	75.0	66.0	73.0	72.6	75.0	68.3	74.4	68.5	75.0	70.5	74.8	70.9	74.9	69.5	74.8	69.1	74.9	68.6	74.8	69.5	75.0	75.0	71.8	74.7	75.0

Figure 46: Comparison of target speed contour (top) and the speed contour as predicted by the calibrated facility after Phase 2

Table 22: Facility travel times based on the target speeds compared to those from facility after Phase 2 calibration

Analysis Period	Target Facility Travel Time (minutes)	Phase 2 Calibration Travel Time (minutes)	Difference (minutes)	Percent (Difference)
#1 6:00 - 6:15	11.98	11.91	-0.08	-0.63%
#2 6:15 - 6:30	11.85	11.96	0.12	0.97%
#3 6:30 - 6:45	11.98	12.14	0.16	1.30%
#4 6:45 - 7:00	12.07	12.49	0.42	3.45%
#5 7:00 - 7:15	12.07	13.22	1.16	9.58%
#6 7:15 - 7:30	12.54	14.15	1.61	12.86%
#7 7:30 - 7:45	14.26	15.32	1.05	7.39%
#8 7:45 - 8:00	16.56	16.47	-0.08	-0.49%
#9 8:00 - 8:15	16.27	16.25	-0.02	-0.10%
#10 8:15 - 8:30	15.45	16.13	0.68	4.39%
#11 8:30 - 8:45	13.76	15.10	1.34	9.74%
#12 8:45 - 9:00	13.08	13.69	0.61	4.70%
#13 9:00 - 9:15	12.07	12.61	0.54	4.48%
#14 9:15 - 9:30	11.92	12.39	0.47	3.94%
#15 9:30 - 9:45	12.13	12.23	0.10	0.84%
#16 9:45 - 10:00	12.37	12.13	-0.25	-1.99%
#17 10:00 - 10:15	12.37	12.06	-0.31	-2.54%
#18 10:15 - 10:30	12.00	12.02	0.03	0.22%
#19 10:30 - 10:45	12.05	11.89	-0.17	-1.39%
#20 10:45 - 11:00	12.39	11.84	-0.55	-4.47%
#21 11:00 - 11:15	12.26	11.83	-0.43	-3.54%
#22 11:15 - 11:30	12.16	11.82	-0.35	-2.86%
Average	12.89	13.16	0.27	2.1%
Avg Absolute Error	-	-	0.48	3.71%

Figure 47 shows the set of pre-breakdown CAFs as estimated by the GA algorithm. It is immediately clear that there exists some “noise" within the generated values, and the capacity of some segments has been adjusted even when no adjustment was needed. This can occur due a lack of sensitivity to the parameter for segments whose D/C ratio is significantly below 1.0. In these cases, neither increasing nor decreasing the capacity has much if any effect on the predicted speeds. Consequently, it may be prudent for an analyst to perform a basic sensitivity analysis to re-adjust some of the estimated CAFs back to the default value. Alternatively, the encoding proposed previously could be adjusted to explicitly constrain the location and/or number of allowed pre-breakdown adjustments. It will be clear for certain facilities, for geometric or other factors, there are a specific number of bottlenecks, or bottlenecks at specific locations, that require pre-breakdown adjustments to be estimated. It is possible to constrain how the set of pre-breakdown CAFs is determined by altering the existing coding for pre-breakdown CAFs proposed earlier. The altered encoding should allow both the location and the value of a pre-specified number of CAFs to be varied by the GA framework. A special case of this encoding can be developed where both the number and location of the CAFs is specified by an analyst, and only the adjustment value is varied by the GA search process.

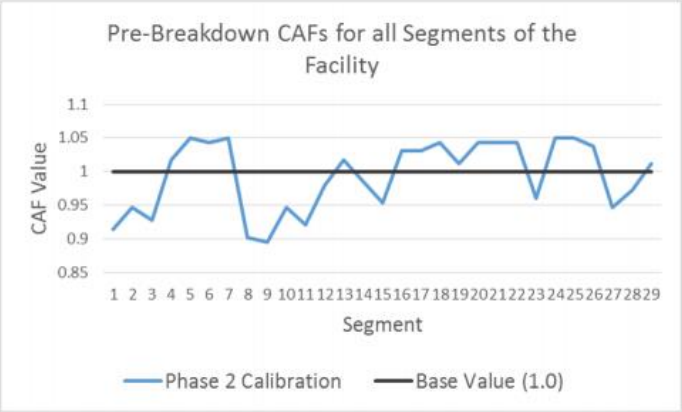

Figure 47: Chart showing the set of pre-breakdown CAFs for all segments of the facility as estimated during the Phase 2 calibration process

If an analyst specifies that n pre-breakdown CAFs should be determined, the encoding will have 2n variables, one segment index variable and one adjustment value for each location. The adjustment can be encoded into a binary string in the same manner as for the full set of adjustments 106 presented previously, but the array of segment locations must be treated as a real-valued array if it is not fixed by the analyst. Unfortunately, the segment locations cannot be encoded as binary values because a single integer value that is not a power of two cannot readily be represented as a binary string. Unlike floating point values, when dealing solely with integers, step sizes and basic rounding cannot be employed as there is no general way to ensure the representation is balanced across the full search range. However, when dealing with an array of integer values, the individual values can maintain their base 10 representation, and the array can be treated in largely the same manner as a binary string. Most common crossover operators would require no adjustment as they simply switch values between arrays. Mutation operators will require slight alterations as they have to consider the range of values for the integer value using a probability distribution (e.g.,

uniform or Gaussian) instead of just the two binary possibilities. While real-value GA encodings such as this are not uncommon, they do lack many of the most desirable properties of a binary encoding, and may result in slower convergence. In the event that the number adjustments is limited to just one segment, an exhaustive search is likely a better option than the GA framework. Further, an exhaustive search is computationally tractable regardless of whether the location of the single adjustment is fixed or allowed to vary. The computational time should not exceed that of the GA approach, and the optimal solution is guaranteed to be found. With a CAF step size of 0.001 and a range of [0.5,1.0], there are 500 potential values for the adjustment. If the location of the adjustment is fixed, the FREEVAL core engine would need to be invoked 500 times, which would have a computational burden equivalent to evolving a population of 100 organisms for 5 generations. This is less than 1% of the effort spent in each of the calibration phases for this case study where a population of 200 organisms was evolved over 400 generations. Even if the location of the adjustment is not fixed, and is allowed to be any of a facility's segments, the burden still remains comparatively small. It is highly unlikely a facility will have more than 50 segments, and if the exhaustive search must be conducted for as many as 50 segments, the computational burden still remains less than 50% of a typical phase of the calibration process. Further, if the step size is limited to 0.01, the burden is reduced by a factor of ten! This special case of allowing a single CAF to be adjusted was explored for the I-540 case study. The exhaustive search approach for the single pre-breakdown capacity adjustment at an unknown segment location was performed. The search determined that the optimal location for the CAF is at segment 15, and the optimal CAF value is 0.94. Table 23 shows a breakdown of the remaining errors in speeds by regime for this special case Phase 2 calibration, and Figure 48 shows the new speed contour. While the reduction in speed error is not quite as good as when the full set of CAFs is allowed to be adjusted, the special case Phase 2 still showed significant improvement over the Phase 1 calibration. Further, it provides a more easily justifiable alteration of capacities for the facility. 107 The adjustment at segment 15 caused the D/C ratio to be above 1.0 for analysis periods 8 and 9 (7:45am-8:15am) leading to the active bottleneck as seen in both the target and predicted contours.

Table 23: Summary results for the Phase 1 calibration run, all errors are the average absolute difference in speed

Error	All Speeds	$v_{i,p} < 65$	$v_{i,p} < 55$	$v_{i,p} < 45$	$v_{i,p} < 35$
Uncalibrated	6.12 mph	12.91 mph	17.21 mph	21.83 mph	36.86 mph
After Phase 1	4.15 mph	7.24 mph	6.55 mph	4.19 mph	7.54 mph
% Improvement	32.09%	43.86%	61.97%	80.78%	79.53%
Phase 2 All CAF	3.73 mph	4.85 mph	4.67 mph	3.32 mph	2.62 mph
% Improvement over Phase 1	10.13%	33.05%	28.55%	20.86%	65.28%
% Improvement over uncalibrated	39.05%	62.43%	72.86%	84.79%	92.89%
Phase 2 Single CAF	3.77 mph	5.77 mph	5.41 mph	3.45 mph	3.73 mph
% Improvement over Phase 1	9.10%	20.26%	17.25%	17.75%	50.57%
% Improvement over uncalibrated	38.27%	55.23%	68.53%	84.19%	89.88%

Analysis Period	Seg. 1	Seg. 2	Seg. 3	Seg. 4	Seg. 5	Seg. 6	Seg. 7	Seg. 8	Seg. 9	Seg. 10	Seg. 11	Seg. 12	Seg. 13	Seg. 14	Seg. 15	Seg. 16	Seg. 17	Seg. 18	Seg. 19	Seg. 20	Seg. 21	Seg. 22	Seg. 23	Seg. 24	Seg. 25	Seg. 26	Seg. 27	Seg. 28	Seg. 29
#1 6:00 - 6:15	65.4	72.6	72.6	72.6	73.0	73.0	73.0	73.0	73.0	73.0	73.4	74.1	74.1	74.1	73.6	73.7	73.7	73.7	72.4	70.5	70.5	70.5	71.8	71.1	71.1	71.1	71.1	72.8	72.8
#2 6:15 - 6:30	68.9	70.4	70.4	70.4	72.5	72.5	72.5	72.1	72.1	72.1	73.3	73.9	73.9	73.9	74.0	74.3	74.3	74.3	74.1	73.4	73.4	73.4	74.5	74.5	74.5	74.5	74.5	72.7	72.7
#3 6:30 - 6:45	73.2	70.8	70.8	70.8	71.1	71.1	71.1	71.5	71.5	71.5	73.1	72.5	72.5	72.5	73.5	73.1	73.1	73.1	72.5	72.0	72.0	72.0	71.7	73.7	73.7	73.7	73.7	72.9	72.9
#4 6:45 - 7:00	72.5	72.6	72.6	72.6	71.3	71.3	71.3	71.6	71.6	71.6	70.8	71.0	71.0	71.0	72.4	71.7	71.7	71.7	71.7	70.8	70.8	70.8	72.0	72.9	72.9	72.9	72.9	73.5	73.5
#5 7:00 - 7:15	73.7	70.3	70.3	70.3	70.7	70.7	70.7	71.9	71.9	71.9	73.3	71.9	71.9	71.9	72.5	72.5	72.5	72.5	72.5	70.8	70.8	70.8	71.7	72.1	72.1	72.1	72.1	73.7	73.7
#6 7:15 - 7:30	68.6	67.6	67.6	67.6	68.4	68.4	68.4	68.4	68.4	68.4	67.4	67.3	67.3	67.3	69.4	68.3	68.3	68.3	69.8	69.1	69.1	69.1	71.7	72.1	72.1	72.1	72.1	71.7	71.7
#7 7:30 - 7:45	67.9	64.7	64.7	64.7	68.6	68.6	68.6	60.9	60.9	60.9	46.5	48.8	48.8	48.8	63.9	62.8	62.8	62.8	59.0	59.1	59.1	59.1	66.4	70.1	70.1	70.1	70.1	70.9	70.9
#8 7:45 - 8:00	71.3	68.7	68.7	68.7	67.8	67.8	67.8	53.9	53.9	53.9	31.5	38.7	38.7	38.7	45.3	46.4	46.4	46.4	36.0	53.9	53.9	53.9	64.8	68.5	68.5	68.5	68.5	68.5	68.5
#9 8:00 - 8:15	71.3	68.1	68.1	68.1	67.1	67.1	67.1	56.1	56.1	56.1	36.8	41.0	41.0	41.0	36.9	43.9	43.9	43.9	44.2	55.1	55.1	55.1	62.3	67.6	67.6	67.6	67.6	70.2	70.2
#10 8:15 - 8:30	72.7	68.7	68.7	68.7	67.5	67.5	67.5	67.3	67.3	67.3	55.9	43.0	43.0	43.0	35.8	43.8	43.8	43.8	42.2	56.9	56.9	56.9	64.6	69.1	69.1	69.1	69.1	71.1	71.1
#11 8:30 - 8:45	70.3	70.8	70.8	70.8	73.0	73.0	73.0	70.5	70.5	70.5	64.3	59.0	59.0	59.0	57.7	54.9	54.9	54.9	46.7	57.0	57.0	57.0	63.8	69.5	69.5	69.5	69.5	70.2	70.2
#12 8:45 - 9:00	71.8	70.9	70.9	70.9	71.1	71.1	71.1	70.1	70.1	70.1	70.3	70.0	70.0	70.0	63.4	54.9	54.9	54.9	57.8	62.4	62.4	62.4	65.7	68.1	68.1	68.1	68.1	70.0	70.0
#13 9:00 - 9:15	73.3	70.9	70.9	70.9	69.7	69.7	69.7	70.3	70.3	70.3	72.9	72.9	72.9	72.9	72.6	73.0	73.0	73.0	73.1	71.2	71.2	71.2	72.5	72.2	72.2	72.2	72.2	73.2	73.2
#14 9:15 - 9:30	73.8	69.8	69.8	69.8	71.3	71.3	71.3	73.6	73.6	73.6	73.3	72.6	72.6	72.6	72.5	73.0	73.0	73.0	72.6	72.3	72.3	72.3	74.4	73.3	73.3	73.3	73.3	73.9	73.9
#15 9:30 - 9:45	70.1	68.5	68.5	68.5	68.3	68.3	68.3	69.8	69.8	69.8	71.4	72.7	72.7	72.7	73.1	73.4	73.4	73.4	73.9	71.7	71.7	71.7	72.1	72.2	72.2	72.2	72.2	73.0	73.0
#16 9:45 - 10:00	67.2	68.7	68.7	68.7	68.2	68.2	68.2	68.1	68.1	68.1	68.9	70.1	70.1	70.1	71.0	71.1	71.1	71.1	71.1	70.5	70.5	70.5	71.9	71.3	71.3	71.3	71.3	72.9	72.9
#17 10:00 - 10:15	69.8	69.1	69.1	69.1	67.4	67.4	67.4	67.7	67.7	67.7	68.1	69.7	69.7	69.7	69.0	70.7	70.7	70.7	71.4	70.7	70.7	70.7	72.7	72.3	72.3	72.3	72.3	72.6	72.6
#18 10:15 - 10:30	72.5	66.9	66.9	66.9	69.1	69.1	69.1	72.7	72.7	72.7	74.4	74.0	74.0	74.0	72.9	72.1	72.1	72.1	72.3	71.1	71.1	71.1	73.5	74.2	74.2	74.2	74.2	73.9	73.9
#19 10:30 - 10:45	69.9	69.8	69.8	69.8	70.9	70.9	70.9	70.5	70.5	70.5	70.7	71.4	71.4	71.4	71.1	71.6	71.6	71.6	73.7	73.3	73.3	73.3	73.3	73.6	73.6	73.6	73.6	73.5	73.5
#20 10:45 - 11:00	69.0	67.0	67.0	67.0	68.0	68.0	68.0	68.3	68.3	68.3	69.4	69.7	69.7	69.7	69.6	70.5	70.5	70.5	71.4	70.8	70.8	70.8	71.5	71.8	71.8	71.8	71.8	73.1	73.1
#21 11:00 - 11:15	68.7	70.4	70.4	70.4	67.8	67.8	67.8	68.0	68.0	68.0	69.5	70.3	70.3	70.3	70.5	73.5	73.5	73.5	74.1	72.0	72.0	72.0	71.1	71.5	71.5	71.5	71.5	72.5	72.5
#22 11:15 - 11:30	68.0	70.3	70.3	70.3	67.7	67.7	67.7	70.4	70.4	70.4	68.1	70.2	70.2	70.2	73.2	73.5	73.5	73.5	72.9	72.2	72.2	72.2	71.4	72.4	72.4	72.4	72.4	72.7	72.7

Analysis Period	Seg. 1	Seg. 2	Seg. 3	Seg. 4	Seg. 5	Seg. 6	Seg. 7	Seg. 8	Seg. 9	Seg. 10	Seg. 11	Seg. 12	Seg. 13	Seg. 14	Seg. 15	Seg. 16	Seg. 17	Seg. 18	Seg. 19	Seg. 20	Seg. 21	Seg. 22	Seg. 23	Seg. 24	Seg. 25	Seg. 26	Seg. 27	Seg. 28	Seg. 29
#1 6:00 - 6:15	75.0	72.1	69.3	74.6	75.0	65.7	73.0	72.2	75.0	68.6	74.4	68.0	74.7	70.6	74.3	70.1	73.9	69.4	74.2	68.6	73.5	68.9	74.3	68.8	73.5	75.0	71.3	74.6	74.8
#2 6:15 - 6:30	75.0	71.9	69.4	74.6	75.0	65.5	72.9	72.1	75.0	68.6	74.5	67.6	74.3	70.4	73.8	69.9	73.3	69.4	73.7	68.3	72.9	68.7	74.0	68.7	73.1	75.0	71.5	74.6	74.5
#3 6:30 - 6:45	75.0	71.6	69.6	74.6	74.8	65.1	72.8	71.7	74.8	68.8	74.5	66.9	73.0	70.1	71.9	69.0	71.5	69.3	72.1	67.5	70.8	68.5	72.6	68.0	71.4	74.6	71.5	74.6	73.6
#4 6:45 - 7:00	75.0	71.1	69.6	74.6	73.4	64.1	72.6	71.2	74.0	68.8	74.5	65.6	70.5	69.7	68.7	67.6	68.3	68.3	69.1	66.2	67.3	67.3	70.2	66.9	68.5	73.8	71.4	74.6	71.5
#5 7:00 - 7:15	74.6	70.5	69.6	73.6	70.1	62.3	68.9	70.4	72.2	68.9	73.3	63.4	66.3	66.3	63.3	63.3	63.3	63.3	64.3	61.8	61.8	61.8	66.2	63.9	63.9	72.2	71.2	73.4	67.9
#6 7:15 - 7:30	73.5	69.9	69.6	72.0	65.4	59.3	63.8	69.7	70.2	68.8	71.8	60.8	62.1	62.1	58.0	58.4	58.4	58.4	59.5	56.4	56.4	56.4	62.4	59.6	59.6	70.5	70.5	72.1	64.3
#7 7:30 - 7:45	72.4	69.4	69.5	70.5	61.3	56.1	59.3	68.3	68.3	68.3	70.1	57.5	52.9	42.3	36.4	56.8	50.6	55.1	38.7	56.8	56.8	56.8	63.0	60.3	60.3	70.8	70.8	72.3	64.7
#8 7:45 - 8:00	72.1	69.2	69.5	69.9	59.1	54.2	56.9	66.9	64.2	57.3	27.8	38.9	41.8	35.4	36.4	49.8	45.4	39.7	35.8	56.9	56.9	56.9	63.3	60.7	60.7	71.0	71.0	72.3	64.8
#9 8:00 - 8:15	72.9	69.5	69.5	70.9	61.4	56.2	59.3	68.0	63.2	43.2	22.4	41.0	43.6	36.2	33.5	47.3	45.8	48.2	36.8	56.9	56.9	56.9	63.8	61.2	61.2	71.2	71.2	72.5	65.2
#10 8:15 - 8:30	74.0	70.1	69.6	72.6	65.8	59.5	64.1	69.6	70.1	68.8	40.2	44.4	45.9	41.5	37.8	47.8	45.2	40.5	35.5	56.9	56.9	56.9	63.9	61.3	61.3	71.2	71.2	72.5	65.3
#11 8:30 - 8:45	74.8	70.7	69.6	74.0	69.9	62.1	68.5	70.4	72.2	68.8	65.4	54.0	55.6	40.2	49.1	45.1	44.6	40.8	35.3	56.9	56.9	56.9	64.1	61.5	61.5	71.3	71.2	72.7	65.7
#12 8:45 - 9:00	75.0	71.2	69.6	74.6	72.8	63.8	71.9	71.1	73.8	68.8	74.5	61.3	65.8	65.8	60.6	59.4	56.9	48.4	36.8	56.9	56.9	56.9	64.2	61.6	61.6	71.3	71.1	72.8	66.1
#13 9:00 - 9:15	75.0	71.6	69.5	74.6	74.5	64.7	72.8	71.6	74.6	68.8	74.5	62.9	68.5	68.5	66.5	66.0	66.0	66.0	69.9	63.7	63.7	63.7	68.7	66.1	66.6	73.2	71.5	74.1	69.8
#14 9:15 - 9:30	75.0	71.9	69.4	74.6	75.0	65.2	72.9	71.9	74.9	68.7	74.5	63.8	70.1	69.6	68.6	67.4	68.0	68.0	68.7	65.9	66.6	66.6	70.4	66.9	68.6	73.9	71.6	74.5	71.4
#15 9:30 - 9:45	75.0	72.1	69.2	74.6	75.0	65.5	72.9	72.1	75.0	68.6	74.4	64.6	71.4	69.7	70.3	68.2	69.7	69.3	70.3	66.6	68.4	68.0	71.5	67.4	70.0	74.3	71.6	74.6	72.4
#16 9:45 - 10:00	75.0	72.2	69.1	74.6	75.0	65.7	73.0	72.3	75.0	68.4	74.4	65.1	72.3	69.8	71.5	68.7	70.9	69.4	71.4	67.1	69.8	68.2	72.3	67.8	71.0	74.5	71.6	74.6	73.2
#17 10:00 - 10:15	75.0	72.3	69.1	74.6	75.0	65.8	73.0	72.4	75.0	68.3	74.4	65.4	72.8	69.8	72.3	69.1	71.7	69.4	72.3	67.5	70.8	68.3	72.9	68.1	71.7	74.7	71.7	74.7	73.6
#18 10:15 - 10:30	75.0	72.3	69.0	74.6	75.0	65.9	73.0	72.5	75.0	68.3	74.4	67.6	74.7	70.3	74.6	70.3	74.2	69.5	74.4	68.6	73.6	68.5	74.5	69.0	73.9	75.0	72.0	74.7	74.8
#19 10:30 - 10:45	75.0	72.4	68.9	74.6	75.0	65.9	73.0	72.5	75.0	68.2	74.4	68.1	75.0	70.5	74.8	70.6	74.7	69.5	74.8	68.9	74.3	68.6	74.8	69.3	74.5	75.0	72.0	74.7	75.0
#20 10:45 - 11:00	75.0	72.4	68.9	74.5	75.0	66.0	73.0	72.5	75.0	68.3	74.4	68.2	75.0	70.6	74.8	70.7	74.8	69.5	74.8	69.0	74.4	68.6	74.8	69.3	74.5	75.0	72.0	74.7	75.0
#21 11:00 - 11:15	75.0	72.4	68.9	74.5	75.0	66.0	73.0	72.6	75.0	68.3	74.4	68.4	75.0	70.6	74.8	70.9	74.9	69.5	74.8	69.1	74.7	68.7	74.8	69.4	74.7	75.0	71.8	74.7	75.0
#22 11:15 - 11:30	75.0	72.4	68.8	74.5	75.0	66.0	73.0	72.6	75.0	68.3	74.4	68.6	75.0	70.6	74.8	71.0	74.9	69.4	74.8	69.3	74.9	68.6	74.8	69.6	74.9	75.0	71.8	74.7	75.0

Figure 48: Comparison of target speed contour (top) and the speed contour as predicted by the methodology after the special case Phase 2 calibration with a single CAF

5.0 CONCLUSIONS

This project focused on the HCM freeway facilities analysis which plays the core role in other freeway analysis types. Other facility-based analysis in HCM is built on freeway facilities methodology such as travel time reliability, Active Traffic and Demand Management (ATDM), or Work Zone analyses. This research focused on the use of avaible data sources to streamline the HCM freeway analysis. Examples of availble data sources were investigated are a) online mapping tools and b) sensor data providing speeds. These data sources can be utilized to aid analysts perform freeway segmentation as well as demand estimation and calibration.

The research team investigated different online mapping services and evaluated information that can be gathered through these data sources. Google Maps API selected to be the best data provider for geometric data needs for freeway analysis. Beside this effort, the project team developed a segmentation procedure that can divide a freeway strech into HCM segments. The resulting HCM segments are completely matching with HCM definitions. The project team implemented the developed segmentation procedure in FREEVAL. Google Maps API also emplyed to assist analysts fill requried information (e.g. sections lengths) automatically. As a result, the entire procedure of segmentatin automated in FREEVAL computational engine.

The project also developed methods to estimate demand and calibrate analysis based on availble sensor data. The most uniform sensor database availble across US is probe-based speed data. There are several number of probe-based speed data providers such as INRIX, Here.com, and etc. The developed models to estimate demand and calibrate FREEVAL to target speed profiles/contours carried out by tuning speed, capacity and demand adjustment factors. The proposed method implemented in FREEVAL, and can be invoked to perform demand estimation and analysis calibration.

The calibration approach uses a genetic algorithm metaheuristic to automate the arduous process of concurrently adjusting large numbers of parameters to ensure the model predicts performances that matches observed real-world conditions. This project presents two encoding approaches for traffic demand estimation and adjustment. Each encoding requires an analyst to have access to average annual daily traffic (AADT) values for each entry and exit node of the facility, and allows general knowledge of demand patterns to be incorporated when available.

Considering model calibration phase, it was found that demand estimation and adjustment using the GA framework was shown to significantly improve upon uncalibrated facilities without any manual adjustments of inputs by the analyst. Combining the approach for demands with key capacity parameters resulted in an even more effective unified calibration framework. Each phase of the calibration shows significant improvement over both the uncalibrated facility and the previous best available calibration. Calibrating for both facility travel time and individual segment speeds in conjunction yields a more accurate model than calibrating facility travel time only and can eliminate cases where closely matching target and predicted travel times are misleading. When

the capacity of every segment along a facility is allowed to be adjusted, it was found that situations may arise where conflicting or unrealistic adjustments occur, likely due to overparameterization.

In summary, the automated system identification approach developed in this project represents a major improvement over the existing best practice for model calibration. The genetic algorithm framework greatly reduces the burden placed on the user and closes the gap between model creation and model utilization, a process that represents the biggest challenge for prospective analysts. Uncalibrated or poorly calibrated models have little to no practical use and consequently facility calibration is critical for utilizing the HCM methodology effectively.

Finally, the genetic algorithm framework in this research dealt strictly with calibrating a facility of the core HCM freeway facilities level. However, with slight modification, the scope of the calibration approach can be greatly expanded. Remaining within the HCM, in the event that data is available, encodings could be developed and studied for calibration of aspects of reliability analysis that spans study periods of months or even years.

6.0 REFERENCES

Blum, C. & Roli, A. (2003). “Metaheuristics in combinatorial optimization: Overview and conceptual comparison”. ACM Computing Surveys (CSUR) 35.3, pp. 268–308.

Carey, M. & Watling, D. (2012). “Dynamic traffic assignment approximating the kinematic wave model: System optimum, marginal costs, externalities and tolls”. Transportation Research Part B: Methodological 46.5, pp. 634–648.

Carey, M. et al. (2014a). “Extending travel-time based models for dynamic network loading and assignment, to achieve adherence to first-in-first-out and link capacities”. Transportation Research Part B: Methodological 65, pp. 90–104.

Carey, M. et al. (2014b). “Implementing first-in–first-out in the cell transmission model for networks”. Transportation Research Part B: Methodological 65, pp. 105–118.

Chiu, Y.-C. et al. (2011). “Dynamic traffic assignment: A primer”. Transportation Research E-Circular E-C153.

Coello, C. A. C. (2002). “Theoretical and numerical constraint-handling techniques used with evolutionary algorithms: a survey of the state of the art”. Computer Methods in Applied Mechanics and Engineering 191.11, pp. 1245–1287.

Daganzo, C. F. (1994). “The cell transmission model: A dynamic representation of highway traffic consistent with the hydrodynamic theory”. Transportation Research Part B: Methodological 28.4, pp. 269 –287.

— (1995). “The cell transmission model, part 2: Network traffic”. Transportation Research Part B: Methodological 29.2, pp. 79 –93.

De Nicolao, G (1997). “System identification: Problems and perspectives”. 12th Workshop on Qualitative Reasoning, pp. 379–386.

Delbem, A. C. et al. (2012). “Efficient forest data structure for evolutionary algorithms applied to network design”. Evolutionary Computation, IEEE Transactions on 16.6, pp. 829–846.

Doan, K. & Ukkusuri, S. V. (2012). “On the holding-back problem in the cell transmission based dynamic traffic assignment models”. Transportation Research Part B: Methodological 46.9, pp. 1218 –1238.

Elefteriadou, L. & Lertworawanich, P. (2003). “Defining, measuring and estimating freeway capacity”. Washington: Transportation Research Board Meeting.

Gendreau, M. & Potvin, J.-Y. (2005). “Metaheuristics in combinatorial optimization”. Annals of Operations Research 140.1, pp. 189–213. 117

Goldberg, D. E. (1989). Genetic Algorithms in Search, Optimization and Machine Learning. 1st. Boston, MA, USA: Addison-Wesley Longman Publishing Co., Inc.

Gomes, G. & Horowitz, R. (2006). "Optimal freeway ramp metering using the asymmetric cell transmission model". Transportation Research Part C: Emerging Technologies 14.4, pp. 244 – 262.

Gomes, G. et al. (2008). "Behavior of the cell transmission model and effectiveness of ramp metering". Transportation Research Part C: Emerging Technologies 16.4, pp. 485 –513.

Hadi, M. et al. (2014). "Pilot Testing of SHRP 2 Reliability Data and Analytical Products: Florida Pilot Site". SHRP 2 Report.

Hallenbeck, M. et al. (1997). Vehicle volume distributions by classification. Tech. rep.

Han, L. et al. (2011). "Complementarity formulations for the cell transmission model based dynamic user equilibrium with departure time choice, elastic demand and user heterogeneity". Transportation Research Part B: Methodological 45.10, pp. 1749 –1767.

Highway CapacityManual(2016). 6th Edition: A Guide forMultimodalMobility Analysis. Washington, D.C.: Transportation Research Board.

Hu, J. et al. (2012). "On linear programs with linear complementarity constraints". English. Journal of Global Optimization 53.1, pp. 29–51.

Juan, W. et al. (2012). "Genetic algorithm for multiuser discrete network design problem under demand uncertainty". Mathematical Problems in Engineering 2012.

Karoonsoontawong, A. & Waller, S. (2006). "Dynamic Continuous Network Design Problem: Linear Bilevel Programming and Metaheuristic Approaches". Transportation Research Record: Journal of the Transportation Research Board 1964, pp. 104–117. eprint: http://dx.doi.org/10.3141/1964-12.

Li, Y. et al. (2003). "A Decomposition Scheme for System Optimal Dynamic Traffic Assignment Models". Networks and Spatial Economics 3.4.

Li, Z.-b. et al. (2014). "Development of control strategy of variable speed limits for improving traffic operations at freeway bottlenecks". English. Journal of Central South University 21.6, pp. 2526– 2538.

Lighthill, M. J. & Whitham, G. B. (1955a). "On Kinematic Waves. I. Flood Movement in Long Rivers". English. Proceedings of the Royal Society of London. Series A, Mathematical and Physical Sciences 229.1178, pp. 281–316.

Lighthill, M. J. & Whitham, G. B. (1955b). "On Kinematic Waves. II. A Theory of Traffic Flow on Long Crowded Roads". Proceedings of the Royal Society of London A: Mathematical, Physical and Engineering Sciences 229.1178, pp. 317–345.

Lim, G. J. et al. (2015). “Reliability analysis of evacuation routes under capacity uncertainty of road links”. IIE Transactions 47.1, pp. 50–63. eprint: http://dx.doi.org/10.1080/0740817X.2014.905736.

Lin, D.-Y. et al. (2011). “A Dual Variable Approximation Based Heuristic for Dynamic Congestion Pricing”. English. Networks and Spatial Economics 11.2, pp. 271–293.

Lin, W.-H. & Ahanotu, D. (1995). “Validating the basic cell transmission model on a single freeway link”. PATH technical note; 95-3.

Ljung, L. (2010). “Perspectives on system identification”. Annual Reviews in Control 34.1, pp. 1–12.

Lo, H. K. (2001). “A Cell-Based Traffic Control Formulation: Strategies and Benefits of Dynamic Timing Plans”. English. Transportation Science 35.2, pp. 148–164.

Lu, C.-C. et al. (2013). “Dynamic origin–destination demand flow estimation under congested traffic conditions”. Transportation Research Part C: Emerging Technologies 34, pp. 16–37.

Luathep, P. et al. (2011). “Global optimization method for mixed transportation network design problem: A mixed-integer linear programming approach”. Transportation Research Part B: Methodological 45.5, pp. 808 –827.

Ma, T. et al. (2015). “Nonlinear multivariate time space threshold vector error correction model for short term traffic state prediction”. Transportation Research Part B: Methodological 76.0, pp. 27 –47.

Malveo, A. E. (2013). Assessing the Impact of Congestion During a Multi-County Evacuation. Tech. rep. DTIC Document.

Maryland CATT Lab, U. of (2008). RITIS:Regional Integrated Transportation Information System. URL: https://www.ritis.org/ (visited on 08/11/2016).

Mitchell, M. (1998). An introduction to genetic algorithms. MIT press.

Morbidi, F. et al. (2014). “A new robust approach for highway traffic density estimation”. Control Conference (ECC), 2014 European, pp. 2575–2580.

Mudchanatongsuk, S. et al. (2008). “Robust Solutions for Network Design under Transportation Cost and Demand Uncertainty”. English. The Journal of the Operational Research Society 59.5, pp. 652–662. 119

Munoz, L. et al. (2003). “Traffic density estimation with the cell transmission model”. American Control Conference, 2003. Proceedings of the 2003. Vol. 5, 3750–3755 vol.5.

Muñoz, L. et al. (2004). “Methodological calibration of the cell transmission model”. American Control Conference, 2004. Proceedings of the 2004. Vol. 1. IEEE, pp. 798–803.

NCDOT (2016). Planning Level Extensions to NCDOT Freeway Analysis Tools. URL: https:// connect.ncdot.gov/projects/planning/Pages/ProjDetails.aspx?ProjectID= 2015-09.

Nisbet, J. et al. (2014). Pilot Testing of SHRP 2 Reliability Data and Analytical Products: Washington.

North Carolina Department of Transportation (2016). Traffic Surveys. URL: https://www.ncdot.gov/projects/trafficsurvey/ (visited on 08/11/2016).

Pascale, A. et al. (2013). "Estimation of highway traffic from sparse sensors: Stochastic modeling and particle filtering". Acoustics, Speech and Signal Processing (ICASSP), 2013 IEEE International Conference on, pp. 6158–6162.

Pascale, A. et al. (2014). "Cooperative Bayesian Estimation of Vehicular Traffic in Large-Scale Networks". Intelligent Transportation Systems, IEEE Transactions on 15.5, pp. 2074–2088.

Richards, P. I. (1956). "Shock Waves on the Highway". English. Operations Research 4.1, pp. 42–51.

Smilowitz, K. & Daganzo, C. (1999). "Predictability of time-dependent traffic backups and other reproducible traits in experimental highway data". California Partners for Advanced Transit and Highways (PATH).

Sobolewski, M. et al. (2014). Pilot Testing of SHRP 2 Reliability Data and Analytical Products: Minnesota.

Stankova, K. & De Schutter, B. (2010). "On freeway traffic density estimation for a jump Markov linear model based on Daganzo's cell transmission model". Intelligent Transportation Systems (ITSC), 2010 13th International IEEE Conference on, pp. 13–18.

Sumalee, A. et al. (2011). "Stochastic cell transmission model (SCTM): A stochastic dynamic traffic model for traffic state surveillance and assignment". Transportation Research Part B: Methodological 45.3, pp. 507 –533.

Sun, H. et al. (2014). "Dynamic Network Design Problem under Demand Uncertainty: An Adjustable Robust Optimization Approach". Discrete Dynamics in Nature and Society 2014.

Tampère, C. & Immers, L. (2007). "An Extended Kalman Filter Application for Traffic State Estimation Using CTM with Implicit Mode Switching and Dynamic Parameters". Intelligent Transportation Systems Conference, 2007. ITSC 2007. IEEE, pp. 209–216.

Travis Waller, S. & Ziliaskopoulos, A. K. (2006). "A Combinatorial user optimal dynamic traffic assignment algorithm". English. Annals of Operations Research 144.1. Copyright - Springer Science+Business Media, LLC 2006; Last updated - 2014-08-30, pp. 249–261.

Ukkusuri, S. V. & Waller, S. T. (2008). "Linear Programming Models for the User and System Optimal Dynamic Network Design Problem: Formulations, Comparisons and Extensions". English. Networks and Spatial Economics 8.4, pp. 383–406.

Ukkusuri, S. V. et al. (2012). “Dynamic user equilibrium with a path based cell transmission model for general traffic networks”. Transportation Research Part B: Methodological 46.10, pp. 1657 –1684.

Waller, S. & Ziliaskopoulos, A. (2001). “Stochastic Dynamic Network Design Problem”. Transportation Research Record: Journal of the Transportation Research Board 1771, pp. 106–113. eprint: http: //dx.doi.org/10.3141/1771-14.

Williges, C. et al. (2014). Pilot Testing of SHRP 2 Reliability Data and Analytical Products: Southern California Pilot Site. Tech. rep.

Xu, T. et al. (2009). “Study on continuous network design problem using simulated annealing and genetic algorithm”. Expert Systems with Applications 36.2, Part 2, pp. 2735 –2741.

Yao, T. et al. (2009). “Evacuation Transportation Planning Under Uncertainty: A Robust Optimization Approach”. English. Networks and Spatial Economics 9.2, pp. 171–189.

Zeng, Q. & Mouskos, K. C. (1997). “Heuristic search strategies to solve transportation network design problems”. Final report to the New Jersey Department of Transportation and the National Center for Transportation and Industrial Productivity.

Zheng, H. & Chiu, Y.-C. (2011). “A Network Flow Algorithm for the Cell-Based Single-Destination System Optimal Dynamic Traffic Assignment Problem”. Transportation Science 45.1, pp. 121– 137. eprint: http://dx.doi.org/10.1287/trsc.1100.0343.

Zhong, R. et al. (2013). “A linear complementarity system approach to macroscopic freeway traffic modeling”. Cyber Technology in Automation, Control and Intelligent Systems (CYBER), 2013 IEEE 3rd Annual International Conference on, pp. 18–23.

Zhong, R. et al. (2014). “Towards automatic model calibration of first-order traffic flow model”. Control Conference (CCC), 2014 33rd Chinese, pp. 3423–3428.

Zhu, F. & Ukkusuri, S. V. (2013). “A cell based dynamic system optimum model with non-holding back flows”. Transportation Research Part C: Emerging Technologies 36, pp. 367 –380.

Ziliaskopoulos, A. K. (2000). “A Linear Programming Model for the Single Destination System Optimum Dynamic Traffic Assignment Problem”. English. Transportation Science 34.1, pp. 37–49.